

GENERAL ELECTRIC

NUCLEAR ENERGY
PROJECTS DIVISION

GENERAL ELECTRIC COMPANY, 175 CURTNER AVE., SAN JOSE, CALIFORNIA 95125
MC 682, (408) 925-5722

MFN-198-79

July 31, 1979

U. S. Nuclear Regulatory Commission
Division of Systems Safety
Office of Nuclear Reactor Regulation
Washington, D. C. 20555

Attention: Frank Schroeder, Acting Director
Division of Systems Safety

Gentlemen:

SUBJECT: ADDITIONAL TLTA INFORMATION

- Reference:
- 1) G. G. Sherwood letter to Frank Schroeder, dated 6/15/79, "Two Loop Test Apparatus (TLTA) Results"
 - 2) R. H. Buchholz letter to Frank Schroeder, dated 7/13/79, "Leibnitz Rule in LOCA Models"

Attached herein is the additional TLTA information requested by NRC during the May 24, 1979 meeting and committed by General Electric in Reference 1. Also included are additional model comparisons as requested by the NRC staff. The requested information is provided in eight attachments which are summarized below for your convenience.

1. A Writeup to Support the May 24 Slides

Attachment 1 is a summary of the May 24 meeting slides which presented the results of the recent TLTA tests. The relevant phenomena controlling the TLTA thermal hydraulic and bundle heatup response are identified and discussed. Comparisons of test results with and without Emergency Core Cooling (ECC) injection and a summary of the peak and low bundle power tests are also provided.

2. Steam Separator ΔP and Break Flow Discussion

519 147

Attachment 2 presents the results from the mass and energy balance obtained from the TLTA data for the tests with and without ECC injection. These results clearly show that for the test with ECC injection, more liquid was entrained out the break and the bulk discharged fluid quality was clearly lower. It is further concluded that fluid conditions discharged from the break led to the differences in depressurization rate observed between the two tests. Attachment 3 provides analysis of the steam separator pressure drop data. The

7908070641

CHANGE: 5/5 X60
ACRS
R ADD: 5/1
W Hodges
H Denzel

preliminary evaluation of the separator ΔP suggested that the steam flow through the separator was lower for the test with ECC injected. Results from Attachment 2 are utilized in Attachment 3 to further substantiate that the flow through the separator was indeed lower. Additional analysis to include the possible effects of liquid entrainment out the separator are also included to demonstrate that the conclusions remain unchanged.

3. TLTA Scaling Discussion

Attachment 4 summarizes the TLTA scaling basis and supporting analysis. It is demonstrated that the relevant BWR LOCA thermal hydraulic phenomena can be evaluated in the TLTA.

4. Vaporization Data Base

Attachment 5 provides further explanation of the facility and method used for the 1974 test which provided the data base for the vaporization correlation. Based on the recent results and data interpretation from the TLTA, it is concluded that the facility and system conditions in TLTA are similar to those of the 1974 vaporization tests.

5. Side Entry Orifice CCFL

Attachment 6 describes the conservatism resulting from not including Side Entry Orifice (SEO) Counter Current Flow Limiting (CCFL) in the General Electric evaluation model. It states that inclusion of SEO CCFL would result in core uncover delay and earlier reflooding which would result in improved heat transfer and lower PCT's.

6. The Grid Spacer Water Accumulation

Attachment 7 provides a discussion of the CCFL characteristics across a bundle. It is concluded that, while there is a potential for water accumulation to exist momentarily when there is a sudden reduction in the bundle inlet flow (e.g., during the flow coastdown period or lower plenum flashing period), accumulation will not occur during the reflood period.

7. Justification of Conservatism of the Heat Transfer Coefficients Used in SAFE

The information provided in Attachment 6 demonstrates that the heat transfer coefficients used in the SAFE Computer Program between the nucleate boiling to the core spray cooling regimes are the appropriate values.

U. S. Nuclear Regulatory Commission
July 31, 1979
Page 3

8. Discussion of Plant Choice For Leibnitz Rule Study

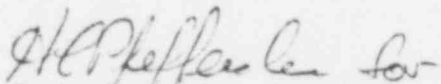
Response to this item was forwarded under separate cover by Reference 2.

9. Additional Evaluation of Model Comparisons

Attachment 8 provides additional evaluation model comparisons of the TLTA tests with and without ECC injection. The comparisons show that the system is calculated to blowdown faster than measured due primarily to an overestimation of the break flow during the early period of the transient.

The information provided here closes out all the TLTA commitments made in Reference 1 and during discussions with the NRC staff. If further clarification is required, please contact R. N. Woldstad at (408) 925-2539 or L. F. Rodriguez at (408) 925-2460.

Very truly yours,



R. H. Buchholz, Manager
BWR Systems Licensing
Safety and Licensing Operation

RHB:gmm/421-423

Attachments

cc: L. S. Gifford (Bethesda)
L. Phillips (NRC)

519 149

ATTACHMENT 1

SUMMARY OF TLTA TEST WITH ECC INJECTION

JULY 1979

1. INTRODUCTION

The BD/ECC-LA phase of the BD/ECC Program was intended to obtain information on the effect of ECC injection on BWR system responses. The original test plan¹ identified a matrix of 20 tests. Six of these tests were selected² by the PMG (Program Management Group) to scope the outcome of the test series.

Four matrix tests plus a repeat of the reference test without ECC injection were completed by September 1978. Preliminary results were presented to the program sponsors and the NRC staff in the ensuing months. Detailed results, interpretations, and conclusions from these tests were presented to the PMG in March 1979 and to the NRC staff in May 1979. This report summarizes the material previously presented.

The report is organized in three sections. The first section summarizes the scenario of the reference tests (average bundle power, average ECC injection). The next section summarizes the differences between tests with and without ECC. The last section summarizes highlights of other tests.

519 150

¹J. C. Wood, A. F. Morrison, "BWR Blowdown/Emergency Core Cooling Program - 64-Rod Bundle Core Spray Interaction (BD/ECC-LA) Test Plan", GEAP-NUREG-21638A, February 1978.

²Contract No. AT(39-24)-0215, "BWR BD/ECC Program Twenty-Ninth Monthly Report", March 1978, Report on 8th PMG Meeting, March 28-29, 1978, at San Jose, Calif.

2. SCENARIO DESCRIPTION OF RESPONSES

System responses are discussed in this section. The configuration of the test apparatus is highlighted first. Control parameters that are imposed on each test are outlined. The reference test (6406/Run 1) scenario is described with the aid of a series of qualitative sketches referred to as "snap shots". Detailed quantitative measurements are presented to substantiate the descriptions.

a. TLTA Configuration

The two-loop test apparatus configuration #5 (TLTA-5) was used to conduct the BD/ECC-1A tests. Details of TLTA can be found in the Description Report¹. A schematic diagram is presented in Figure 1; salient features of TLTA-5 are:

- Integral system
- Full size bundle
- Full power
- Prototypical pressure and temperature
- ECCS

b. Controlled Parameters

Controlled parameters refer to those quantities whose transient responses are designed and controlled to be similar to those predicted for a reactor counterpart. Included and shown in Figure 2 are: Bundle power, steamline flow, ECC injection flow characteristics, and drive pump coastdown.

519 151

¹W. J. Letzring, editor, "BWR Blowdown/Emergency Core Cooling Program Preliminary Facility Description Report for the BD/ECC-1A Test Phase", GEAP-23592, December 1977.

The bundle power, ECC pump rated flow conditions and the temperature of the ECC water are parameters in the BD/ECC-1A test. Table 1 shows the variation of parameters in the matrix tests.

The steam line flow (Figure 2a) is controlled during tests, by the response of the pressure control valve. This valve closes and opens in response to the vessel pressure. The set point for the valve was 1050 psi. The valve closed completely at ~12 sec. for the reference test (Figure 2a).

The ECC injections in the reference test are shown in Figure 2b. The HPCS was activated at 27* sec.; injection begins immediately. The LPCS and LPCI were activated at 37* sec.; actual flow begins at 76 sec. for LPCS and 88 sec. for LPCI. Both the timings and the ECCS pump operating characteristics were designed² to simulate the characteristics of the BWR ECCS.

The bundle power transient is shown in Figure 2c. The power supplied to the bundle was programmed to simulate the stored heat and fission decay heat (based on ANS + 20%) of a BWR bundle. The capability of the mechanical controller had limited the close simulation to only 50 seconds. Beyond that time, the power supply was held constant. It becomes increasingly higher than the fission decay heat calculated from ANS + 20% reaching ~1.8 times the ANS value at the end of the test (~300 sec.). A detailed discussion of the bundle power supply has been reported previously³.

Coastdown of the intact loop drive pump begins immediately in response to the loss of power (Figure 1d). The response of pump coastdown is governed by the inertia of the rotating components. The inertia of the test pump has been designed to simulate that of the BWR counterpart.

c. Scenario of Reference Test

(1) Early Responses

The responses from BD/ECC-1A tests, before HPCS injection at 27 sec.,

²C. G. Hayes, "BWR Blowdown/Emergency Core Cooling Program - ECC System Calibration and Performance Verification", NEDG-21956, July 1978.

³Transmittal, G. W. Burnette (GE) to E. L. Halman (NRC) and M. Merilo (EPRI), Contract No. NRC-04-76-215, Informal Monthly Progress Report for January 1979.

*NOTE: The time delay of 27 sec. for HPCS and 37 sec. for LPCS is designed to simulate the startup of diesel generator and opening of valves.

are similar to those of the previous, 8x8 BDHT tests (with no ECC). The early responses are governed by the liquid level in the downcomer region (Figure 3a). This level reaches the jet pump suction plane at 7.6 sec. and the recirculation line suction inlet at about 10.5 seconds (Figure 3a).

The bundle inlet flow drops in response to the loss of jet pump flow in the broken loop, it then coasts down (Figure 3b) following the drive pump (Figure 2d). The flow reaches a near zero value when the jet pump suction is uncovered at ~ 7.6 sec. The flow surge associated with lower plenum flashing occurs at ~ 11.8 seconds shortly after recirculation line suction uncover.

The system depressurization rate increases after the recirculation line suction uncover (Figure 3c) due to the increased volumetric discharge that accomplish this transition from predominantly liquid to vapor blowdown.

(2) "Snap Shots" Presentation

A series of pictorial depictions - snap shots - of the system at selected instants of the transient is presented in Figure 4. These snap shots convey an overview of the thermal-hydraulics responses of the TLTA sequentially. They show the qualitative characterization of the conditions in the system and are backed up with detailed, quantitative plots as appropriate.

The first snap shot (Figure 4a) depicts the system conditions at the onset of HPCS injection which occurs at ~ 27 seconds shortly after LPF (lower plenum flashing). This instant is a demarcation of difference in boundary conditions between tests with and without ECCS. Substantial mass inventory is seen in the upper plenum (see also Figure 5 for detail). This inventory was transferred there as a result of LPF which redistributes fluid from the lower plenum to the core and the upper plenum. An apparent continuum of liquid (or two-phase mixture) keeps the bundle in nucleate boiling (see also Figure 7 for thermal response details).

519 153

As the blowdown proceeds and mass inventory continues to deplete from the lower plenum, the receding two-phase level reaches the jet pump exit plane at ~ 34 seconds as shown in Figure 5. The flashing lower plenum fluid discharges with increasing vapor fraction through the jet pumps. The void fraction in the jet pump increases, reducing the hydrostatic head and therefore the pressure difference across the jet pump. Accordingly, the

pressure drop across the bundle path, which is in parallel with the jet pump path, also decreases. This decreased pressure difference reduces the vapor up flow and correspondingly the hold up of liquid, due to CCFL, within the bundle. The liquid continuum within the bundle is no longer sustained, and the level drops below the bottom of heated length (BHL) at ~40 seconds (Figure 4b and also Figure 5 for detail).

At 40 seconds (Figure 4b), the bundle is filled by a vapor continuum in place of the liquid continuum. Heater rods begin to dryout and bulk heat-up occurs (see Figure 7 A and 7B). By contrast, the upper plenum inventory remains essentially unchanged during this period: HPCS replenishes the loss while CCFL prevents complete draining into bundle or bypass.

The vapor flow at the top of the bundle diminishes with the reduction in vapor upflow from the lower plenum through the bundle. Another contributing factor is the reduction in heat transfer that accompanies the loss of the liquid continuum.

The CCFL conditions at the upper tieplate shift in response to reduced vapor flow from the bundle. Accordingly, an increased amount of liquid drains into the bundle (Figure 4c), and a few of the previously dried-out rods are seen to rewet. During this period (~64 seconds), rewetting is limited to the upper portion of the bundle.

LPCS injection begins at ~76 seconds. The injection rate increases towards the rated flow as the system pressure decreases. The upper plenum inventory is maintained by this LPCS mass influx in conjunction with that of HPCS. The vapor upflow from the lower plenum, in the meantime, diminishes as the rate of system depressurization decreases. The liquid downflow at the upper tieplate increases as the CCFL conditions shift at ~90 seconds (Figure 4). Rewetting of previously dried-out thermocouple locations are seen at the bottom as well as the upper part of the bundle.

Also at ~90 seconds, LPCI begins to flow into the bypass region in increasing amount (until rated flow has been reached). The net vapor outflow from this region decreases as the influx of subcooled ECC water condenses some of the steam. The CCFL condition at the bypass outlet shifts to allow the liquid in the upper plenum to drain more rapidly into the bypass region (Figures 4e and 8). More fluid is now in the bypass region and less in the upper plenum. The hydrostatic head is, therefore, increased in the bypass relative to the upper plenum. Therefore, more vapor flows through the bundle until

the pressure drop across the bundle equalizes the hydrostatic head in the bypass region. The increased vapor upflow contributes to an increase in bundle heat transfer which results in a decrease in the bulk heatup rate at ~105 seconds (Figures 7A and 7B).

As the bypass region is being filled, some liquid drains into the guide tube and, alternatively, into the lower plenum. The mixture level in the lower plenum rises. This level rises steadily and at a faster rate after the guide tube is completely full. The jet pump exit becomes sealed by the rising mixture level at ~150 seconds (Figure 4f). As the mixture fills the jet pump, the hydrostatic head and hence the pressure drop across the jet pump increases. The pressure drop across the bundle increases correspondingly with increased vapor flow from the lower plenum. The increased vapor flow contributes to a further increase in bulk heat transfer that results in the decrease in bundle heat-up rate noted in Figure 7A & 7B at ~150 seconds.

The bundle begins to reflood as the lower plenum level continues to rise at a more rapid pace after the bypass region has become full (Figure 4g). The reflooding of the bundle results in rapid quenching below the mixture level (see Figure 7A and 7B). The extent of the bundle reflood is limited to the height corresponding to the jet pump suction plane (see Figure 8 for additional details). The mixture level reaches its height limit at ~220 seconds. The system is maintained at quasi-steady state for the balance of the test which ends at ~300 seconds.

d. Detailed Responses

The details of responses shown in Figures 5 to 8 were the bases from which the scenario for the reference test was constructed. Certain details in these figures have been cited in the preceding discussion. Additional observations are discussed here.

The two-phase mixture levels (Figure 5) are based on differential pressure measurements as well as conductivity probes. The lower plenum level reaches the jet pump exit plane at about 34 seconds. This level remains there, at the jet pump exit plane, until it rises later when the lower plenum refills (Figure 8).

519 155

The level is maintained at the jet pump exit until the bypass fills. The jet pump flow path height plays a major role in system responses as will be discussed later (Section 3).

Plots of nodal density (Figure 6) provide information on system inventory distribution. The nodal density of the heated length is seen to be highly voided after 40 seconds. Only the node below the heated length, Node 21, and the top node which includes the upper tieplate and part of the upper plenum, Node 31, show any significant liquid inventory.

519 156

3. COMPARISON OF TESTS WITH/WITHOUT ECC

Comparisons of data from average-power tests with and without ECC are made in this section. Data from Test 6406/R1 (average power, average ECC) will be compared with those from Test 6406/R3 and/or Test 6007/R26 (average power, no ECC).

The system depressurization rate is seen to be lower for the test with ECC after approximately 65 seconds (Figure 9). The cause of this difference is discussed at length in Attachment 2. In essence, the attachment shows that the flow emanating from the lower plenum for the test with ECC has a higher moisture content as well as a higher discharge rate through the jet pump. The combined effect is a sequential reduction of volumetric flow through, first, the drive/blowdown line and then the suction/blowdown line. Slower depressurization results from these lower volumetric flows through the breaks.)

The system mass inventory is higher, as expected, for the test with ECC. In the upper plenum (Figure 10a), the fluid is prevented from completely draining due to CCFL at the upper tieplate. In the test without ECC, the inventory there depletes steadily as it continues to flash throughout the transient. In the test with ECC, the core spray maintains the inventory until ~100 seconds. At that time, the LPCI has taken effect in the bypass region to reduce the vapor up flow and therefore allows the upper plenum fluid to drain into the region (see also Section 2). The ECC injection rate is given in Figure 10d.

The bundle mass inventories for the two tests are virtually the same (Figure 10b). In both tests, the bundle is filled with a vapor continuum after ~ 40 seconds. The mass inventory is derived from the bundle pressure drop measurements which show nearly identical responses for the tests with/without ECC (see Figure 11). The transition from liquid to vapor continuum is shown to occur between 34 to 40 seconds. In the test with ECC, reflooding causes liquid accumulation in the lower part of the bundle later in the transient (~200 seconds).

The lower plenum mass for the test with ECC is maintained rather constant from 35 seconds to 120 seconds (Figure 10c). The fluid discharged through the jet pump is balanced by the ECC fluid draining from the upper plenum. For the test without ECC, in contrast, the mass inventory in the lower plenum depletes continuously as the fluid flashes off throughout the transient.

The bypass region mass inventories for the two tests are similar prior to LPCI injection (Figure 10e). Following the LPCI injection (~90 seconds), the bypass region refills for the test with ECC. This filling became more rapid as the core spray fluids drain from the upper plenum.

The guide tube mass inventories (Figure 10f) also show similar response. Discernible difference between the tests occurs when ECC fluid in the upper plenum begins (~75 seconds) to drain into and accumulate in the guide tube.

The responses in the guide tube and especially the bypass region are important in understanding the related response in the bundle. This is because the bypass region and bundle are parallel paths connecting the lower plenum to the upper plenum. The bypass region dominates the hydraulic response along the path since there is more mass inventory there.

The two-phase levels at different regions in TLTA are shown in Figure 12. The level plots provide information on fluid distribution along each flow path and within each region. They are derived from detailed differential pressure measurements. Measurements from conductivity probes (level probes) are also used as supplementary information.

The upper plenum two-phase levels reflects the mass inventories shown in Figure 10a. In the case with ECC, the mixture level holds up longer because of the core spray fluid.

519 158

The mixture level in the bundle drops to the bottom of the heated length at ~40 seconds. The level remains below the heated length until later when the bundle refloods in the case with ECC.

The lower plenum mixture level falls rather rapidly after lower plenum flashing, reaching the jet pump exit plane at ~34 seconds. The level in the test with ECC lingers at this elevation until it rises later in the transient (~120 seconds). In contrast, the level for the test without ECC falls and holds momentarily at the exit plane then falls below the jet pump exit at 65 seconds.

In the bypass region, the levels for the two tests are initially similar. For the test with ECC, the level rises later (~98 seconds) as the LPCI flows and the spray fluid drains into the region. Similarly, the level in the guide tube rises later for the case with ECC.

As a consequence of the difference in hydraulic responses for the two tests, the thermal responses are also different. In the test without ECC, bundle rewetting and heat-up rate reduction are not observed.

The thermal responses for the two tests are compared in Figure 13. The lower part of the bundle (Figure 13a) is cooler in the test without ECC for the first ~100 seconds. This is consistent with an earlier observation (Figure 12) that the mixture level stays longer there for that test.

Responses from the upper part of the bundle (Figure 13b) provide evidence of improved heat transfer with ECC. A temperature difference of 375°F is seen at ~150 seconds between the tests at 90" elevation - location of the peak cladding temperature for the test without ECC.

519 159

4. HIGHLIGHTS OF SIGNIFICANT DIFFERENCES OF OTHER TESTS WITH ECC INJECTION

a. Average Power, Low ECC Test (6405/Run 3)

Responses from this test are, in general, similar to those from the reference test as can be seen from Figure 14. The system pressure of the two tests with ECC starts deviating from that of the test without ECC at ~65 seconds. The difference, as has been mentioned in Section 3, is due to higher liquid content in the break flow through the drive/blowdown line. The difference at ~100 seconds between the two tests with ECC is due to the same effect, i.e., difference in liquid content in the break flow through the suction/blowdown line. The lower ECC flow results in lower liquid fraction in the downcomer region at that time.

The lower ECC injection also causes a slower system refill as expected. Nevertheless, the responses and phenomena observed are similar. The overall thermal response of the bundle shows that less ECC fluid results in higher cladding temperature at the peak power plane (Figure 15).

b. Peak Power, Low Flow and High Temperature ECC Test (6414/Run 3)

The parameters for this test were intentionally chosen to provide an upper bound, bundle heat-up response. The ECC system was degraded to have low flow, high temperature for the test conducted with peak bundle power (6.49 mw). Nevertheless, the system response from this test is comparable with that from the average power, average ECC test. The hydraulic response of the bundle for the peak power test is similar to that of the average power as shown by the comparison of pressure drop across the bundle (Figure 16). Because of the higher bundle power, the temperature response of the bundles is different, as can be seen from Figure 15. It is seen that the peak power bundle has higher temperature as expected. A temperature difference of ~450°F is observed at ~170 seconds when the peak power test was terminated.

c. Low Power, High ECC Test (6401/Run 4)

The goal of this low power (1.62 mw), high spray flow test was to obtain a data base of system response with particular emphasis on draining of the upper plenum through a peripheral-power bundle. Significant differences of hydraulic responses are seen in this test as compared with the reference test. The differences are:

- more liquid drains into the bundle due to the combined effect of higher spray flow and lower bundle power,
- CCFL at side entry orifice holds up liquid in the bundle throughout the test,
- the bundle is kept well cooled (below 600°F) throughout the transient (Figure 15) due to the liquid holdup, and
- Subcooling of upper plenum fluid leads to a significant increase of liquid down flow into the bundle.

TABLE 1. TEST PARAMETERS FOR DD/ECC 1A TESTS

● ECC FLOW VARIATION TESTS

<u>TEST NO.</u>	<u>POWER</u>	<u>ECCS FLOW</u>	<u>ECC TEMPERATURE</u>
6007/26 ⁺	5.05 MW	NO	~
6405/3	5.05 MW	LOW	~120°F
6406/1*	5.05 MW	AVE	~120°F

+ REPEATED AS 6406/3

* REFERENCE TEST

● POWER VARIATION TESTS

<u>TEST NO.</u>	<u>POWER</u>	<u>ECCS FLOW</u>	<u>ECC TEMPERATURE</u>
6401/4	1.62 MW	HIGH	~120°F
6414/3	6.49 MW	LOW	~200°F

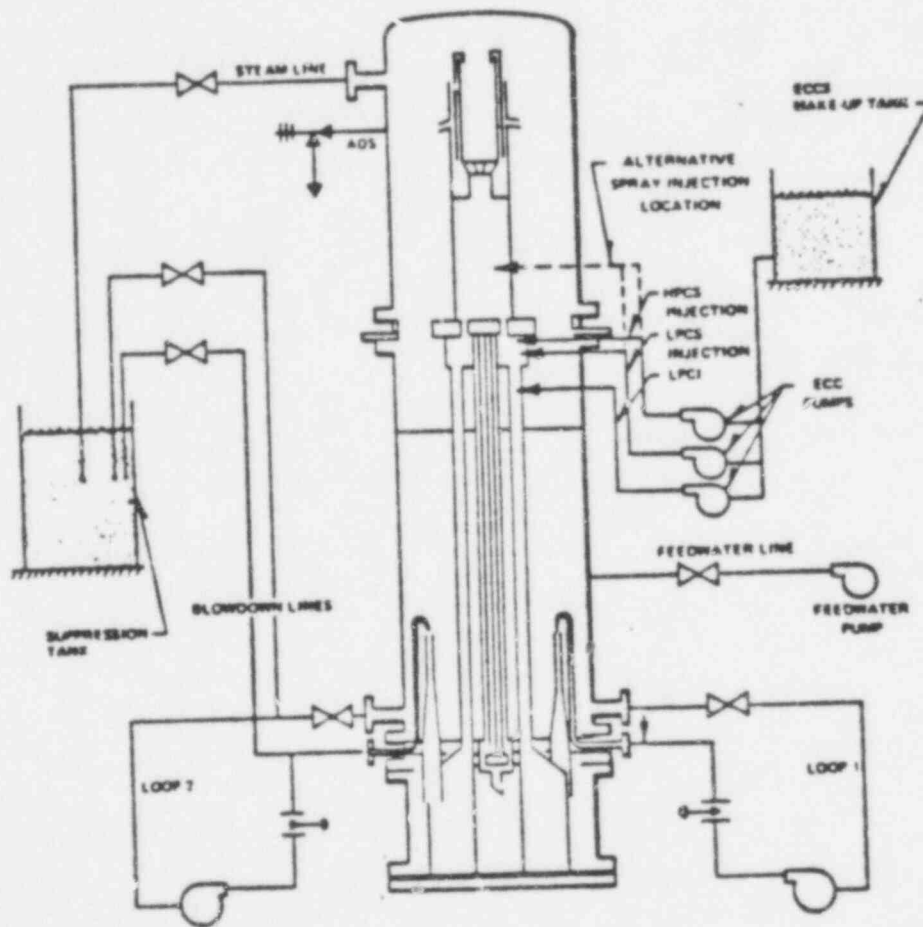


FIGURE 1, TLTA5 (TWO LOOP TEST APPARATUS CONFIGURATION 5)
WITH ECCS (EMERGENCY CORE COOLING SYSTEMS)

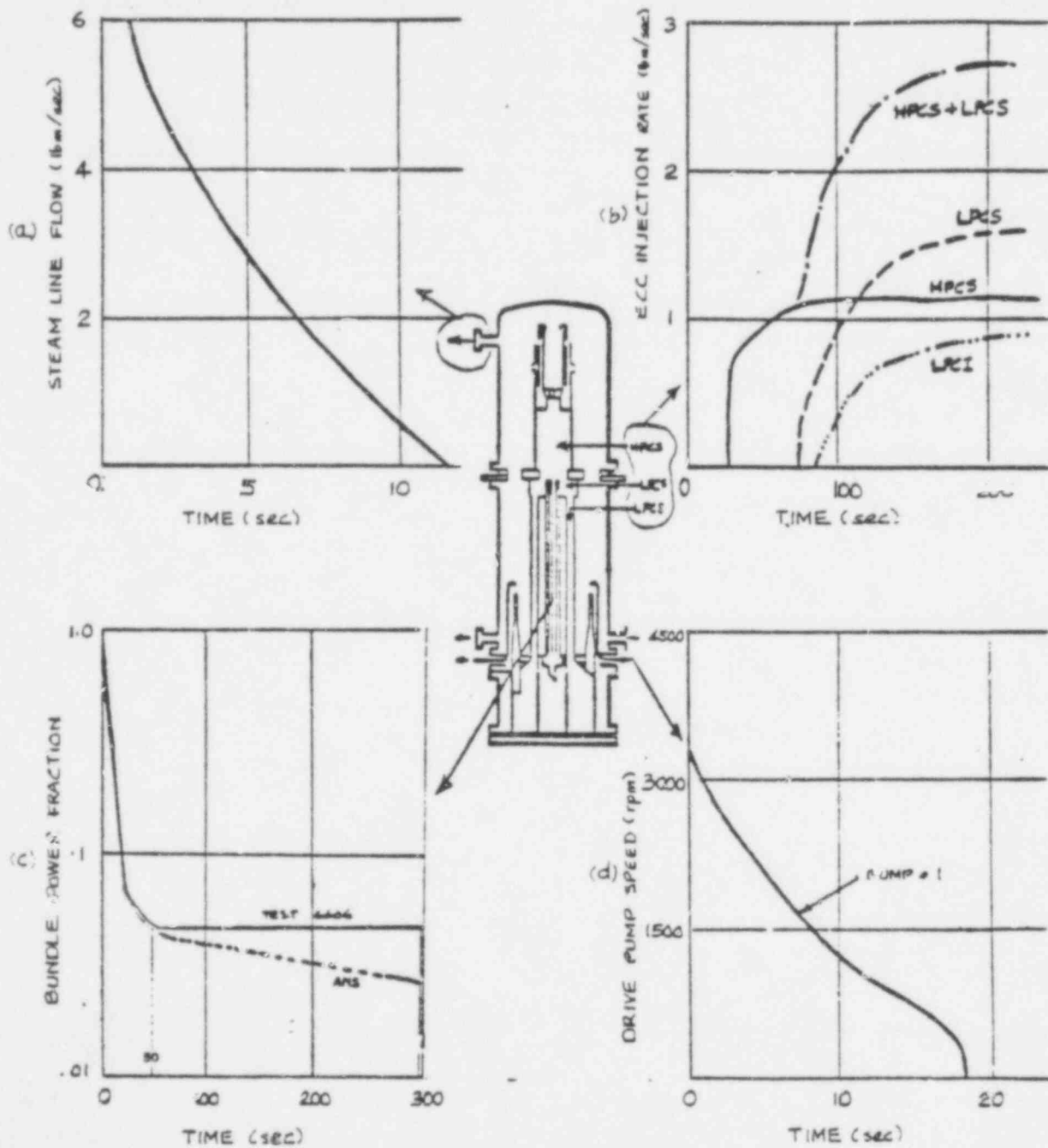


FIGURE 2, CONTROLLED PARAMETERS RESPONSES OF REFERENCE TEST (6406 RUN 1 AVERAGE POWER, AVERAGE ECC).

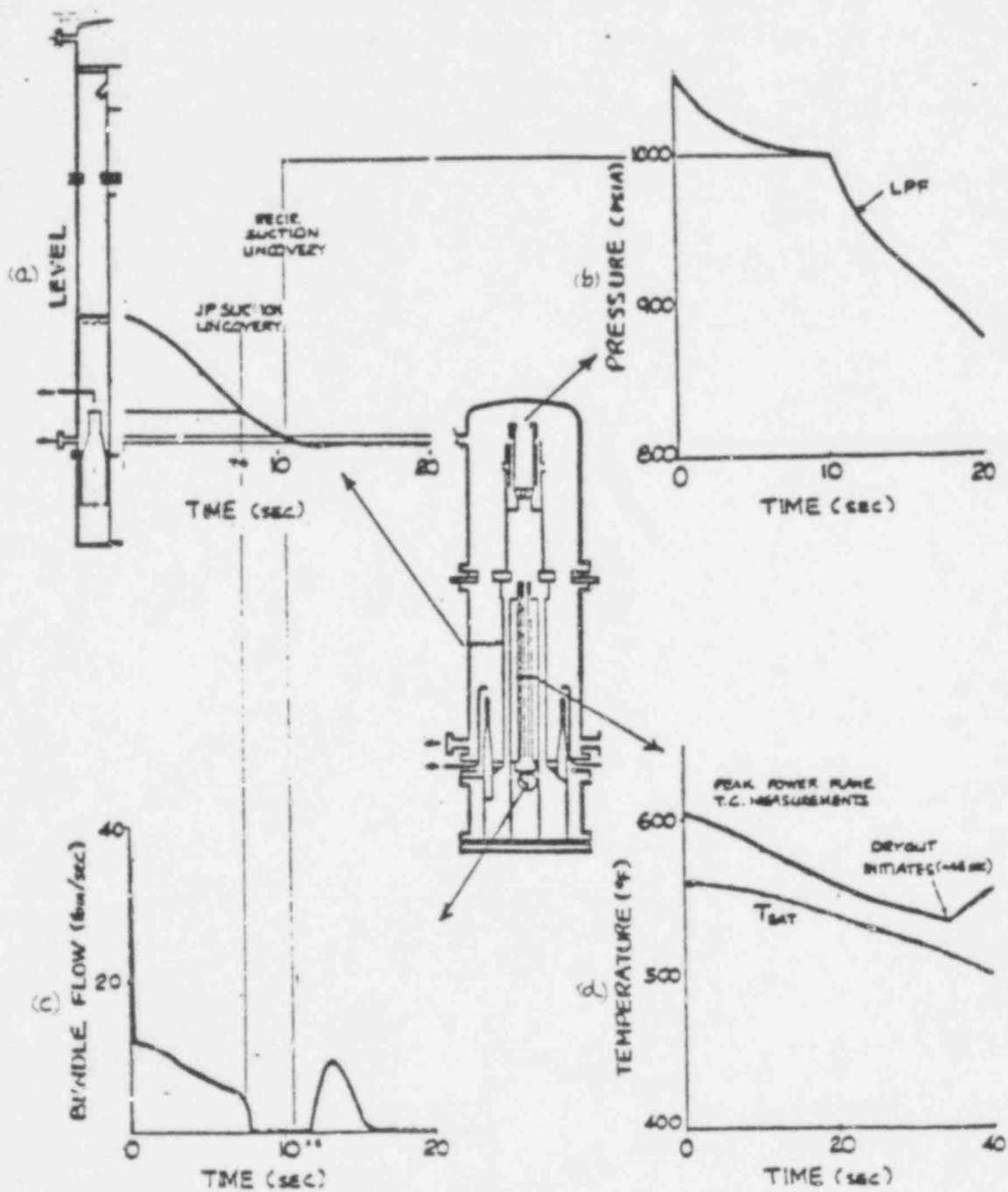
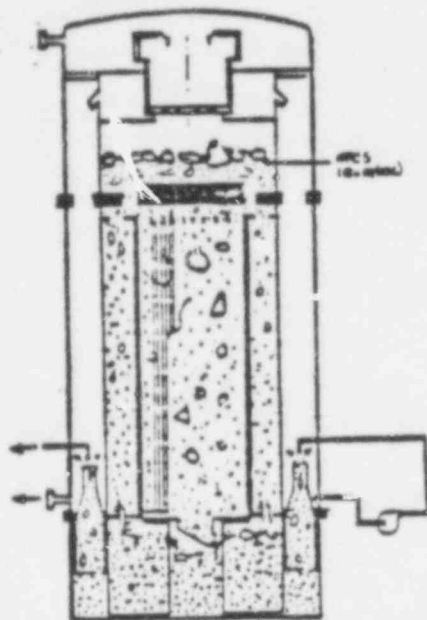
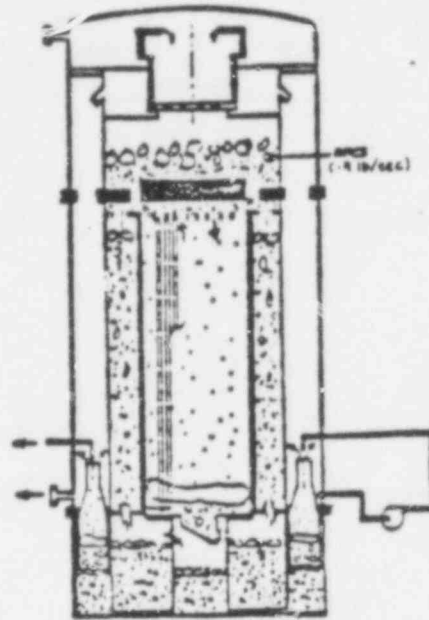


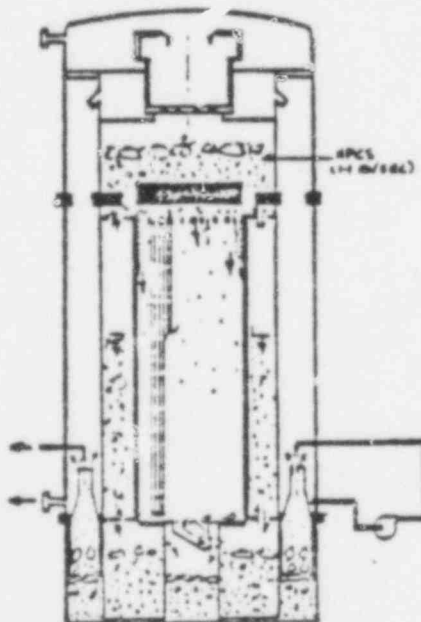
FIGURE 3, SYSTEM RESPONSES IN THE EARLY STAGE OF THE BD/ECC TRANSIENT FOR THE REFERENCE TEST (6406 RUN 1, AVERAGE POWER, AVERAGE ECC)



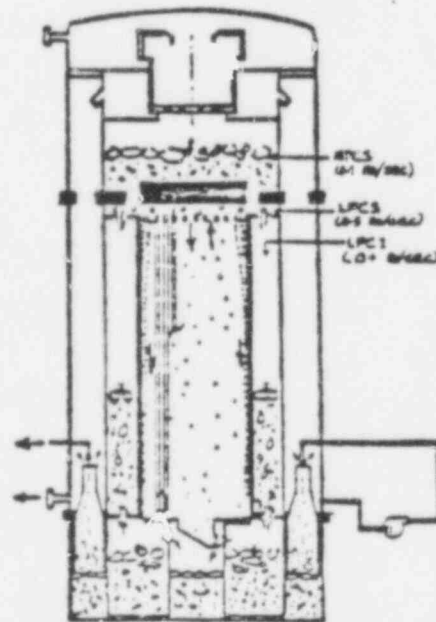
a. 6406/1 HPCS Flow Inception (27 sec)



b. 6406/1 Jet Pump Exit Exposure (~40 sec)



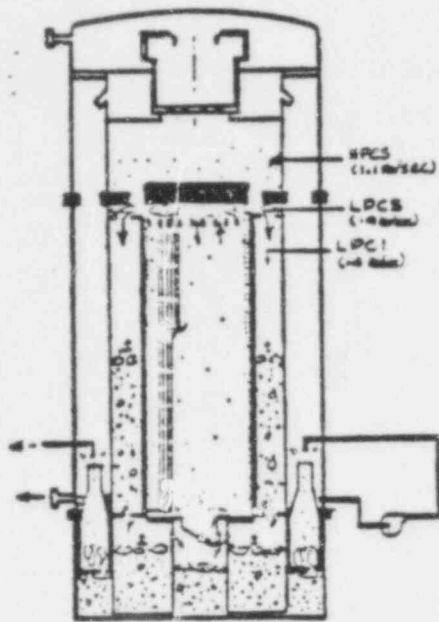
c. 6406/1 P Difference Discernible (~64 sec)



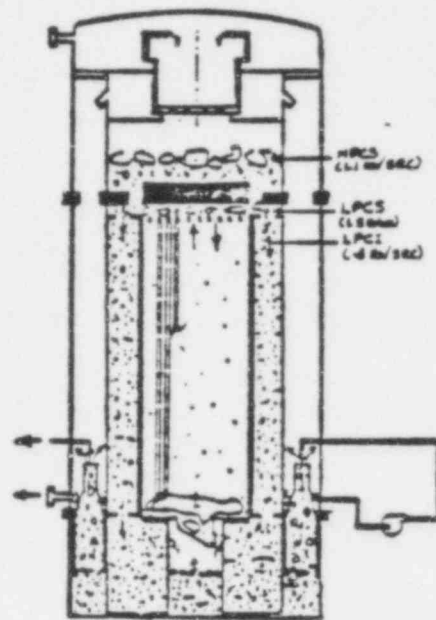
d. 6406/1 LPCS and LPCI Injecting (~90 sec)

519 166

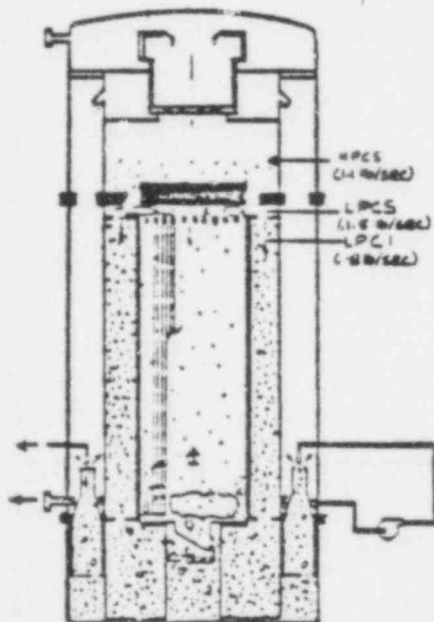
FIGURE 4, SNAP SHOTS AT SELECTED INSTANCES FOR THE REFERENCE TEST (6406 Run 1, AVERAGE POWER, AVERAGE ECC).



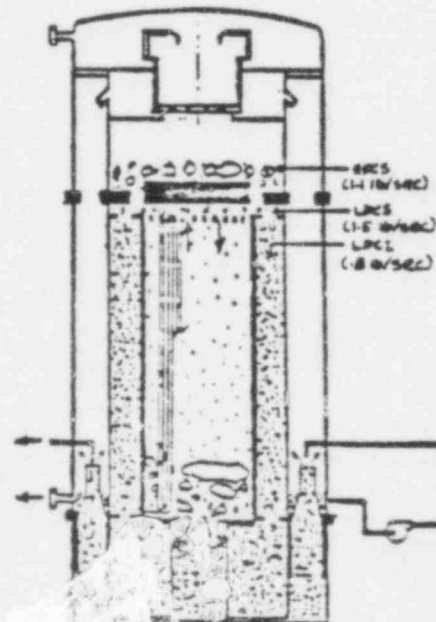
e. 6406/1 CCFL Breakdown at Bypass (~105 sec)



f. 6406/1 Jet Pump Refilled With Liquid (~150 sec)



g. 6406/1 System Filling (~160 sec)



h. 6406/1 A Refilled (~160 sec)

FIGURE 4, SNAP SHOTS AT SELECTED INSTANCES FOR THE REFERENCE 167 TEST (6406 RUN 1, AVERAGE POWER, AVERAGE ECC) (CONTINUED)

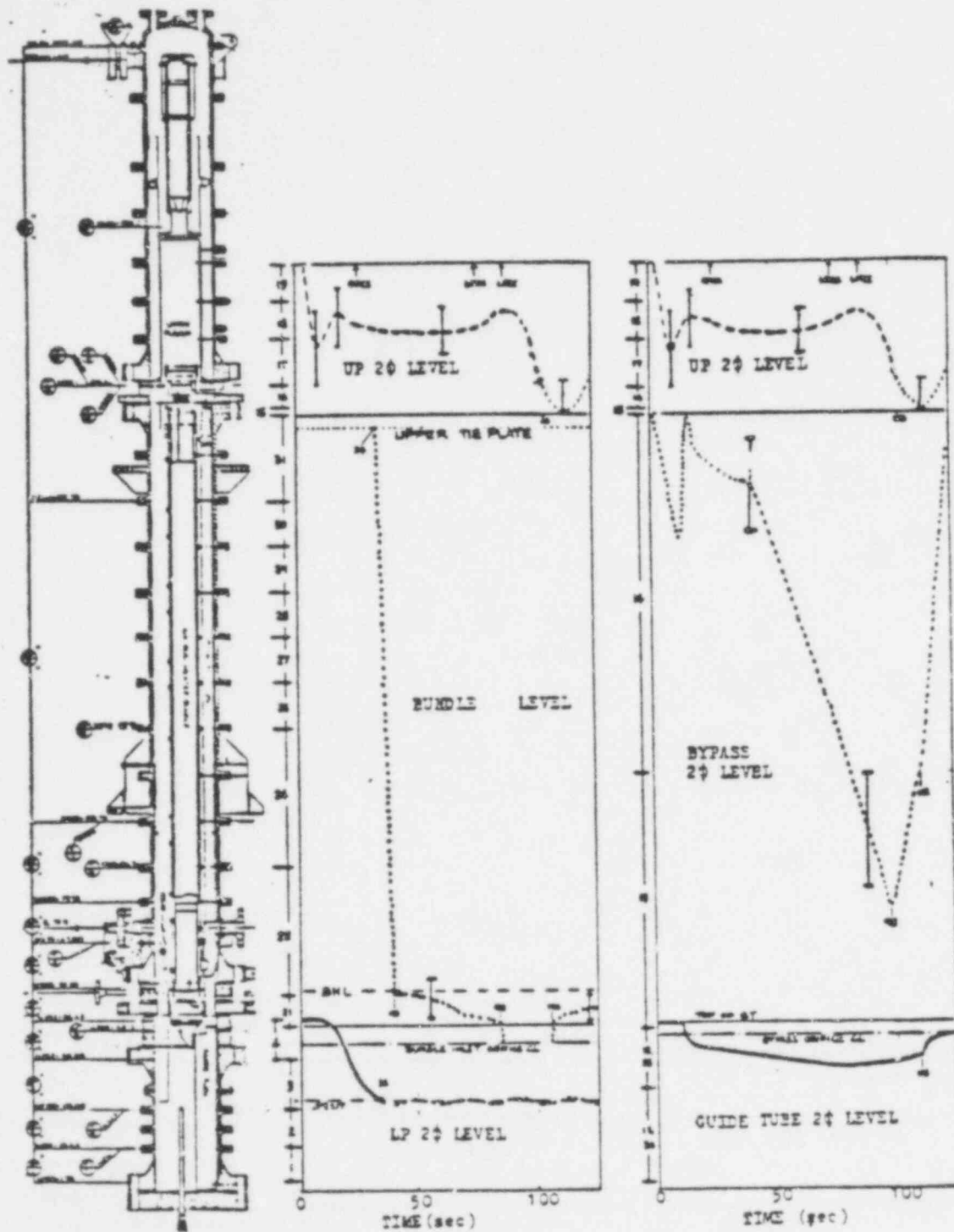


FIGURE 5, TWO-PHASE MIXTURE LEVEL RESPONSES FOR THE REFERENCE TEST (6406 Run 1, AVERAGE POWER, AVERAGE ECC)

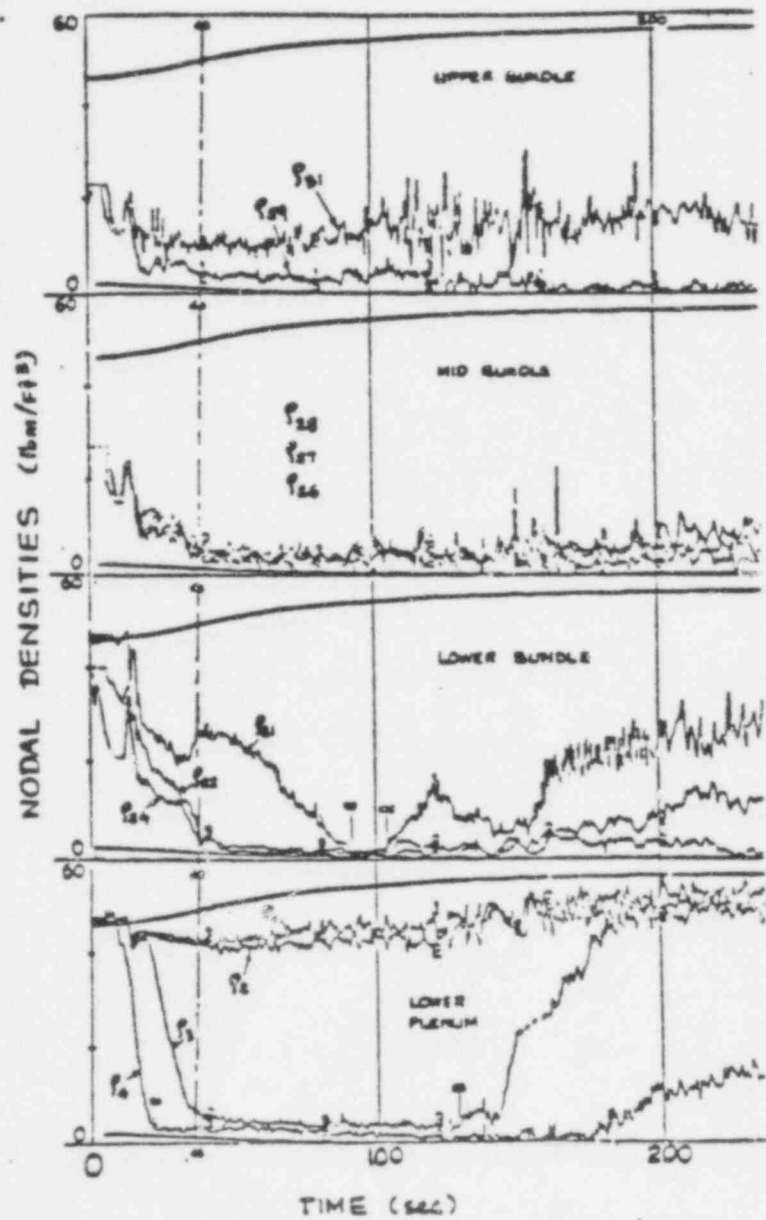
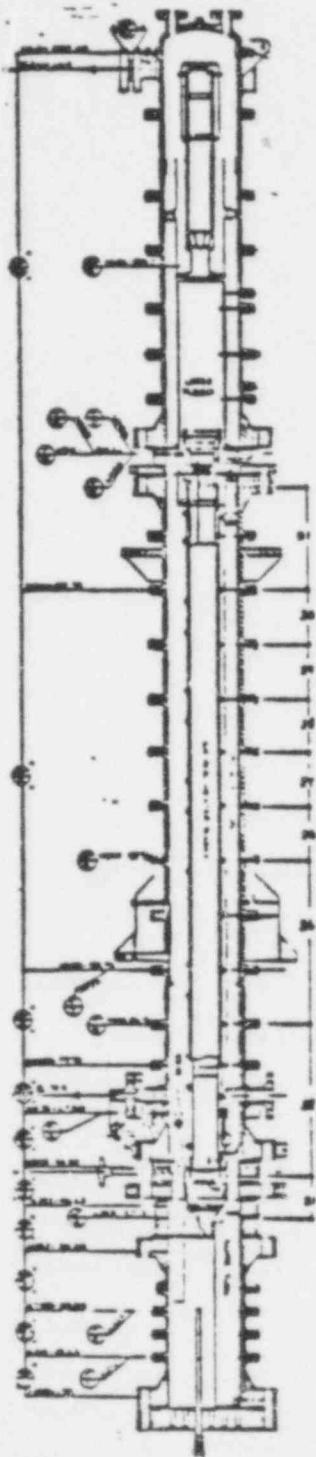


FIGURE 6, NODAL DENSITIES IN LOWER PLENUM AND BUNDLE OF THE
 REFERENCE TEST (6406 RUN 1, AVERAGE POWER, AVERAGE ECC)

519 169

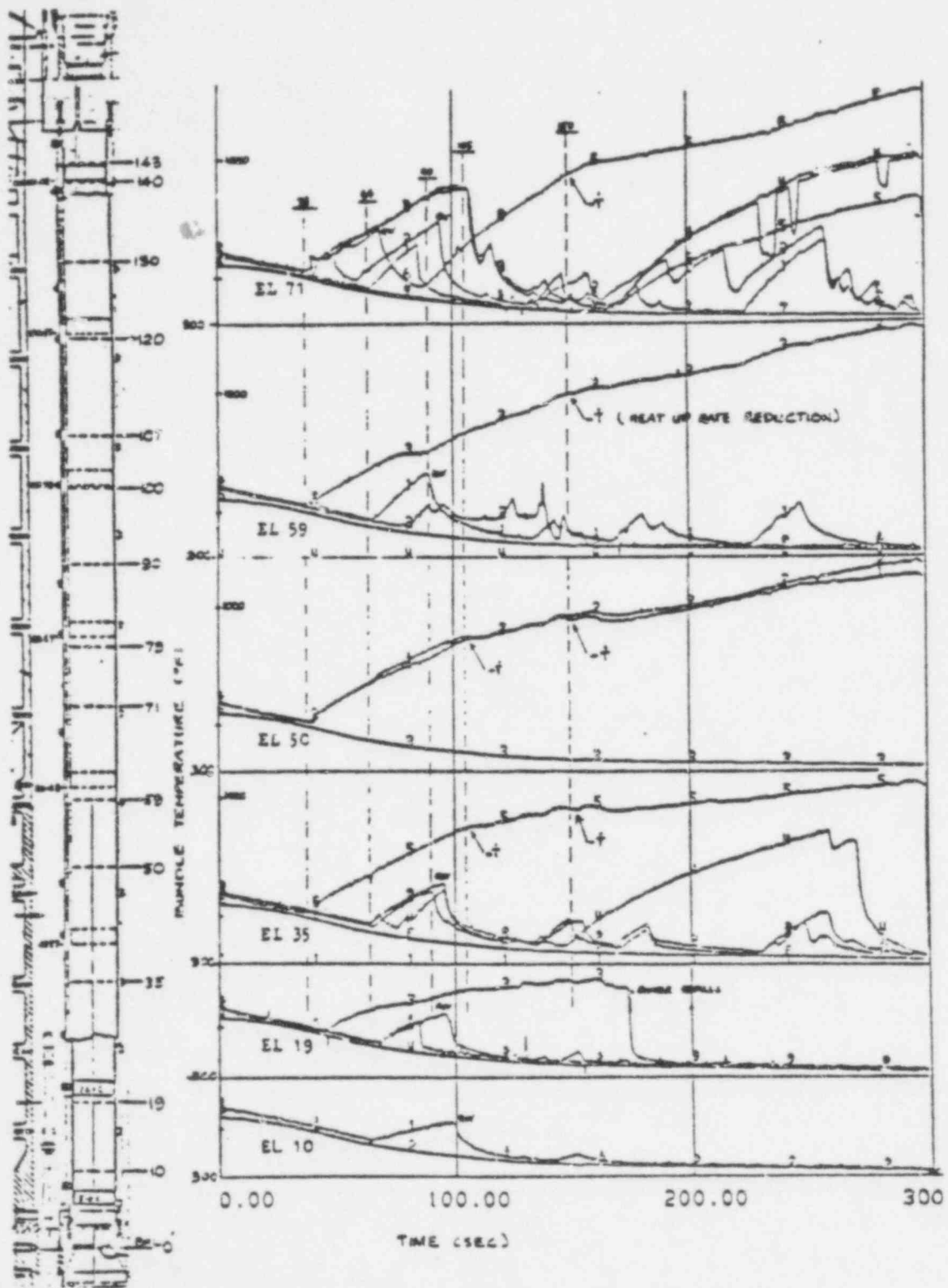


FIGURE 7A, TEMPERATURE RESPONSES OF LOWER HALF OF BUNDLE FOR THE REFERENCE TEST (6406 RUN 1, AVERAGE POWER, AVERAGE ECC)

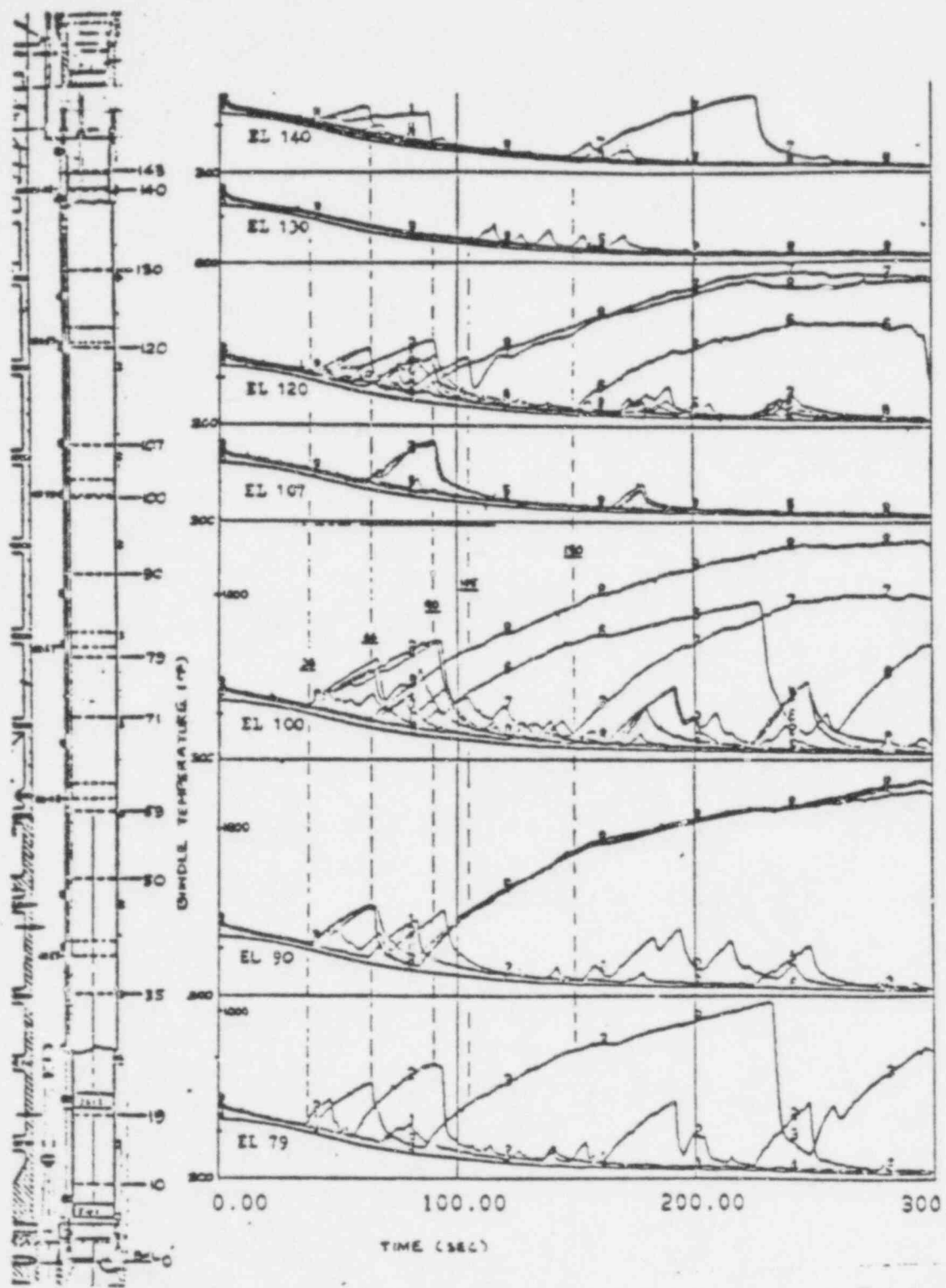
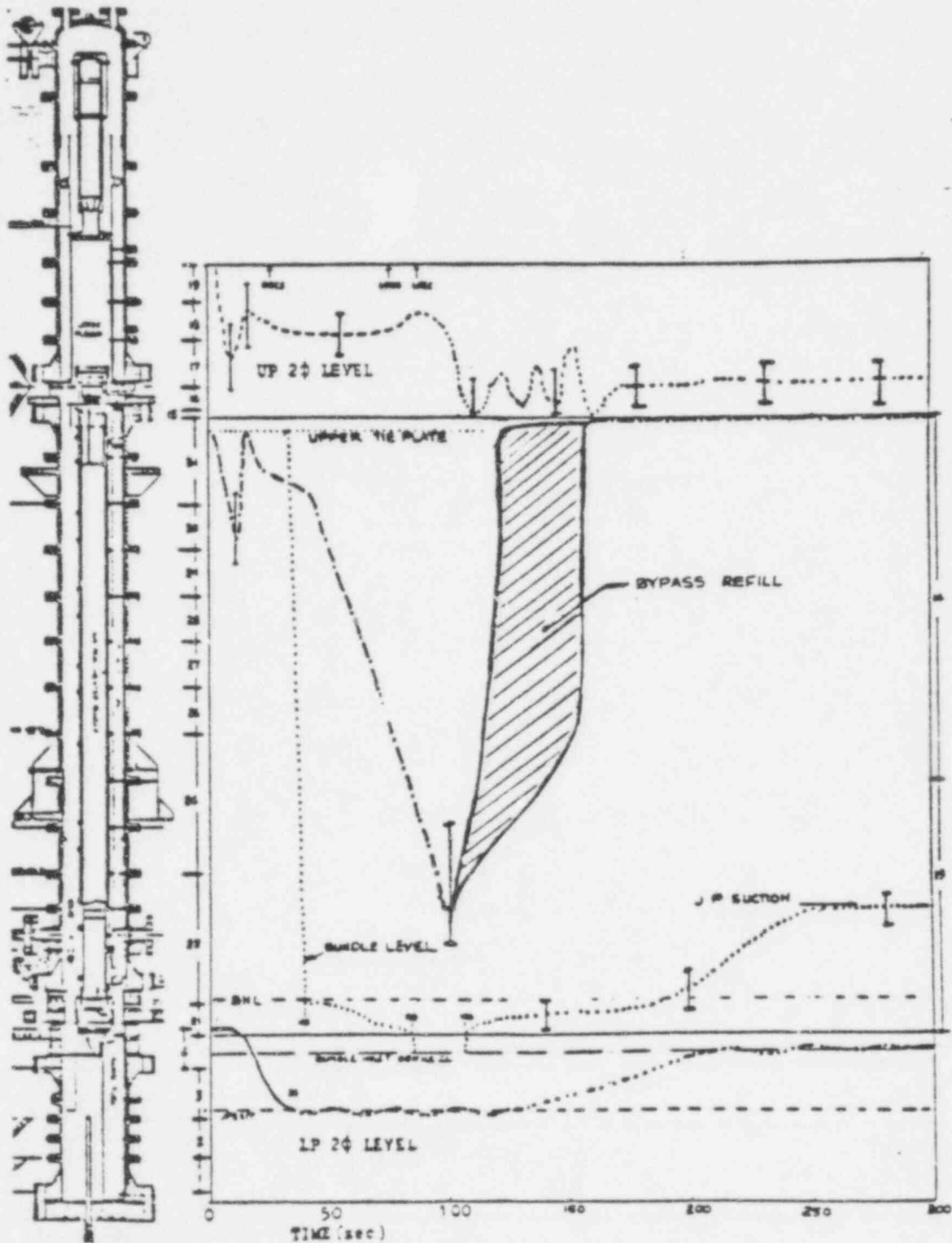


FIGURE 7B, TEMPERATURE RESPONSES OF UPPER HALF OF BUNDLE
 FOR THE REFERENCE TEST (6406 RUN 1, AVERAGE
 POWER, AVERAGE ECC)



519 172

FIGURE 8, TWO-PHASE MIXTURE LEVEL RESPONSES ILLUSTRATING BUNDLE REFILL FOR THE REFERENCE TEST (E401 RUN 1, AVERAGE POWER, AVERAGE ECC).

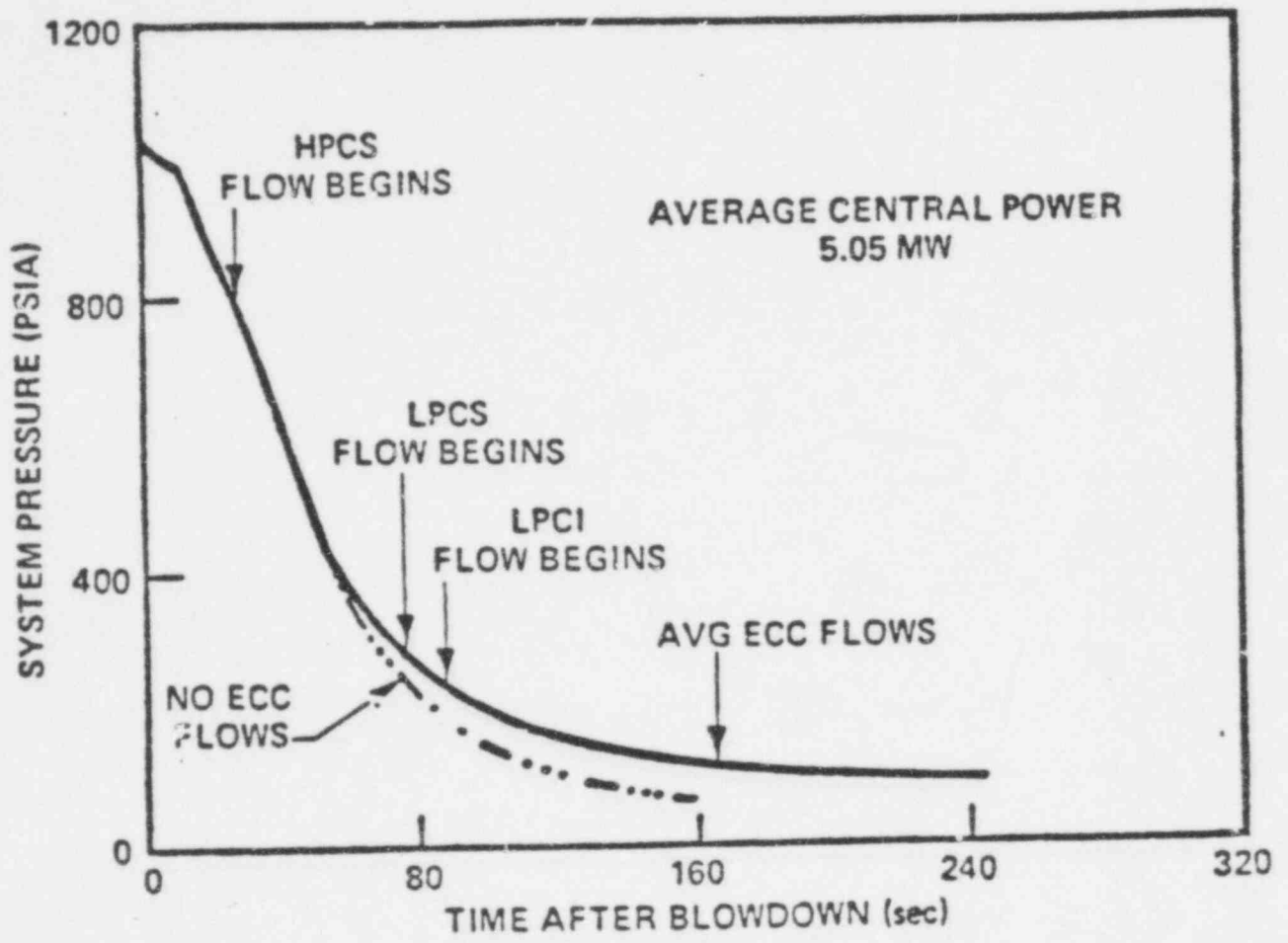


FIGURE 9, COMPARISON OF SYSTEM PRESSURE RESPONSES BETWEEN TESTS WITH/WITHOUT ECC.

519 173

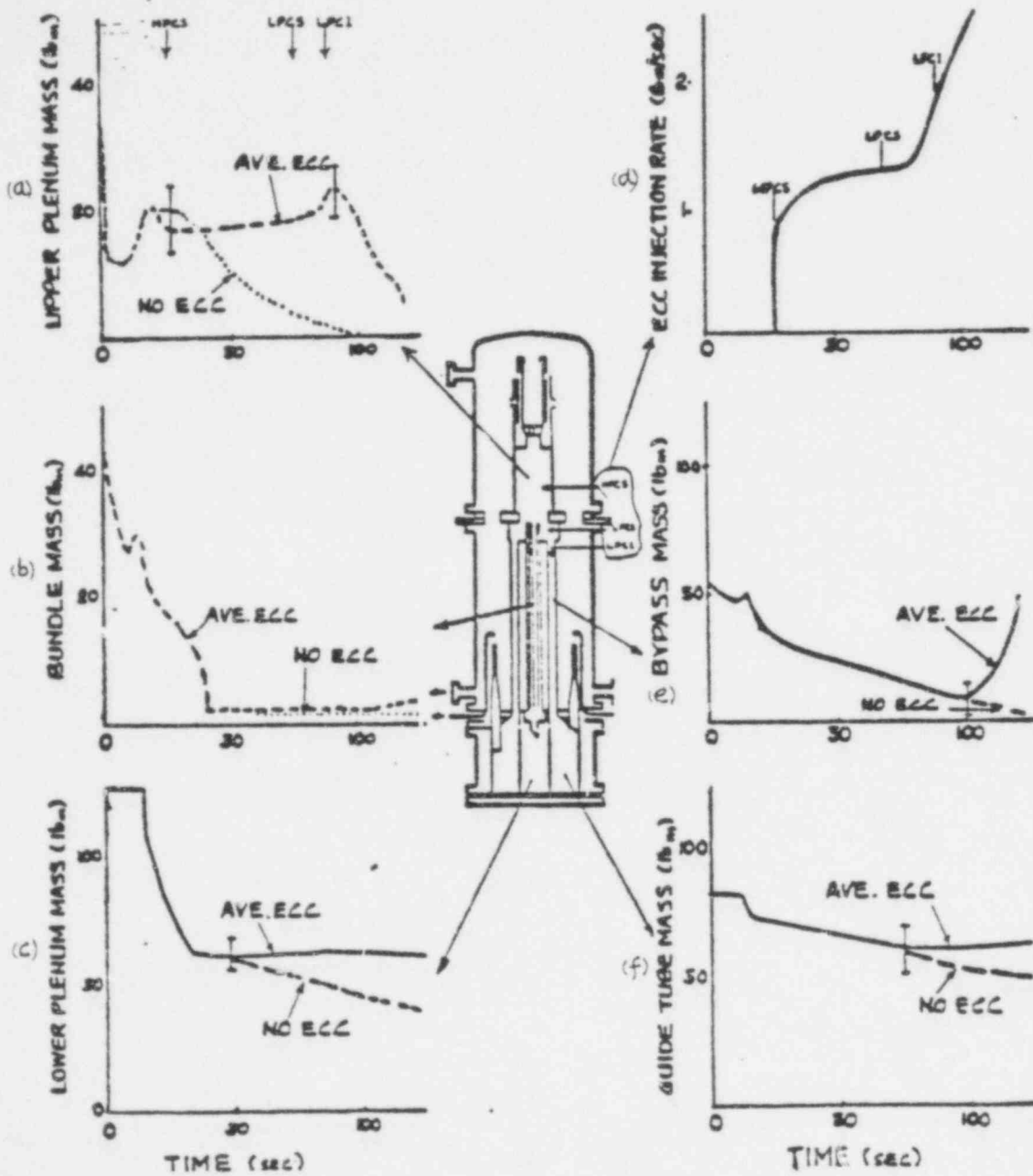


FIGURE 10, COMPARISON OF MASS INVENTORIES BETWEEN TESTS WITH/WITHOUT ECC.

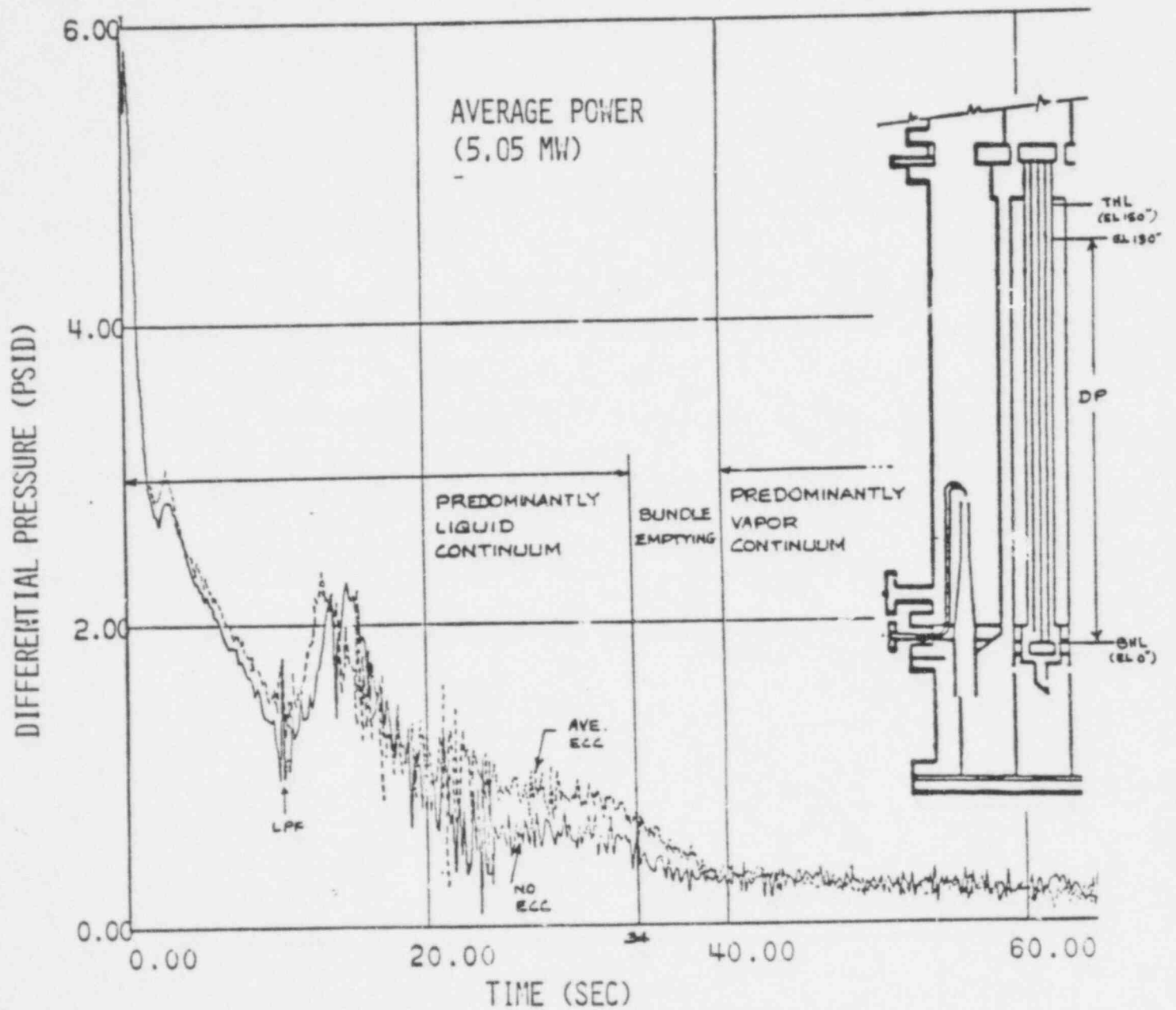


FIGURE 11, COMPARISON OF BUNDLE DIFFERENTIAL PRESSURES BETWEEN TESTS WITH/WITHOUT ECC.

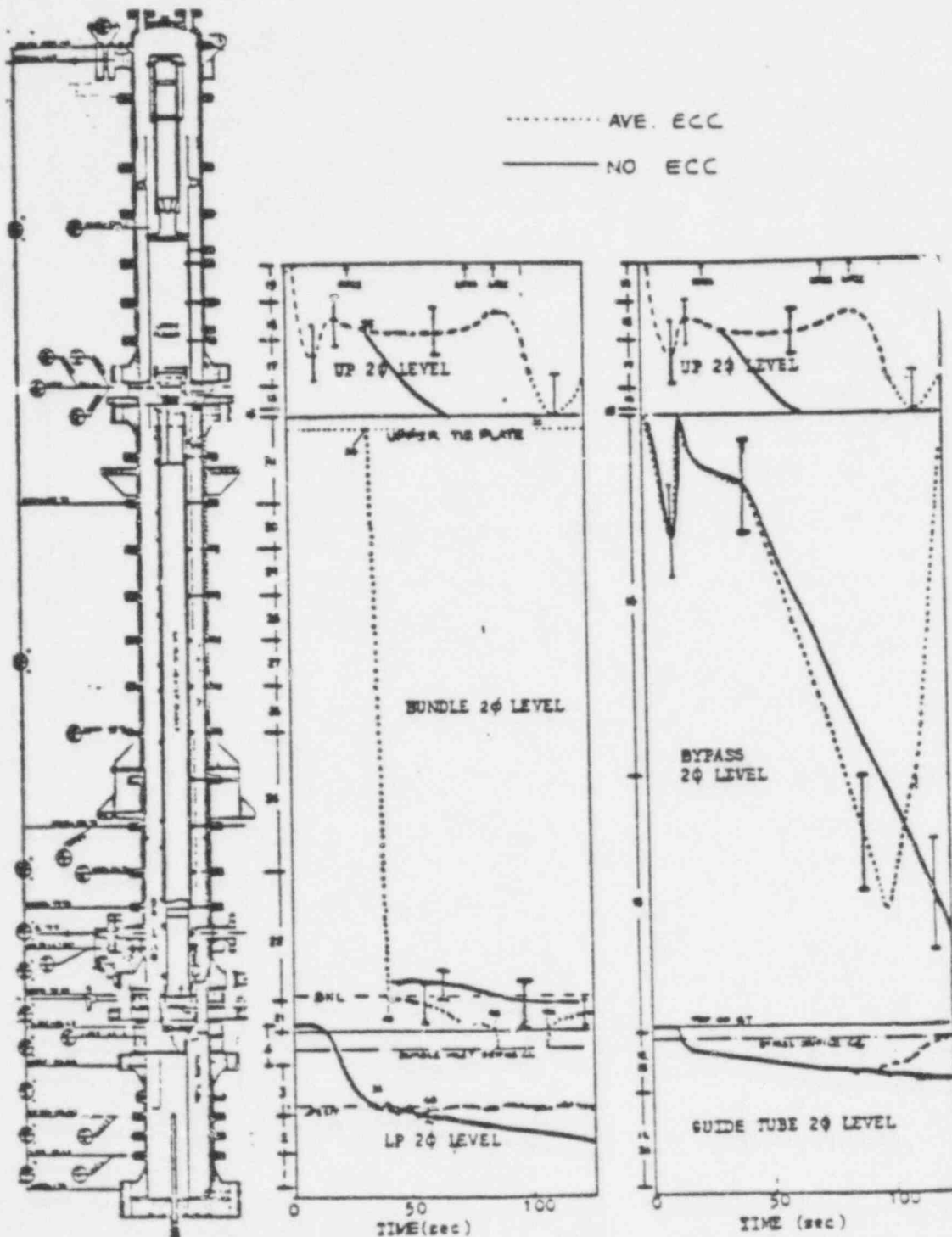
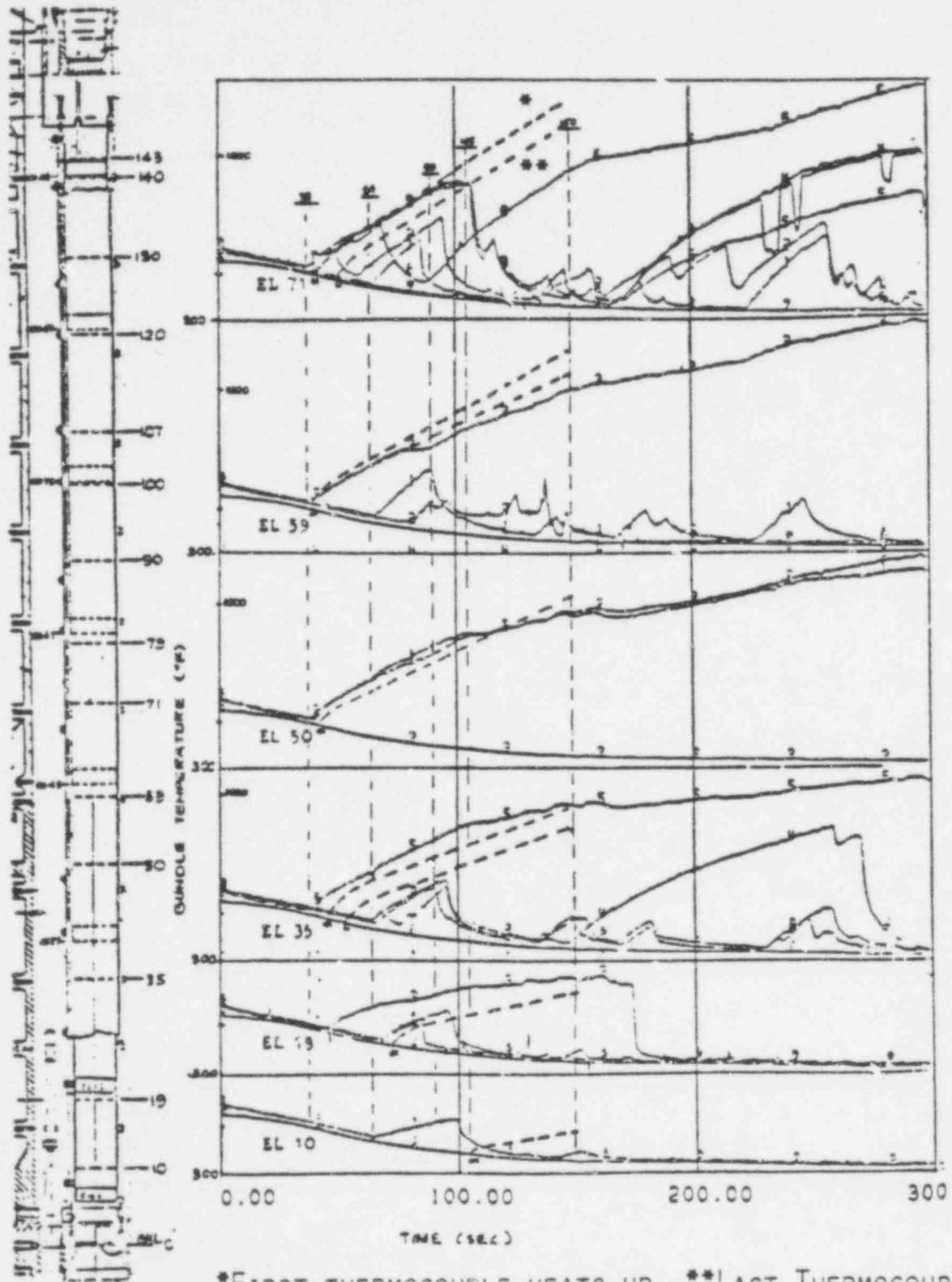


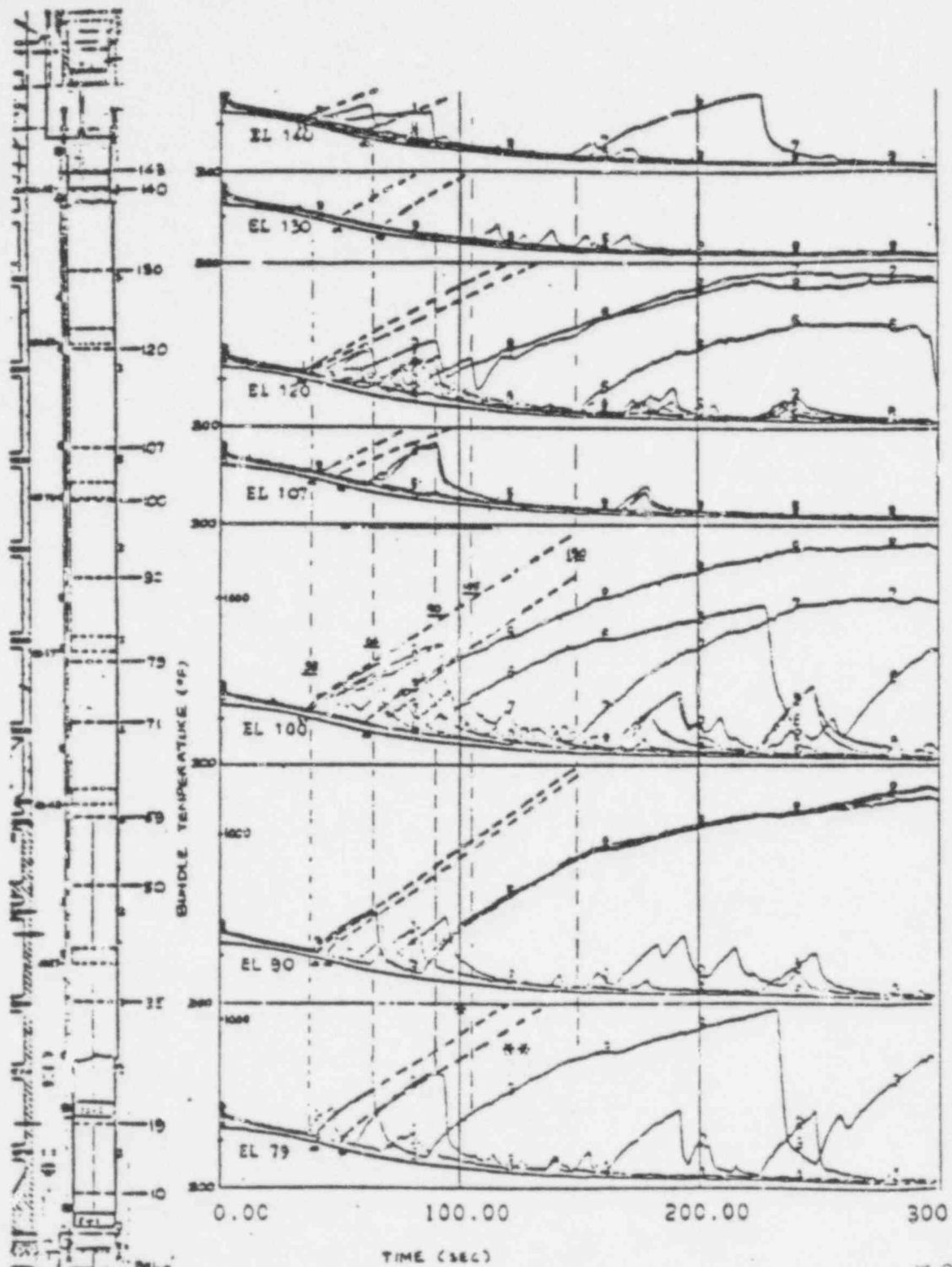
FIGURE 12, COMPARISON OF MIXTURE LEVEL RESPONSES BETWEEN TESTS WITH/WITHOUT ECC

176



*FIRST THERMOCOUPLE HEATS UP, **LAST THERMOCOUPLE HEATS UP

FIGURE 13A, COMPARISON OF TEMPERATURE RESPONSES IN LOWER HALF OF BUNDLE BETWEEN TESTS WITH/WITHOUT ECC.



*FIRST THERMOCOUPLE HEATS UP, **LAST THERMOCOUPLE HEATS UP

FIGURE 13B, COMPARISON OF TEMPERATURE RESPONSES IN UPPER HALF OF BUNDLE BETWEEN TESTS WITH/WITHOUT ECC.

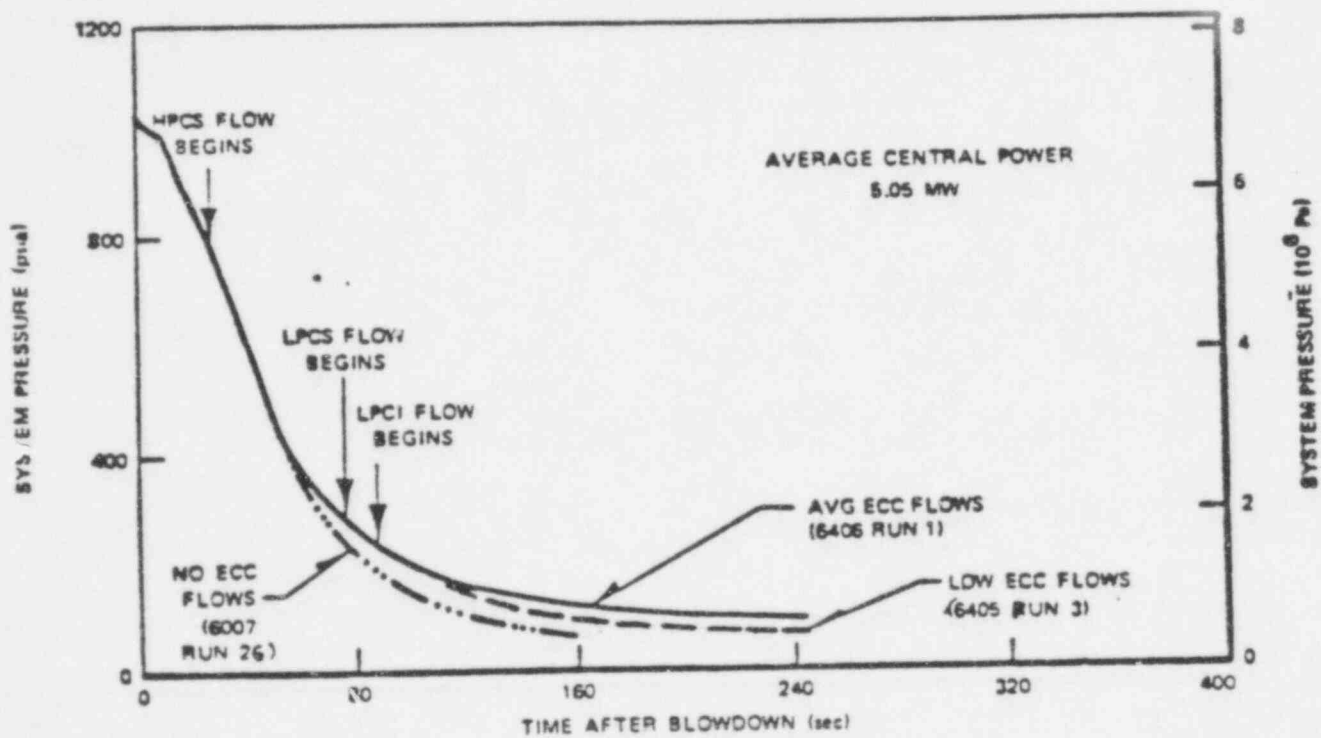


FIGURE 14, COMPARISON OF SYSTEM PRESSURE RESPONSE OF AVERAGE POWER TESTS.

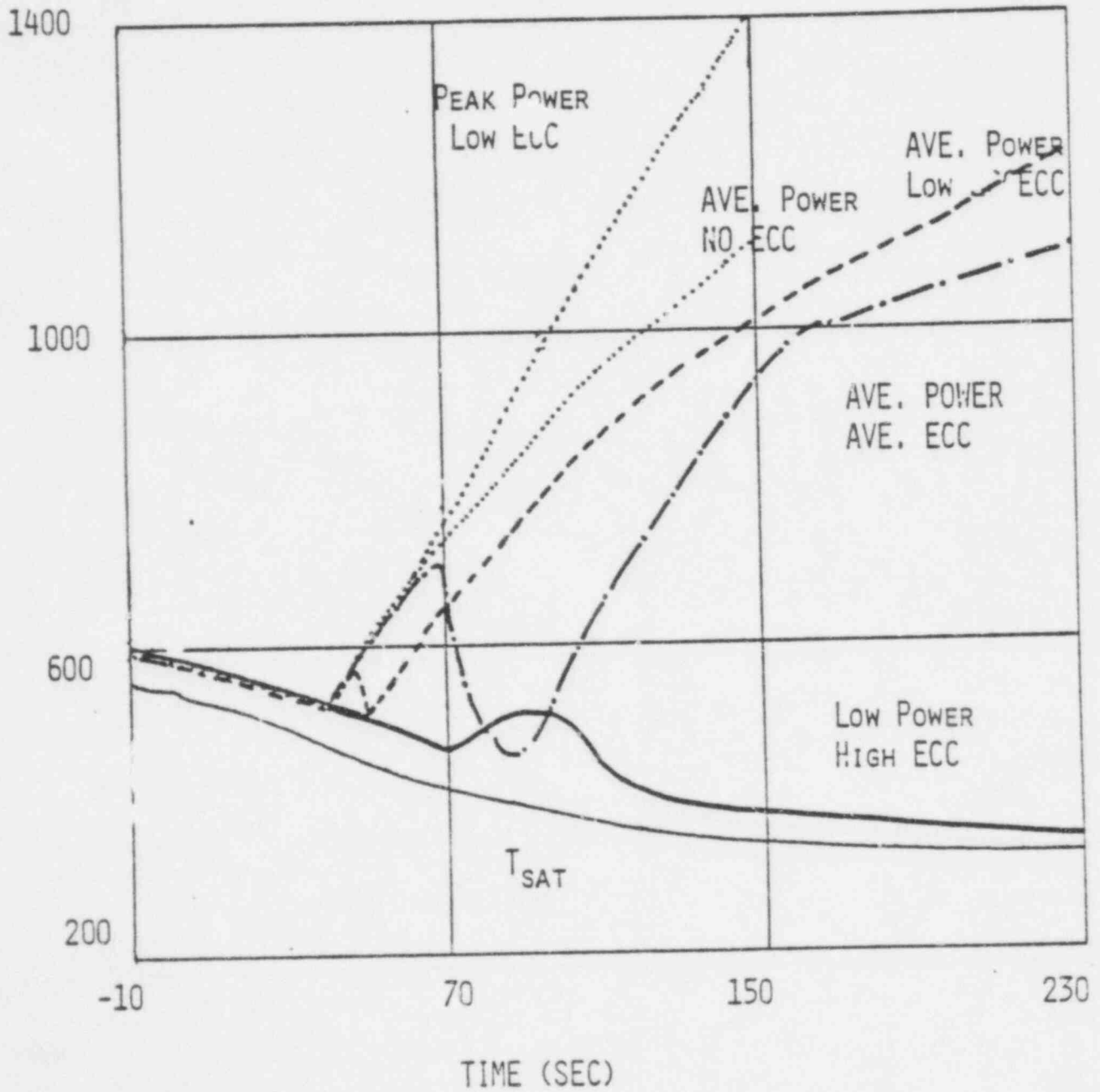
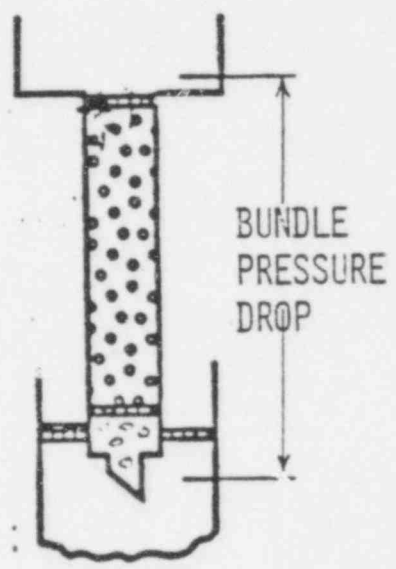
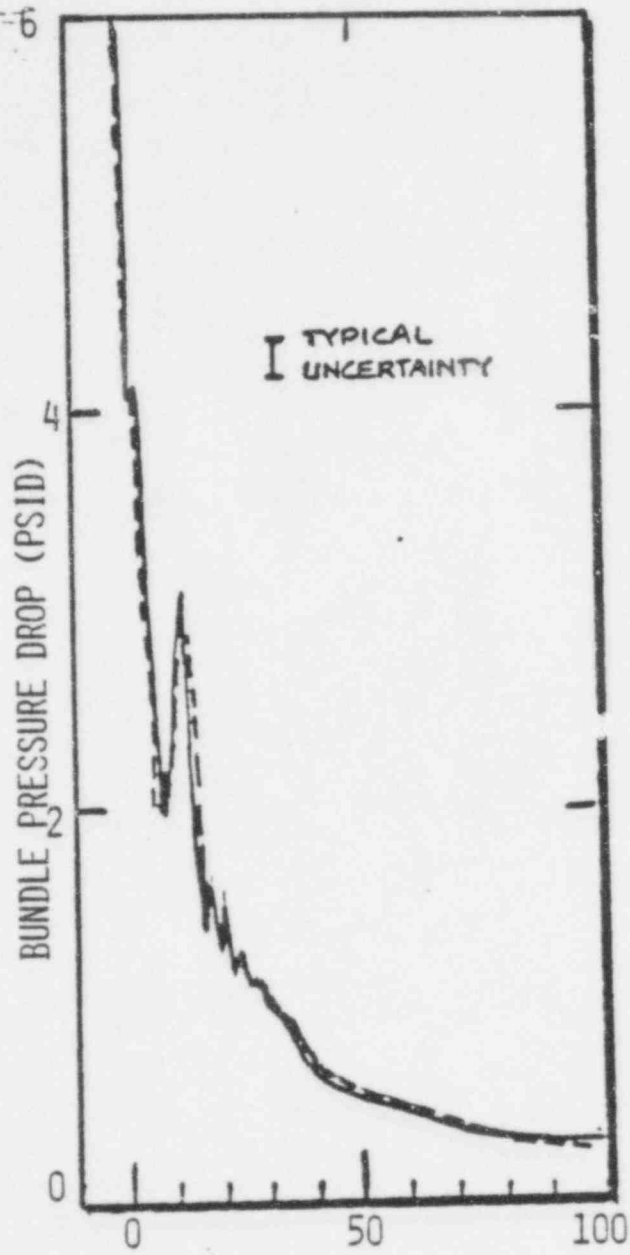


FIGURE 15, COMPARISON OF CLADDING TEMPERATURES AT PEAK-POWER ELEVATION (71")



— AVE. POWER TEST (640E/1)
 - - - PEAK POWER TEST (6414/3)

519 181

FIGURE 16, COMPARISON OF BUNDLE INLET TO OUTLET DIFFERENTIAL PRESSURES.

TLTA BREAK FLOW STUDY

July 1979

INTRODUCTION

Comparisons of the nodal two-phase fluid conditions in the TLTA upstream of the break planes (both suction and drive lines) indicated a substantial difference in density between nominal power tests with and without ECC injection (Figure 1). This Figure shows that the fluid density upstream from the break planes was higher for the test with ECC injection after approximately 60 seconds. Additionally, it is observed that the fluid in the lower plenum and jet pumps follows the same increasing density trend while the test without ECC injection indicates a decreasing density trend throughout the transient. Further interpretation of Figure 1 leads to the preliminary conclusion that the break volumetric flux was lower for the test with ECC injection. It was postulated that this density change was responsible for a corresponding deviation of the break plane quality and ultimately, the total system pressure response.

Through further analyses and supporting calculations, substantiation of the break flow comparisons and the effect on system blowdown response are provided herein. The differences in break mass flow rate and break quality were found to be responsible for deviations in system depressurization response for tests with and without ECC.

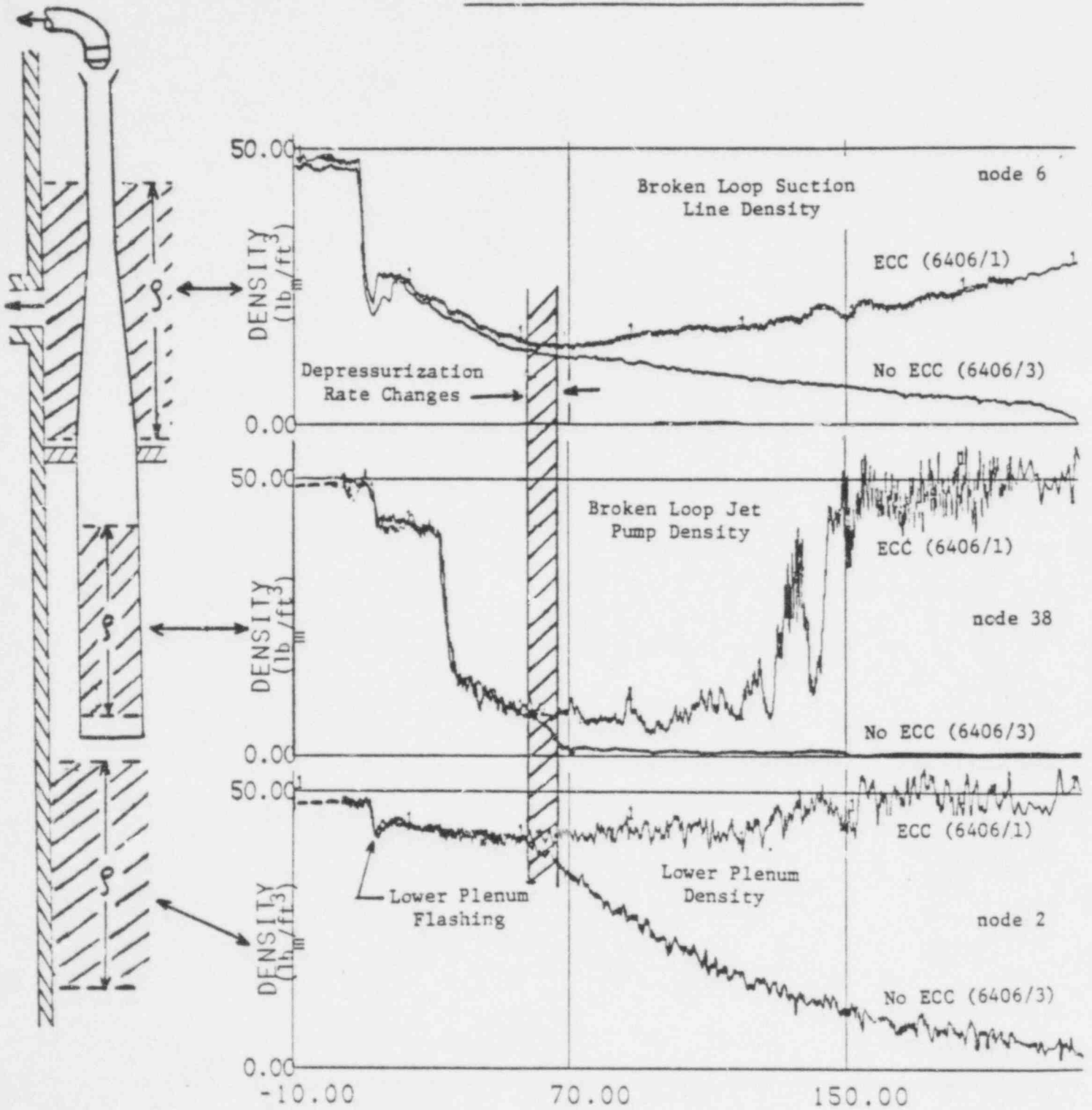
ANALYSIS

Break Flow Data

A total system mass balance was used to derive the mass rate of change from which the break flow rate was determined. Figure 2 shows the break flow comparison between the two tests. It is important to note that beyond approximately 60 seconds,

519 182

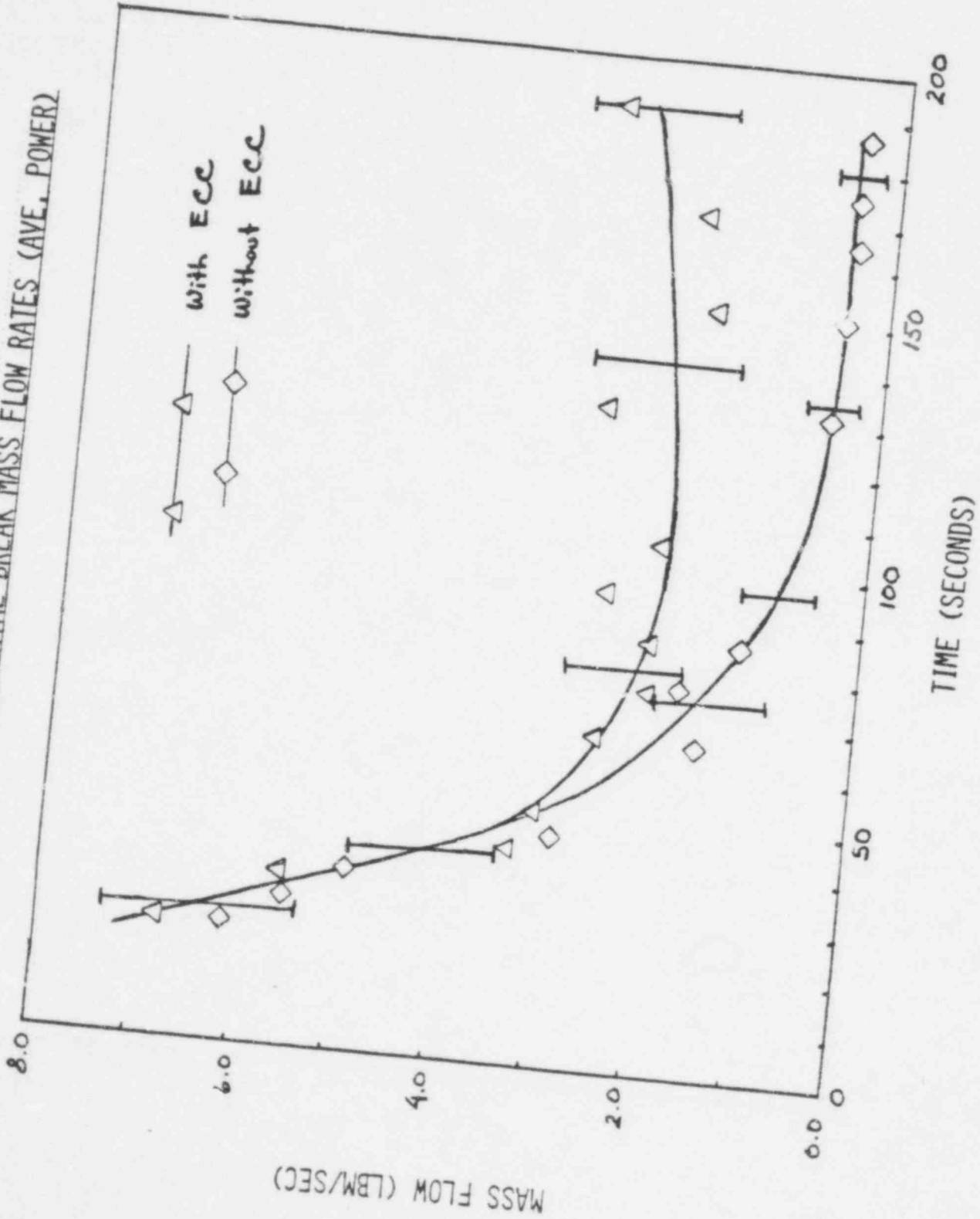
FIGURE 1: BREAK FLOW DENSITY COMPARISON



TIME (SECONDS)

519 183

FIGURE 2: EXPERIMENTAL BREAK MASS FLOW RATES (AVE. POWER)



there is a considerable difference in the break flow rates and that the test with ECC injection indicates substantially higher break flows which is consistent with the higher liquid density shown in Figure 1. The uncertainty margin exhibited in this Figure represents the experimental uncertainty of the data. The deviance between the two curves gives further indication of a lower break quality and volumetric flux for the test with ECC injection.

Additional experimental substantiation of these differences in break quality is obtained from the comparison of the density measurements taken from the annulus region upstream of the suction line break (Figure 1). As a lower bounding approximation, this density can be separated into a collapsed liquid level in the nodal region. For the test with ECC injection, the collapsed mixture level partially covers the break exit area throughout the transient while the test without ECC injection indicates an almost non-existent collapsed mixture level. Such a comparison demonstrates that there is little or no potential for liquid entrainment out the break for the test without ECC injection.

Derivation of Break Flow Quality

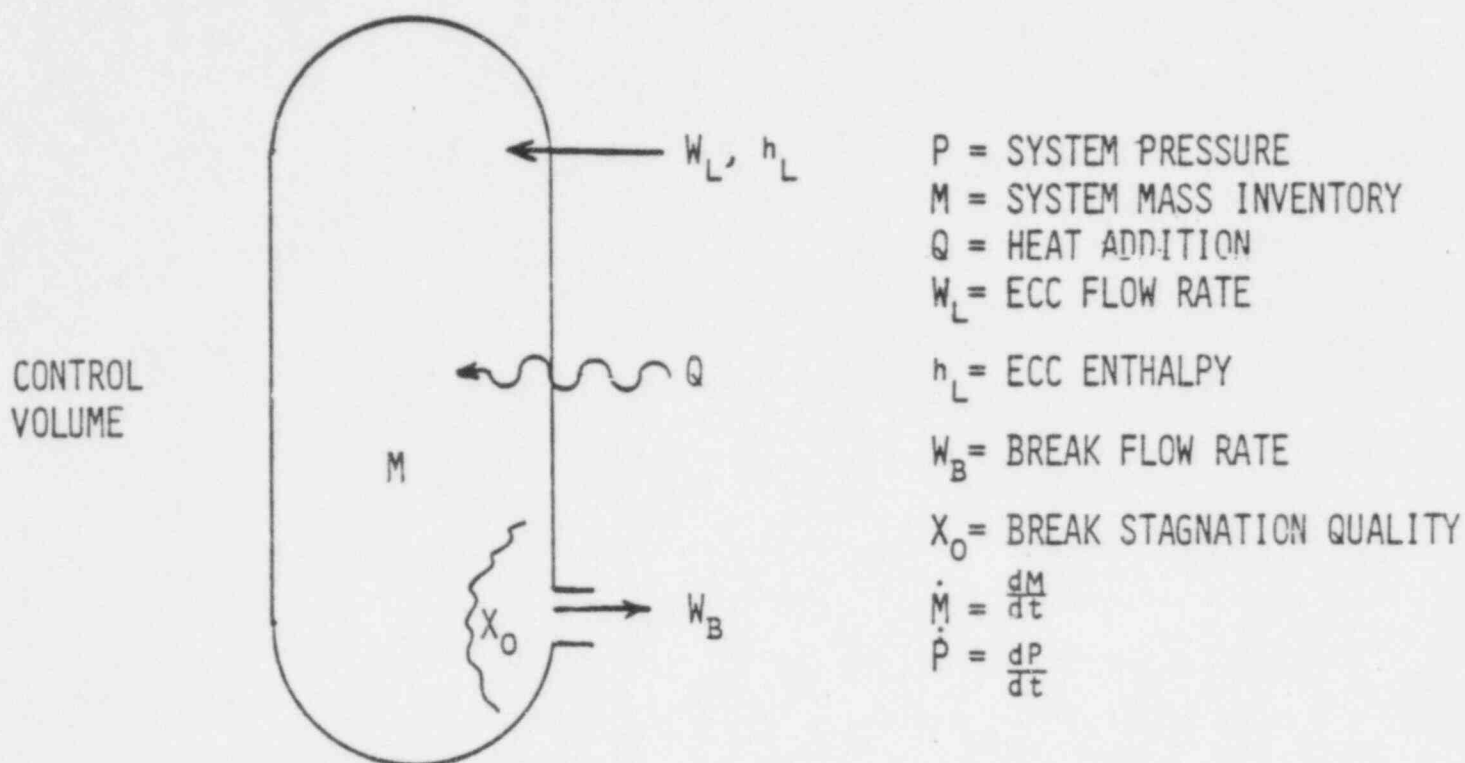
By utilization of the continuity and energy balances in conjunction with a simple control volume, the rate of system pressure change may be determined. The technique for determining this value is outlined in Figure 3.

As a first approximation, the total heat transfer to the system can be estimated as the sum of the bundle input power and stored heat from the vessel walls. Previous analyses (Reference 1) were used to approximate the stored heat contribution. The values of Q and X_0 were then varied over a reasonable range to optimize the calculation of system pressure response.

The derived break flow quality which best matched the depressurization data is shown in Figure 4 for the tests with and without ECC. The uncertainty band indicates the variation in break quality for a range of $\pm 25\%$ of the assumed heat input, Q .

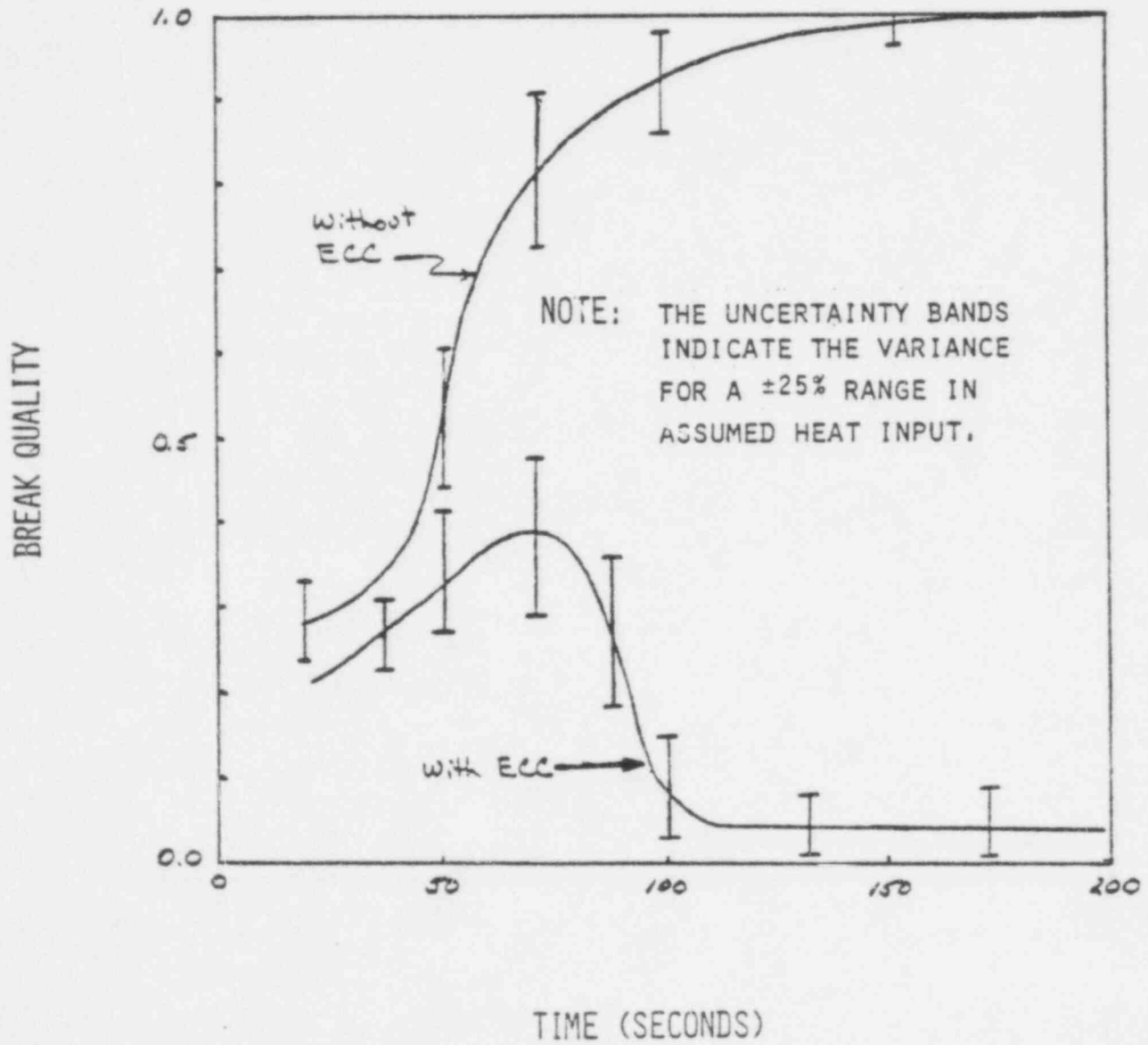
This calculation clearly indicates a substantial difference in break quality between the two tests. The lower quality observed in the test with ECC injection indicates a decreased volumetric flux exiting through the break, thus diminishing

FIGURE 3: COMPUTATIONAL SCHEMATIC



1. MASS BALANCE: $W_B = W_L - \dot{M}$
2. ENERGY BALANCE: $\dot{P} = f_N (P, M, \dot{M}, X_O, W_L, h_L)$
3. MEASURED CONDITIONS: $M, \dot{M}, P, \dot{P}, W_L, h_L$
4. REMAINING FACTORS: X_O, Q
5. BASED ON BUNDLE POWER INPUT AND STORED HEAT APPROXIMATION, Q CAN BE BOUNDED
6. VARY X_O UNTIL PRESSURE DECAY MATCHED

FIGURE 4: COMPARISON OF COMPUTED BREAK QUALITY



the rate of depressurization. The results of this calculation are consistent with both the postulated and experimental justifications proposed to determine the cause of the depressurization rate discrepancy between the two tests.

CONCLUSIONS

By performing a mass balance on the TLTA system, it has been shown that the break flow rate for the test with ECC injection was clearly higher during the ECC period of the transient due to liquid accumulation in the vicinity of the break.

An independent mass and energy balance analysis on a simple representation of the TLTA further substantiates the increased flow observed for the test with ECC injection. In addition, the break quality is shown to be substantially lower for the test with ECC beyond about 50 seconds.

The combined effect of higher break flow rate, lower break quality, and corresponding lower volumetric break flow are responsible for the differences in depressurization rates between the tests with and without ECC.

REFERENCES

1. GEAP-23592, EWR Blowdown/Emergency Core Cooling Program Preliminary Facility Description Report for the BD/ECC-LA Test Phase, W. J. Letzring, December 1977.

ATTACHMENT 3

EVALUATION OF TLTA SEPARATOR

PRESSURE DROP

July 1979

INTRODUCTION

Preliminary analysis of the steam separator pressure drop, shown in Figure 1, qualitatively indicated that the net core region steam flow rate was lower for the average power test with ECC injection when compared to an identical test without ECC cooling. This lower flow was postulated to result from the effects of condensation caused by the subcooled ECC injection. Further data analysis on the separator have been performed to substantiate the mass flow rate trends defined previously and are discussed herein.

A mass and energy balance has been performed on the TLTA by utilization of the data and a simple blowdown analysis (see the TLTA Break Flow Study for discussion). By initialization of the calculation with the experimental data, and further utilizing the measured mass balance (i.e., break flow), the heat addition to the fluid and the break quality were varied until the measured system pressure response was matched. As a result, the net system vapor generation rate has also been determined. Conclusions from this analysis, and from an independent flow analysis of the separator pressure drop, are utilized to demonstrate that the differences in net vapor flow from the core region support the earlier preliminary conclusions.

ANALYSIS

The total pressure drop across the separator is composed of the sum of the irreversible losses and the elevation head. This may be expressed as:

$$\Delta P_{\text{Total}} = \Delta P_{\substack{\text{irreversible} \\ \text{losses}}} + P_{\substack{\text{elevation} \\ \text{head}}}$$

DIFFERENTIAL PRESSURE (PSID)

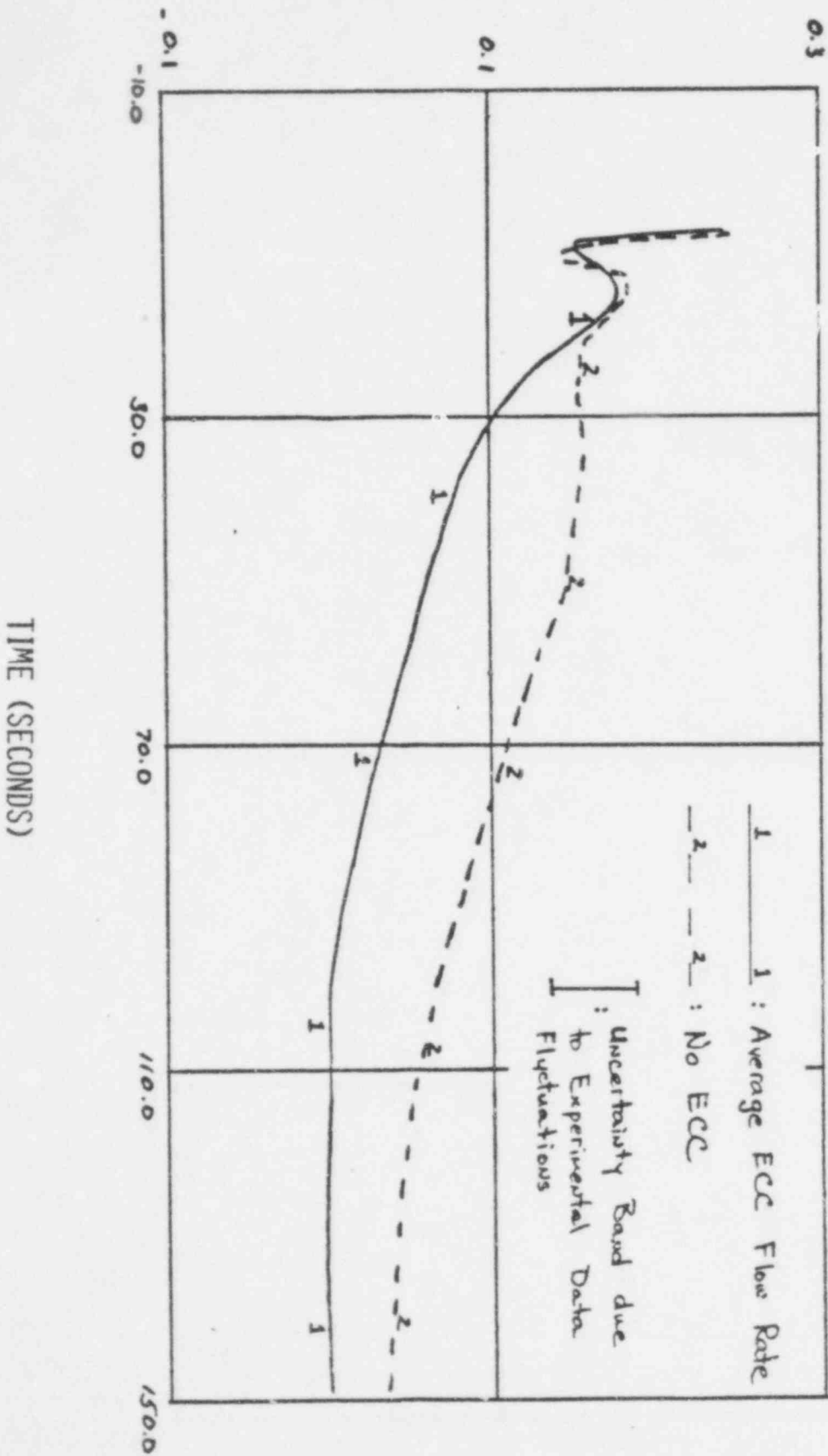


FIGURE 1: STEAM SEPARATOR PRESSURE DROP (AVE. POWER)

519 190

Assuming zero liquid entrainment in the steam flow through the separator (examination of this assumption is presented below) yields:

$$\Delta P_{\text{irreversible losses}} = K \frac{\dot{M}^2}{2g_c \rho}$$

$$\Delta P_{\text{elevation}} = \rho h \frac{g}{g_c}$$

The irreversible loss coefficient, K , can be obtained from the flow geometry of the separator as shown in Figure 2. The flow path has been idealized as a series of abrupt flow area changes which contribute to the form losses (i.e., entrance, exit, area restrictions) in addition to other frictional losses of the form $f \frac{L}{D}$. Based on the resistance shown and assuming fully developed turbulent flow, the total loss coefficient was calculated to be 5.03. Results from similar full sized separator tests (Ref. 1 and 2) verify that the calculated loss coefficient was found to be within 10% of the experimental value.

Thus, the irreversible losses may be expressed as:

$$\Delta P_{\text{irreversible losses}} = 5.03 \frac{\dot{M}^2}{2g_c \rho}$$

Utilizing the calculated net system vaporization rate and the above equation, a reasonable estimate of the irreversible pressure losses may be obtained. The total predicted separator pressure drop is then determined by summing the irreversible losses with the elevation head.

Figure 3 shows the comparison between the calculated and experimental pressure losses based on the above assumptions. The calculated ΔP is seen to closely follow the same trends and magnitudes as the data. These comparisons confirm that the measured pressure drop across the separator provides reasonable approximation of the mass flow rate through the separator.

ENTRAINMENT SENSITIVITY STUDY

The sensitivity of the separator pressure drop to liquid entrainment was investigated in order to assess the assumption of zero liquid entrainment. The

FIGURE 2: ILTA STEAM SEPARATOR

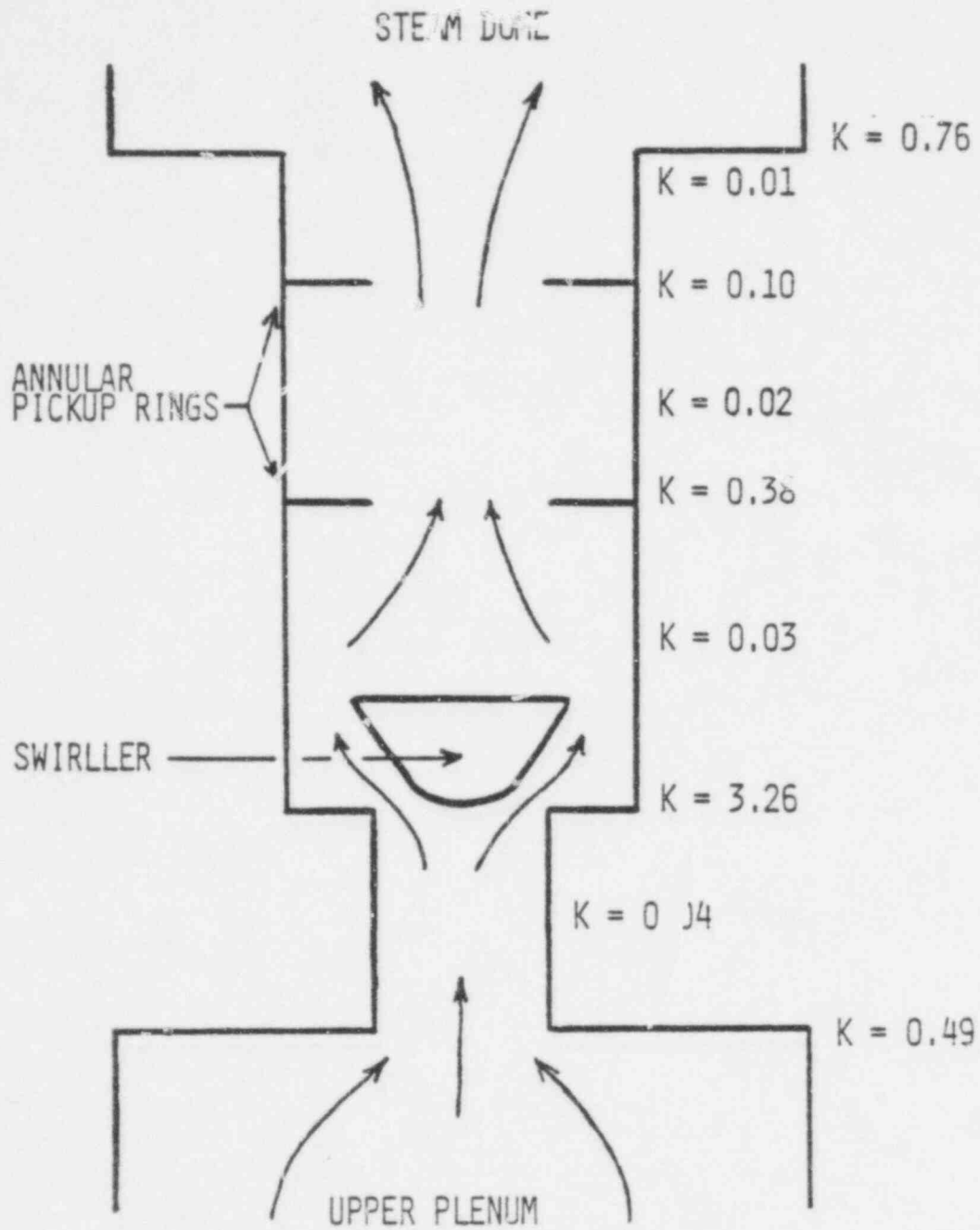
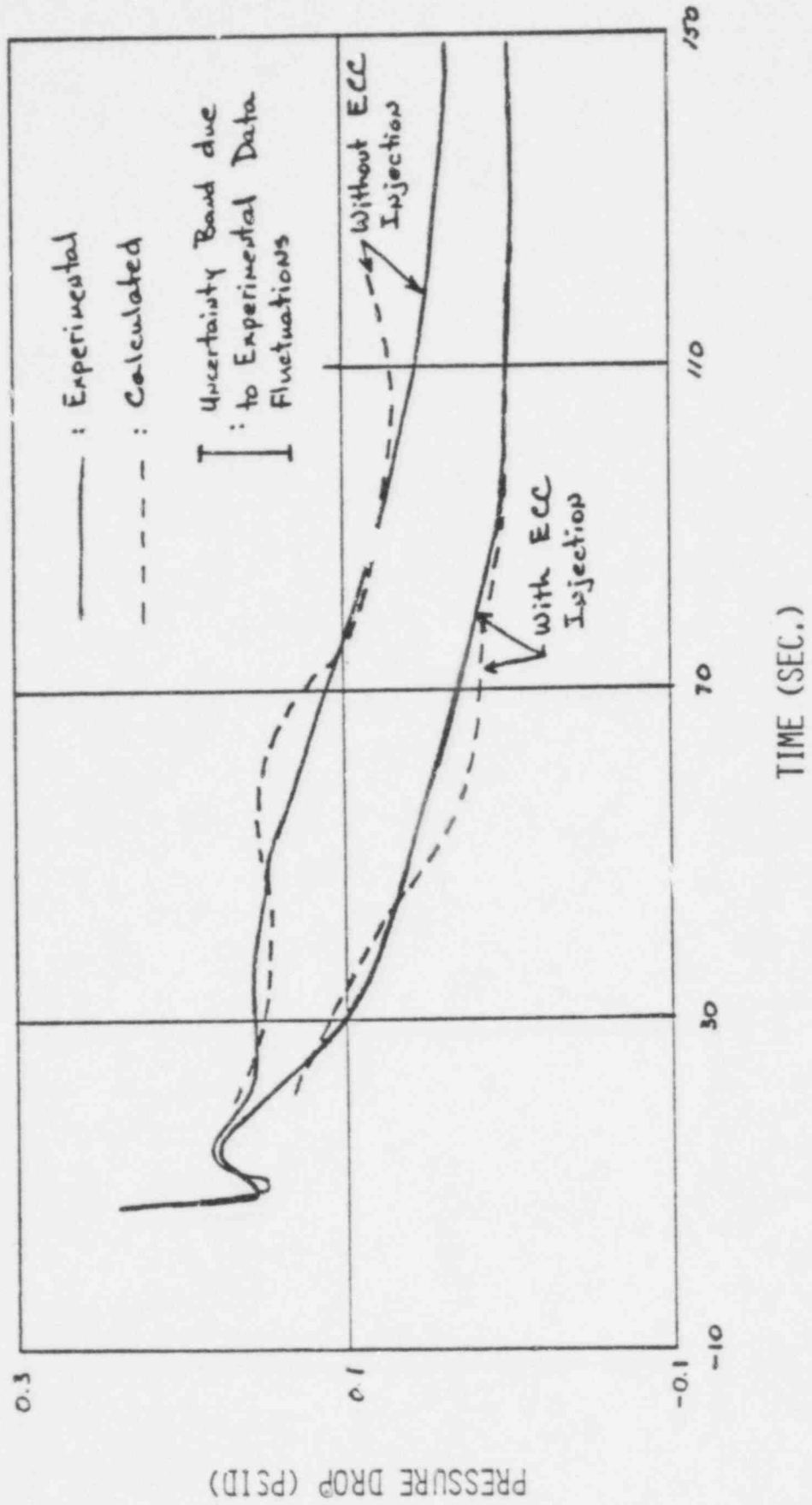


FIGURE 3: COMPARISON OF CALCULATED AND EXPERIMENTAL
STEAM SEPARATOR PRESSURE DROPS



results (presented in Figures 4 and 5) indicate that the maximum mass flow rate and irreversible pressure drop occur with zero entrainment.

The irreversible losses shown in Figure 4 were determined from subtraction of the implied elevation head from the maximum experimental pressure drop. It is seen from Figure 4 that the total separator pressure drop would equal the elevation head at a void fraction of 0.96. Thus, this corresponds to the maximum entrainment which could flow out of the separator for the pressure condition measured.

Calculations of the separator mass flow rate based on the implied irreversible pressure drop are shown in Figure 5. It is important to note that the maximum flow rate would occur with zero entrainment. The comparison of separator pressure drop in Figure 1 suggests that the mass flow rate through the separator was lower for the test with ECC injection. The results shown in Figure 5 indicate that the separator flow rate was even lower for the ECC injection case (most likely to have entrainment) than that determined by assuming zero entrainment (Figure 3). Therefore, the possible presence of liquid entrainment does not change the conclusion that less vapor flowed through the separator for the test with ECC than for the test without ECC.

CONCLUSION

The above study further substantiates that the measured pressure drop across the steam separator in the TLTA provides an adequate indication that the flow rate through the separator for the test with ECC injection was lower than for the test without ECC.

REFERENCES

1. Wolf, S., and Moen, R. H., "Advances in Steam-Water Separators for Boiling Water Reactors", ASME Paper No. 73-WA/Pwr-4, 1973.
2. Kudirka, A. A., and Swan, C. L., "Performance of Production Steam Separators for the 1967 Product Line", December 1969.

FIGURE 4: EFFECT OF ENTRAINMENT ON
SEPARATOR PRESSURE DROP

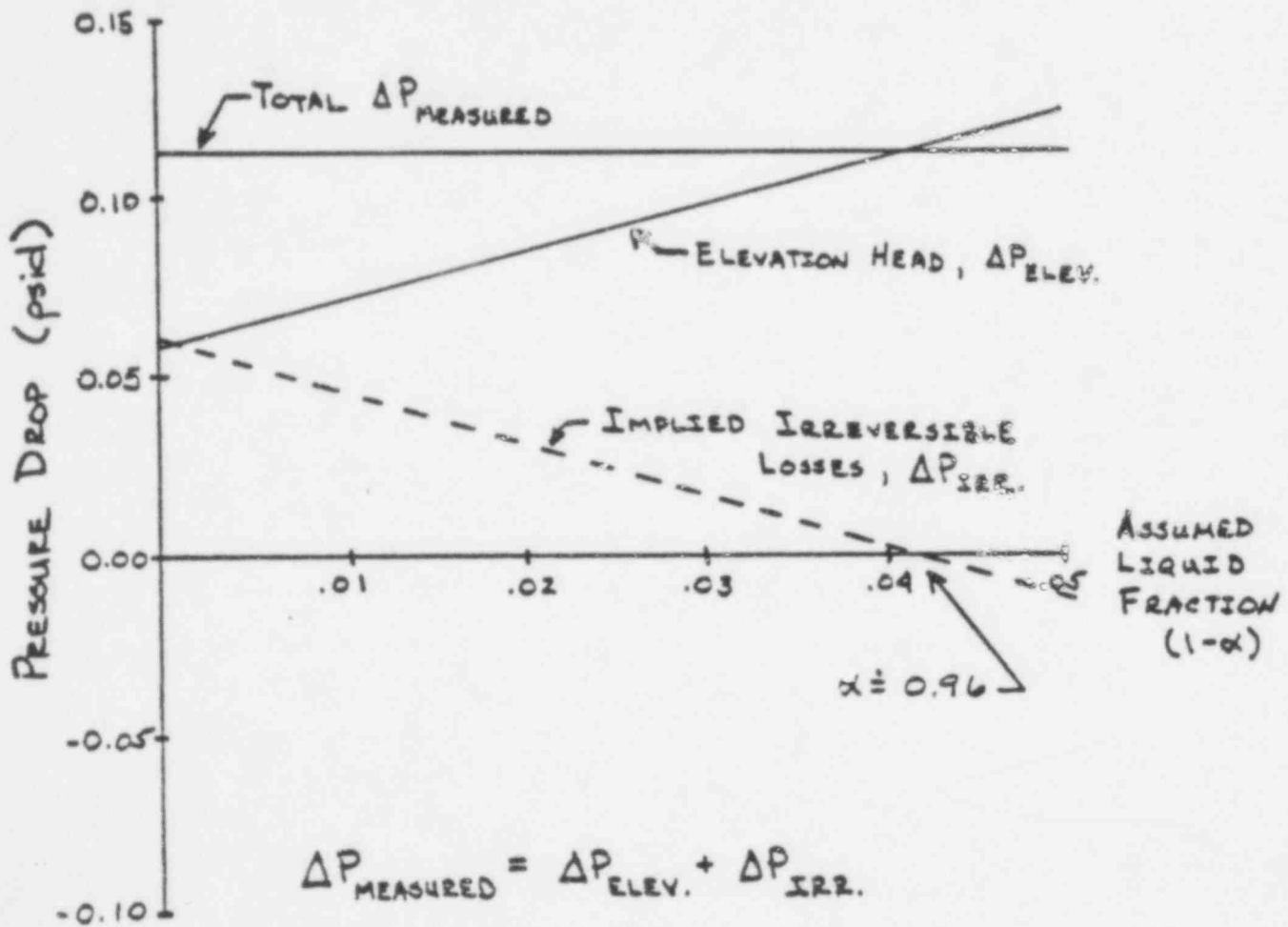
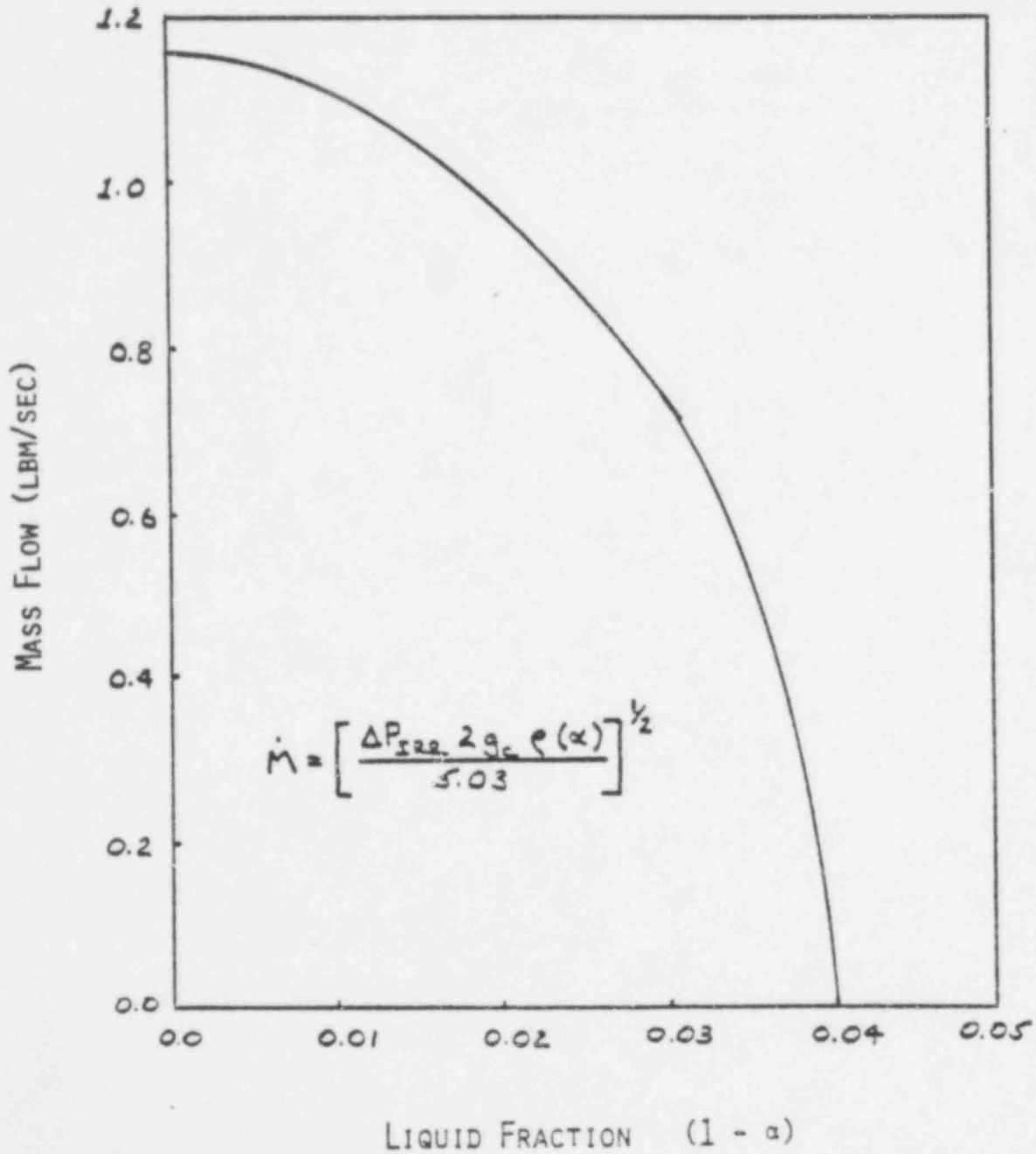


FIGURE 5: EFFECT OF ENTRAINMENT ON
MASS FLOW RATE



ATTACHMENT 4

TLTA SCALING BASIS

BACKGROUND

In the TLTA the core region is sized to accommodate one full-size test bundle and this condition formed the primary basis for the scaling of the remainder of the test apparatus. Thus, in the context of the 624 nuclear fuel bundles in the reference BWR/6-218, the scaling objective was to scale the volume, mass, energy and flow rates on a 1 to 624 ratio compared to the reactor. One-to-one scaling of linear dimensions of the different regions and internal components, except in the case of the bundle, was found impractical. The consequences of the above compromise is the subject of this discussion.

A detailed description of the TLTA and a thorough discussion of the scaling basis and compromises are presented in Reference 1. However, for completeness some of the discussion from Reference 1 is repeated herein.

The original TLTA (denoted TLTA-1) was built several years ago² and was originally scaled to a BWR/4-218 plant. The test apparatus has undergone a number of modifications and scaling changes. The present basis is a BWR/6 and the test facility is denoted TLTA-5.

JET PUMPS

The scaling basis for the jet pumps is to preserve an equivalent mass flux between the BWR pumps and the test pumps with the scaled mass flow of 1/62.4 of the reactor jet pumps through the test jet pumps. The above scaling factor of 62.4 is a consequence of 624 fuel bundles and 10 pumps in each recirculation loop of the test apparatus. This scaling factor would have required a 1/62.6 or 1/7.9 scaling of the linear dimensions of height and diameter. The jet pumps used in the previous BDHT program² were designed on a 1/7.5 linear scaling basis

to represent a BWR/4 and resulted in a pump mass flux and velocity of only 90% of that in the reference BWR/6 pumps. Since the jet pumps in the TLTA have been scaled down in height as well as in diameter, the initial momentum in the TLTA jet pumps are estimated to be about 1/10th of that in the reference BWR/6. Consequently, the flow in the broken loop jet pump of the TLTA is expected to reverse much more rapidly and earlier, and to allow the core flow to drop quicker than for the reference BWR/6 under similar circumstances. Evaluation model prediction comparison in Figure 1 is indicative of this scaling compromise.

DOWNCOMER

The TLTA downcomer cross-sectional area is not scaled with respect to the reference reactor. On the other hand, the downcomer cross-sectional area is made sufficiently large to locate the jet pumps. This scaling choice results in a larger downcomer area than a properly scaled value $(\frac{1}{(624)^{1/3}})^2$ of the reactor downcomer area and will result in too low a fluid velocity in the TLTA. In order to maintain the correct scaled fluid inventory in the downcomer, the initial level is lower in the TLTA than for the BWR.

The initial water level in the TLTA annulus and the jet pump height are based on the scaling of the corresponding reactor volumes, and this results in a much lower elevation head above the TLTA jet pump exit than the corresponding value for the reference BWR. The elevation head in the bundle, however, is closely matched between the TLTA and the reference BWR since the heater bundle is full length. Under these circumstances, it is expected that a larger fraction of the intact recirculation loop flow into the lower plenum will be diverted to the broken loop jet pump path of the TLTA since the TLTA reverse-flow path has a lower elevation head. This would result in a lower core flow in the TLTA up to the time of the jet pump suction uncover, as shown in Figure 2. This reduced core flow in the TLTA, as compared to the reactor core flow would be expected to lead to a higher heatup, (i.e., yield higher cladding temperatures) in the TLTA heater bundle. However, calculations of the peak heater rod temperature for the core-average bundle power indicate that the rods remain well cooled throughout the coastdown period and closely approximate that of the reference fuel bundle. This has later been confirmed by the actual reference power tests (Test 6406/Run 1). The short jet pumps are not expected to introduce any significant compromise for the average power bundle during the flow coastdown period as

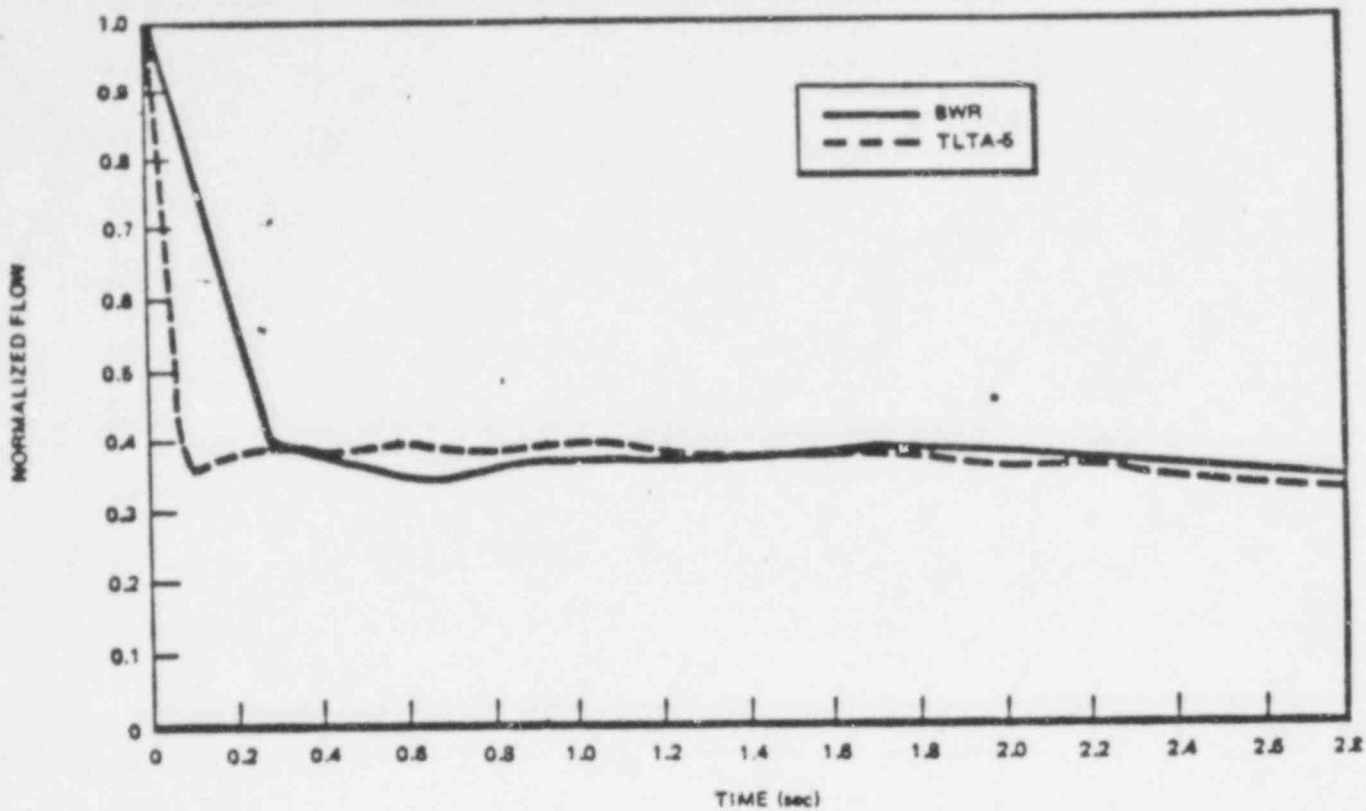


FIGURE 1
Effect of Jet Pump Length on Early Core Inlet Flow Coastdown - LAMB Predictions

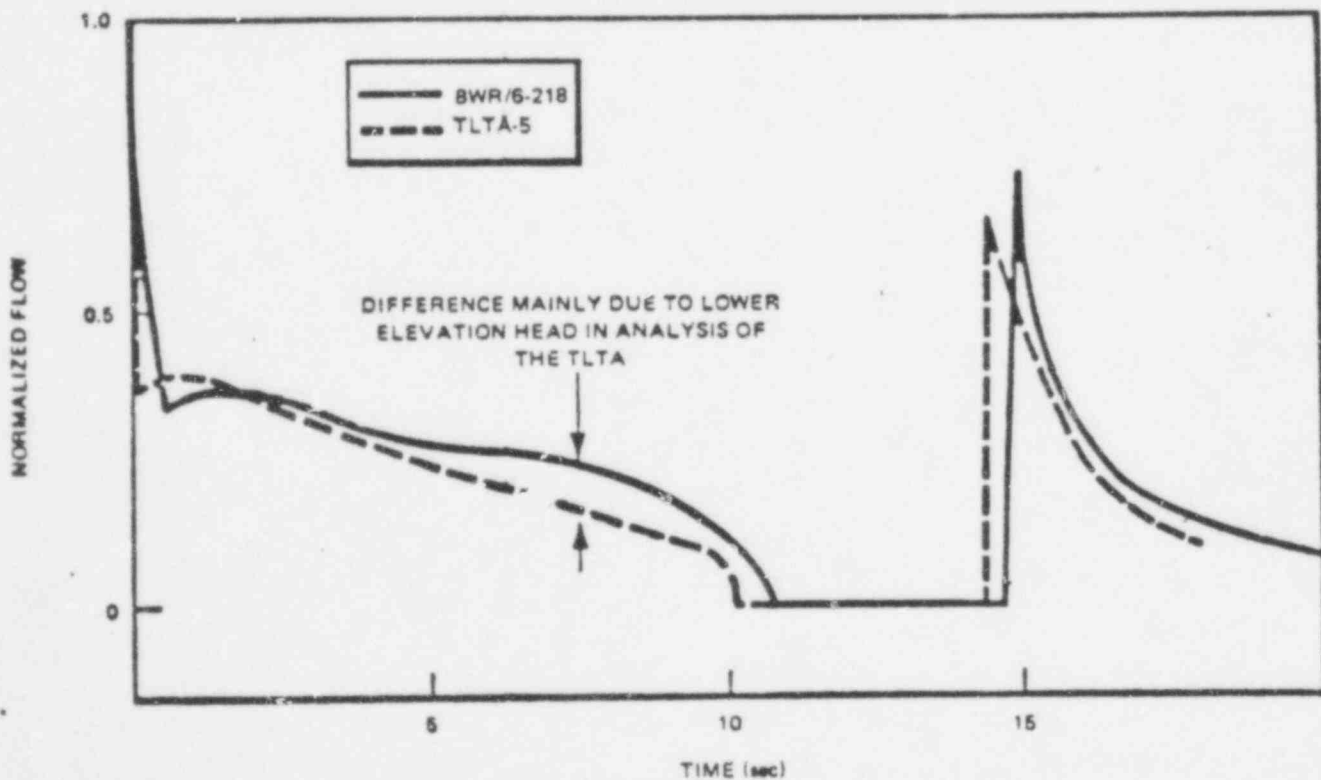


FIGURE 2
Effect of Lower Downcomer Elevation Head on Core Flow Coastdown

measured by the peak clad temperature. On the other hand, the early rapid core flow coastdown, that results from the unscaled inertia, is expected to result in an atypical core heatup response for the peak power bundle. This is also confirmed by the peak power test results (Test 6414).

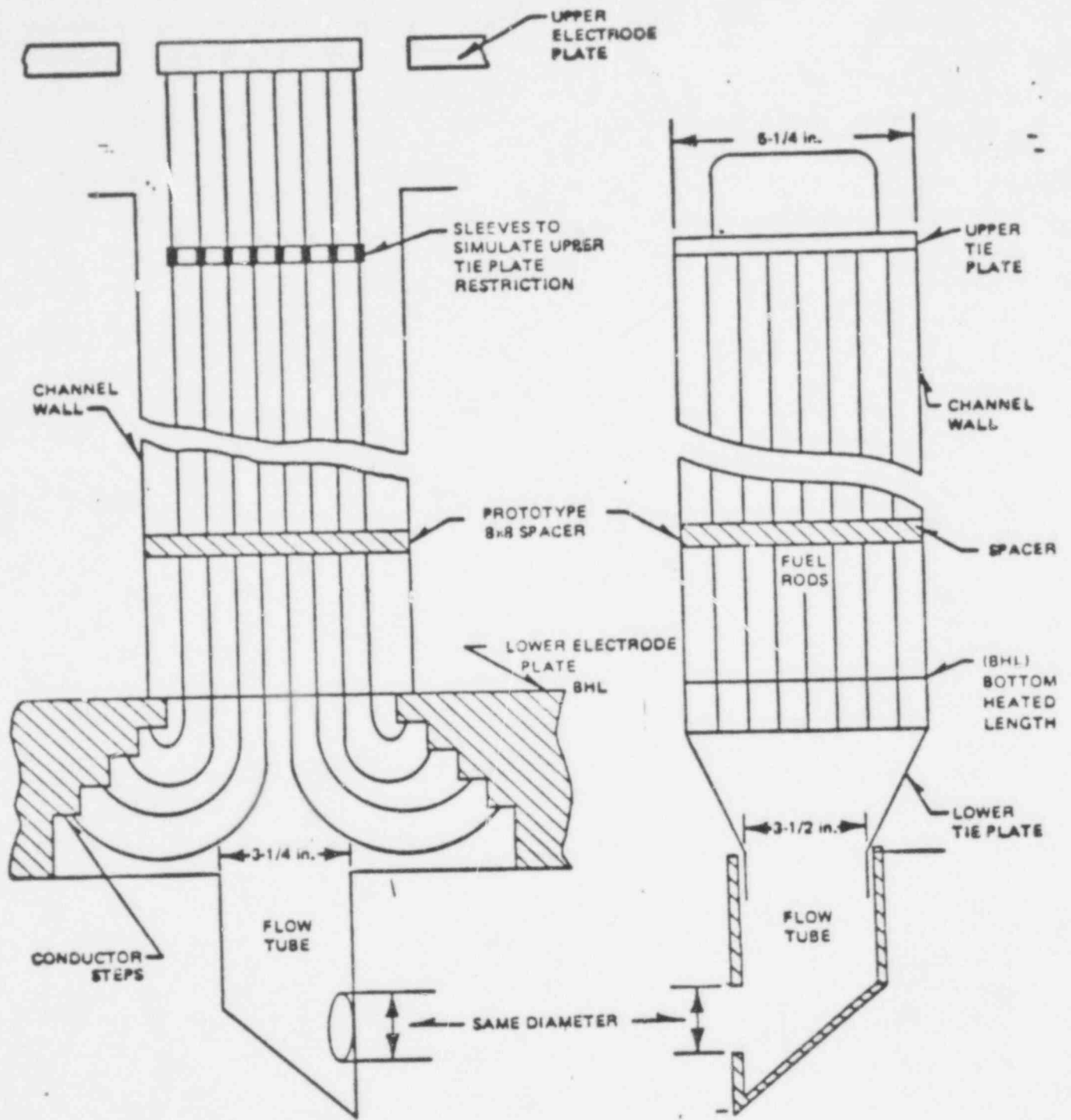
SEPARATOR

The TLTA separator is designed so that the mass flux rate in it matches the scaled reactor value. On this basis the separator pressure drop, mainly due to the expansion and contraction losses and the entrance swirler losses, will be closely matched with that of the reference BWR.

The fluid inertia in the TLTA separator is low by a factor of about 4 as compared to that of the reference BWR because of the separator's shorter length². This would tend to allow the flow through the separator and, hence, through the core to decrease faster than in the reference BWR. However, as shown in Reference 2, the core-flow during the coastdown will not be affected as much as in the case of the short jet pumps.

BUNDLE LOCAL RESTRICTIONS

The test bundle geometry has a one-to-one similarity with the reference reactor bundle at the inlet, exit, and along most of its length. However, at the entrance to the test bundle, the flow path differs from that of the reference BWR, as shown in Figure 3. There are also minor variations between the two bundles at the exit. These geometrical differences could contribute to at most an additional 10% in the pressure drop across the inlet region of the test bundle assembly as compared to a reactor assembly, due primarily to the sudden expansion and contraction in the lower electrode plate flow path, as shown in Figure 3. A large variation in the core inlet orifice was empirically shown to have a negligible effect on the core-flow transient during the blowdown phase of a DBA². Under the ECC mode these small deviations in the local pressure drops are of little significance since the CCFL characteristics at the minimum flow path areas, viz., the bundle inlet and outlet restrictions, dominate the core-flow transient, and the test bundle has CCFL characteristic essentially the same as the reference BWR.



(a) TLTA HEATER BUNDLE ASSEMBLY

(b) BWR CORE INLET/BUNDLE ASSEMBLY

FIGURE 3

Comparison of BWR Fuel Bundle and TLTA Heater Bundle Assemblies

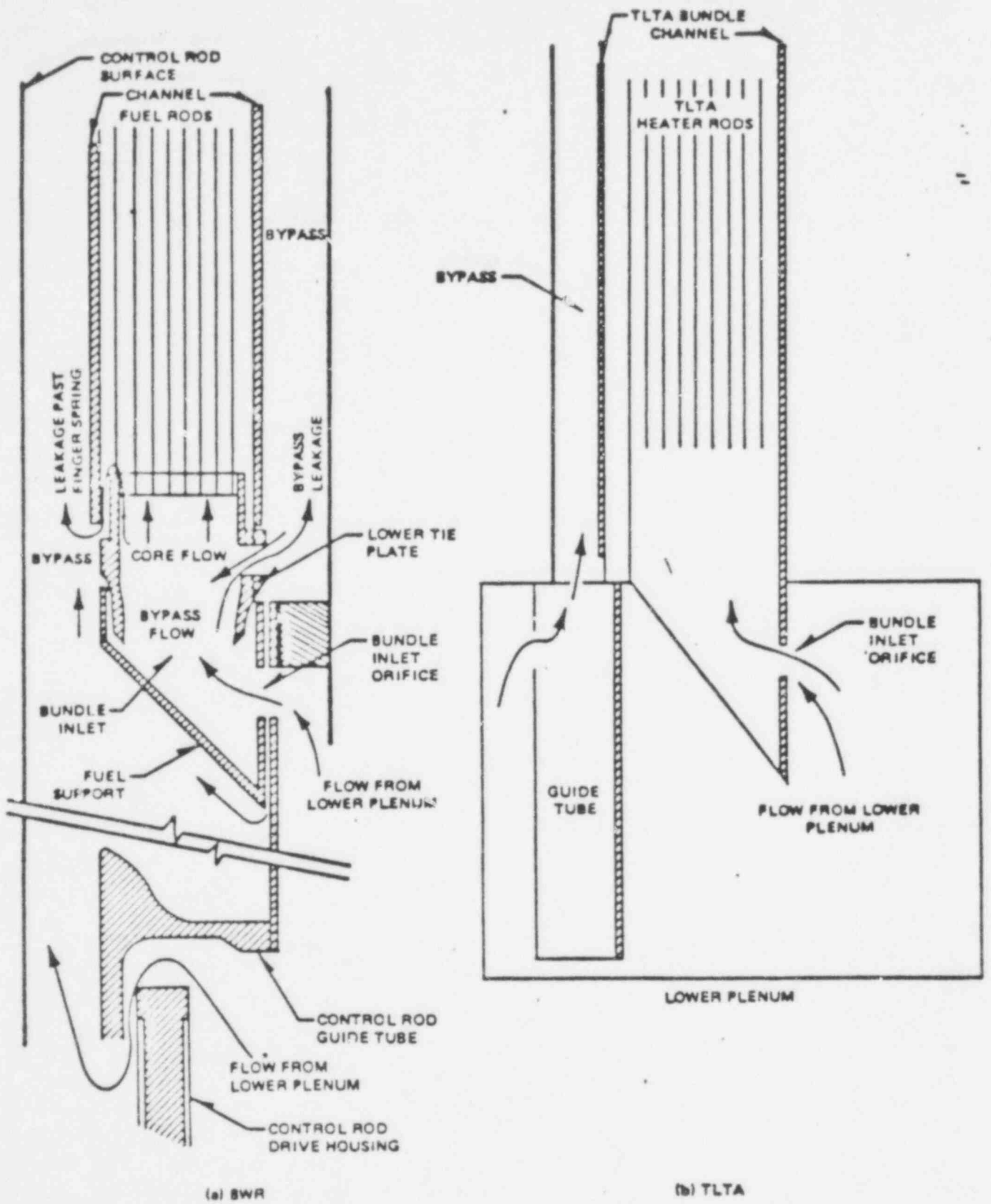


FIGURE 4
 Details of BWR Fuel Bundle and TLTA Heater Bundle Inlet Regions

during the blowdown phase since it has been shown, as reported in Reference 2, that a variation of $\pm 50\%$ in the bypass flow area has a negligible effect on both the system and bundle response.

LOWER PLENUM

The scaling of the lower plenum (LP) is on a volume basis only. This scaling basis leads to a short lower plenum, which is approximately 20% of the height of the reference BWR lower plenum with a surface to volume ratio several times that of the reference BWR. The effect of these two compromises on the core inlet flow, jet pump flow, and system response is discussed below.

STORED HEAT

During a blowdown transient, the vessel wall and internals are a source of energy for steam generation in the wetted regions of the TLTA and the reference BWR. Figure 5 compares the energy rates for the TLTA during a typical blowdown test. As seen in this figure, the energy transfer from the vessel and internals can be significant late in the transient for a time greater than 40 seconds. During this period, the LP is the major contributor of the vessel's energy to the system. The surface area of the TLTA's LP is approximately 5 times that of the scaled value for the reference BWR. This translates into approximately 5 times the stored energy transfer from the wall to the system. The heat transfer of the stored energy from the LP wall and internals to the fluid in a BWR/6 and the TLTA are compared in Figure 6. For this comparison the entire surface area of the LP was assumed to be well cooled throughout a typical blowdown transient. A comparison is also shown with a 3/16 inch (4.76 mm) thickness of insulation on the TLTA wall. The installation of insulation on the inside wall of the TLTA's LP alleviates the non-scaled energy transfer from the wall to the fluid in the LP over the entire BD/ECC period. The use of a 3/16 inch (4.76 mm) thick layer of insulation was considered the most practical in light of the effectiveness and geometric constraints.

519 203

Although these results show that the heat transfer rate will still be slightly higher in the TLTA's LP, this heat source is less than 10% of the energy transfer rate from the bundle, which is typically 200 to 300 kW. Therefore,

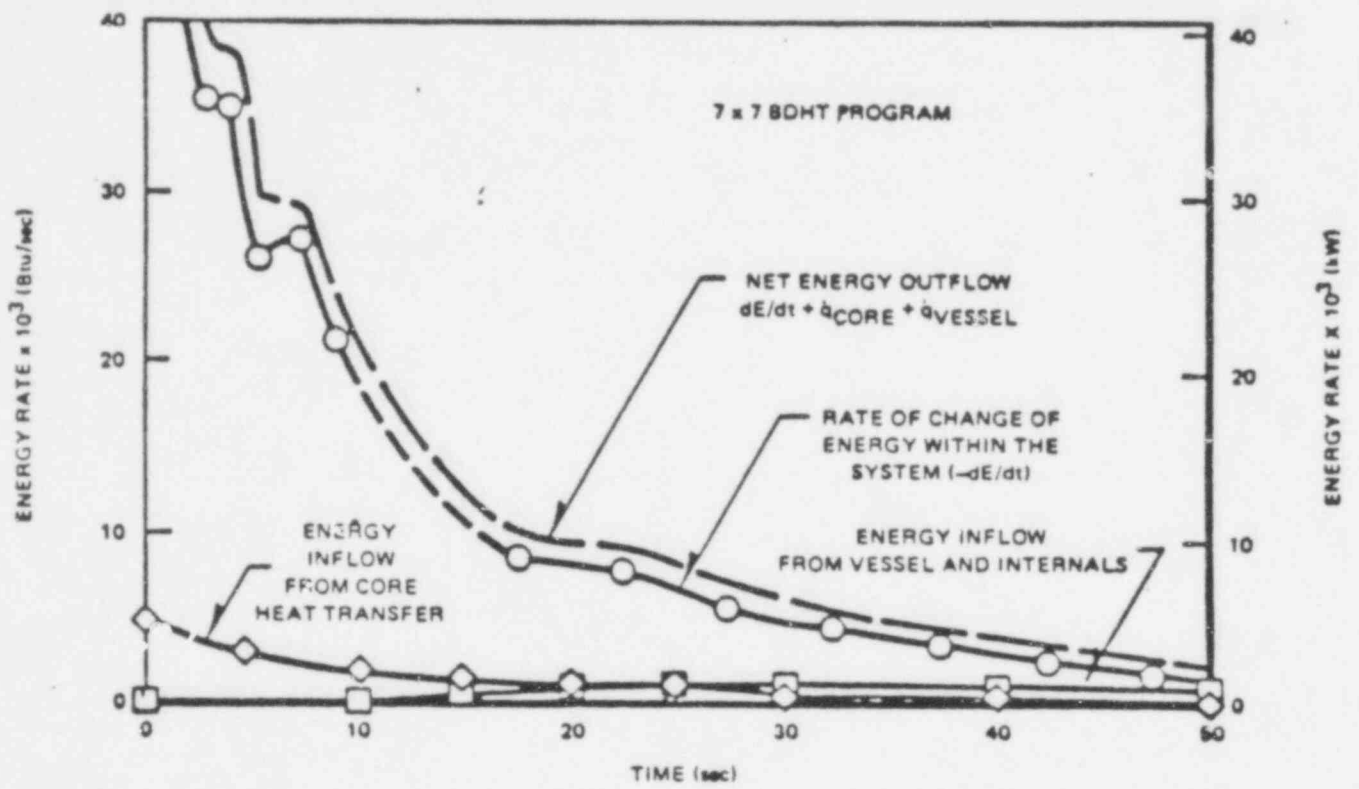


FIGURE 5
Energy Rates Within TLTA-1

519 204

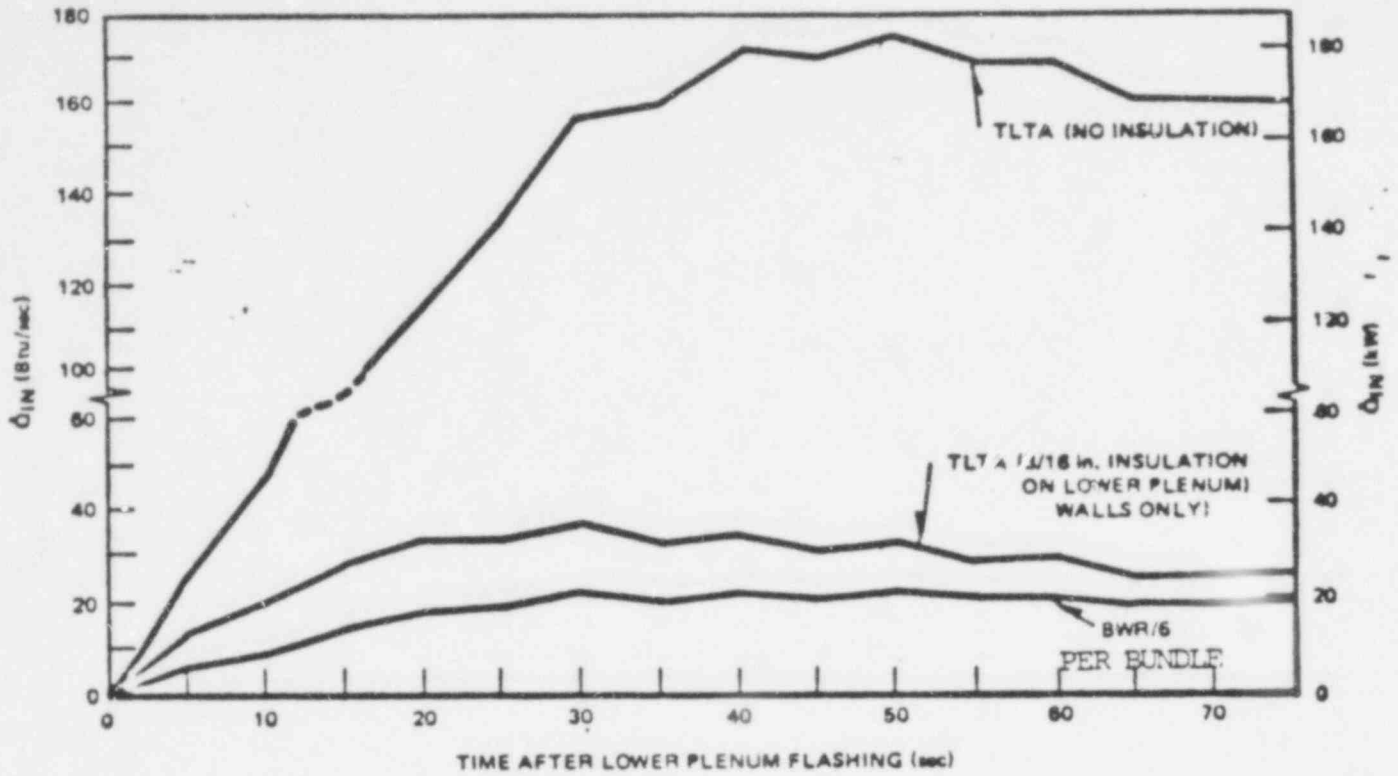


FIGURE 6

Effect of Insulation on Stored Energy Transfer Within Lower Plenum

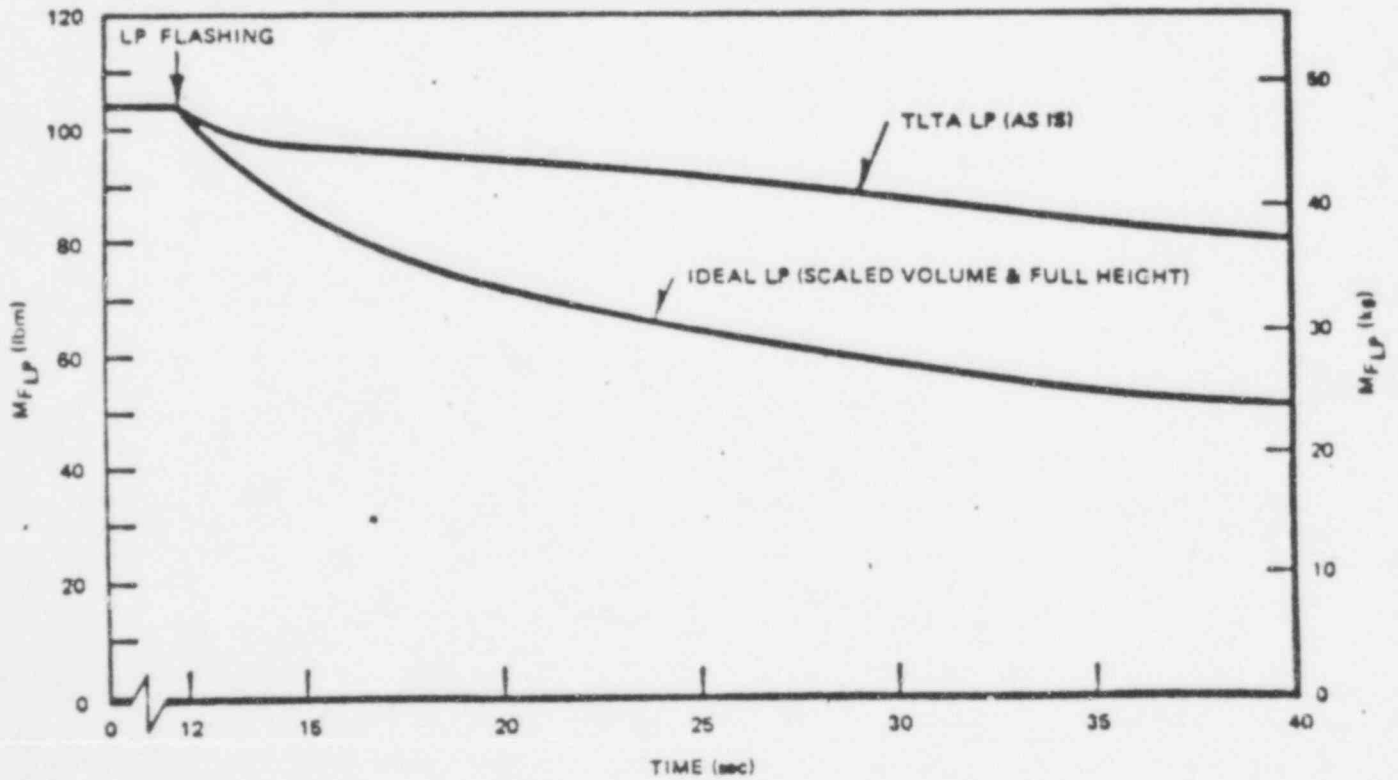


FIGURE 7

Effect of Lower Plenum Height on Lower Plenum Inventory

319 205

the inclusion of this insulation material has achieved the desired effect of minimizing energy transfer from the stored heat source. Preliminary analysis of the first BD/ECC-LA tests suggested that the insulation material was not as effective in minimizing the heat transfer from the walls of the lower plenum. However, recent test evaluations and inspection indicate that the insulation material is approximately 75% effective.

LENGTH EFFECTS

Volume scaling of the LP is sufficient for obtaining a real time response during the early blowdown period when the LP liquid is subcooled. From the time of flashing onward, the height of the LP can play a dominant role in determining the fluid inventory and mass-flow rate out of the LP.

During the onset of the LP flashing surge, the major driving force for the fluid loss from the LP is the displacement of fluid by the steam being generated within the liquid. The amount of fluid displaced at any given time depends on the difference in the quantity of steam generated within the two-phase mixture and the amount leaving the two-phase mixture. The steam generated from the saturated liquid is due to depressurization and the heat transfer from the metal internals and vessel wall. The buoyant force on the steam is its driving force. Thus, the rate at which the vapor can leave the system is governed by the relative velocity of steam rising within the two-phase mixture and the distance the vapor must travel. Since the LP of the reference BWR is much taller than the LP in the TLTA, the time it takes for the steam to leave the two-phase mixture is much longer in the reference BWR than in the TLTA. Thus, the reference BWR will have more mass discharged out of its LP than the TLTA during the initial flashing surge.

A one-dimensional transient thermal-hydraulics code which utilizes a drift-flux model, was used to obtain an estimate of the difference in the inventory of an "ideally" scaled BWR LP, i.e., exact geometric scaling in volume and height, versus the actual TLTA LP. The fluid inventory remaining in the LP for both cases is compared in Figure 7. The void distribution in the LP at 20 seconds after the break, i.e., approximately 8 seconds after LP flashing, is shown in Figure 8. The shaded integral areas in Figure 8 - between 0 and 3.1 ft. for the TLTA and between 0 and 15 ft. for BWR - depict the liquid fraction of the respective LP inventories.

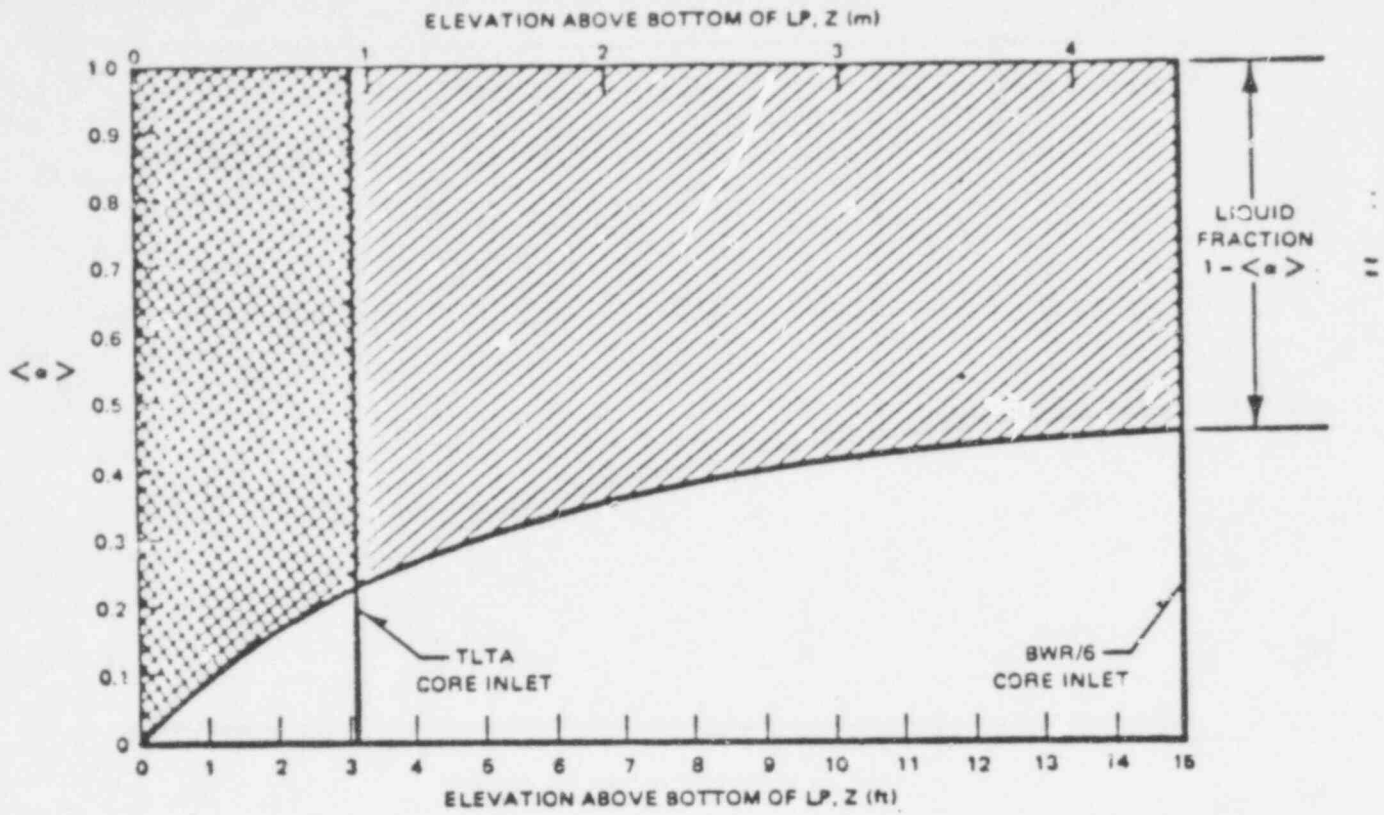


FIGURE 8
 Void Distribution Inside the Lower Plenum About Eight Seconds
 After Lower Plenum Flashing

519 207

The liquid fraction gives an indication of the fluid mass in the LP. For this case the estimated difference in the liquid volume normalized by the LP's total volume is

$$\frac{V_f}{V_{total}} \Big|_{TLTA} = 0.83 \quad \text{versus} \quad \frac{V_f}{V_{total}} \Big|_{BWR/6} = 0.67$$

This will lead to approximately 25%^{*} more steam being generated in the LP of the TLTA due to depressurization than in the LP of the reference BWR subsequent to the flashing surge. Therefore, the steam flow to the core inlet during post LP flashing will be higher in the TLTA than in the reference BWR. This difference is expected to have an effect on the inventory in the bundle because steam inlet flow affects CCFL at the bundle inlet and exit. The increased steam flow will also have an effect on the bundle heat transfer because both the two-phase mixture level and steam cooling above the mixture level are steam inflow dependent. This can lead to a difference in the real time response and possibly in the magnitude of the response, but it is not expected to compromise any phenomena occurring within the core flow path.

During the post lower plenum flashing (LPF) period, the effect of the jet pump exit locations on the TLTA internal flows was reevaluated. For the 7x7 and 8x8 BDHT tests, the jet pump discharge or exit was located at the top of the lower plenum, i.e., above the core inlet elevation. In contrast, the reference BWR jet pump discharge is well below the core inlet. Following the LPF surge the two-phase level drops into the lower plenum, uncovers the jet pump flow path in the TLTA, and results in an alternate flow path to vent the steam. Such venting of steam from the lower plenum occurs later in the reference BWR with its jet pumps located much lower in the lower plenum and immersed in the two-phase mixture. Steam due to flashing and stored heat could be diverted from the TLTA core, and this may lead to an atypical core-flow response later in the transient.

In order to preserve the phenomena of core inlet uncover relative to jet pump uncover and the subsequent system response, the jet pump discharges are extended into the lower plenum of the TLTA. Because of the relatively short TLTA lower plenum and the known differences in void and mass distribution between the TLTA and the reference BWR, no simple basis could be established, a priori, to determine how far to extend the jet pumps. The maximum extension possible is limited by the TLTA auxiliary heaters. At this elevation the fluid volume between jet pump exits and core inlet is scaled to about 1 to 624 of the

* $\frac{.83 - .67}{.67}$
 .67

corresponding value in the reference BWR and so the maximum extension was chosen. The recent test results have shown the importance in the uncovering of the jet pump. Shortly after uncovering, the liquid continuum which was present in the bundle is lost and bulk heatup was observed. Hence, it is crucial that the location of the jet pump exits are scaled to assure that the timing of this event is realistic of a reactor behavior.

RECIRCULATION LOOP

The recirculation loops are designed on the basis that the NPSH available at the inlet to the recirculation loops has sufficient margin over the required NPSH. This results in larger recirculation lines and excess recirculation loop volumes. These are not expected to significantly affect the overall system response through lower plenum flashing. However, following lower plenum flashing, the excess volume in the recirculation loop (intact side) is expected to have a significant effect on the response of the system.

The calculations for the system response were extended to the time period beyond lower plenum flashing. The results of these calculations are illustrated in Figures 9, 10 and 11. Precise scaling of the volume in the intact recirculation loop results in a faster depressurization of the system than that in the TLTA-5, as seen in Figure 9. This deviation in the response of the system is a result of two factors. First there is less total mass within the system in the case of scaled loop, as shown in Figure 10, and, second, there is less two-phase flow discharging from the scaled recirculation loop line into the annulus and out through the break. This is represented by the slight difference in the calculated annulus mass in the post LPP period, as shown in Figure 11. As a result of this comparative study, it was decided to isolate the unscaled portion of the intact recirculation loop during the transient. This modification has recently been made. The modified test apparatus, denoted TLTA-5A, will include a more representative recirculation loop volume.

BREAK AREAS

519 209

The main break-flow path is through the break in the recirculation suction line and the TLTA break geometry and size were scaled to provide 1/624 of the

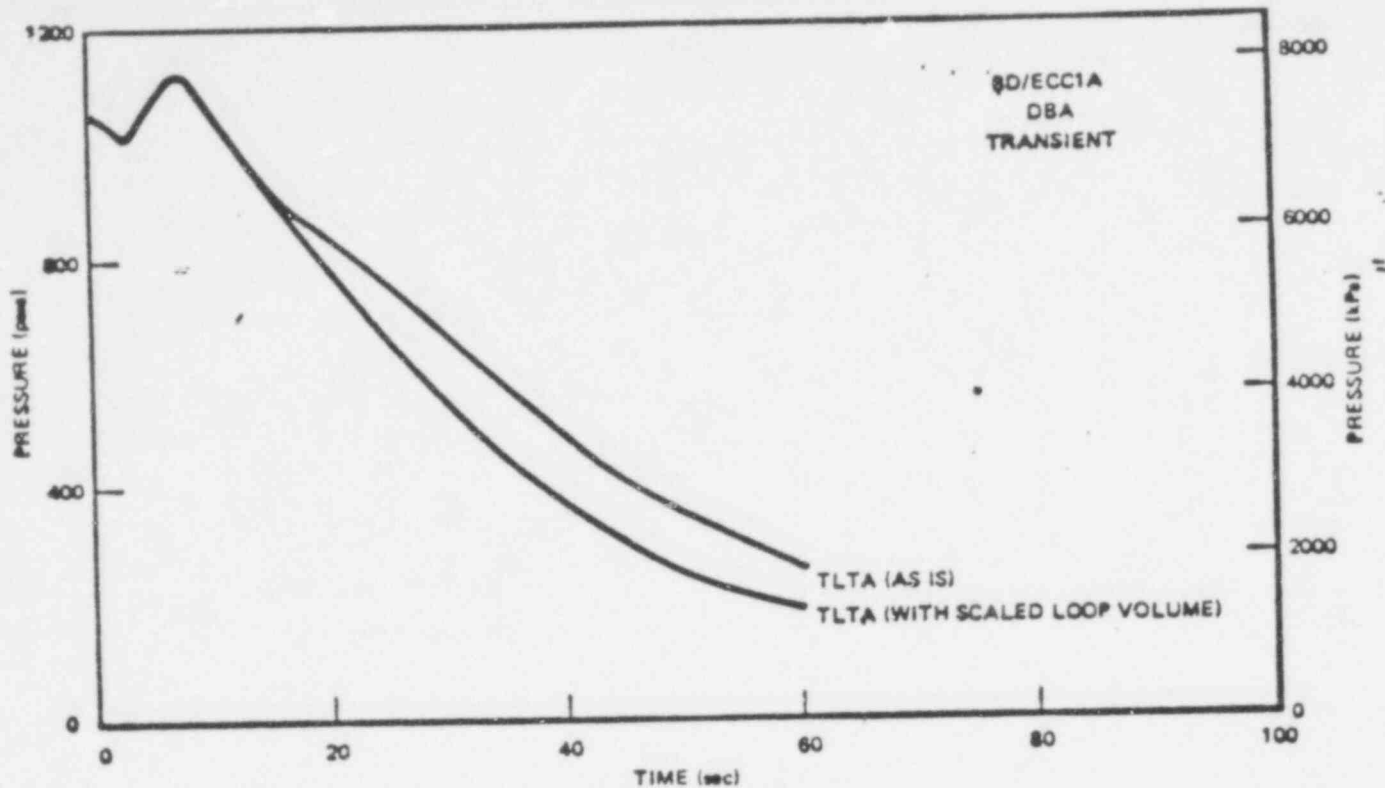


FIGURE 9

Comparison of System Pressure Response in TLTA for Intact Loop Volumes

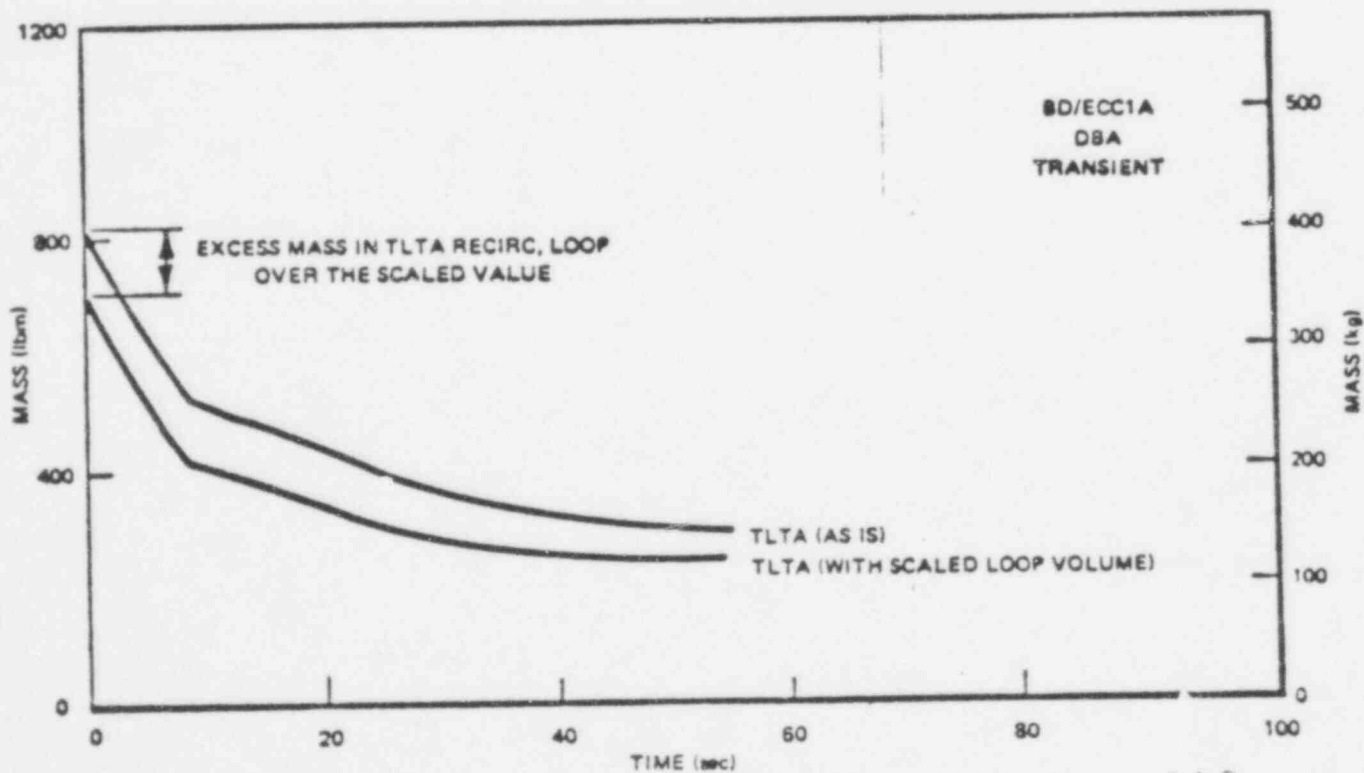


FIGURE 10

Comparison of System Inventory Response in TLTA for Intact Loop Volumes

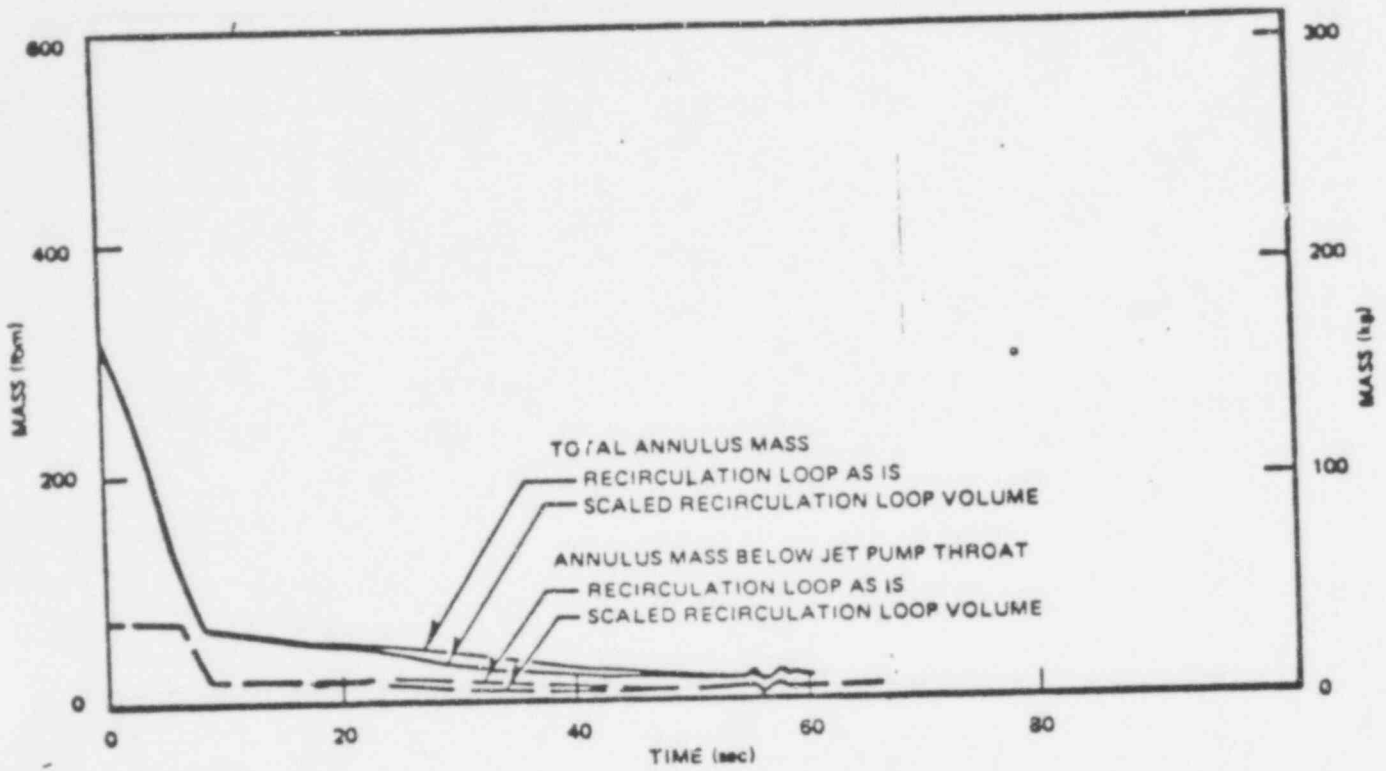


FIGURE 11

Comparison of Regional Inventory Response in TLTA for Scaled and Unscaled Loop Volumes

519 211

reference reactor break-flow area in the TLTA.

The second break-flow path is through the jet pump drive line of the broken loop, the limiting area in a reactor is at the jet pump nozzle. The TLTA jet pump nozzle area of 0.00112 sq. ft. (0.000104 m²) based on a BWR/4 is twice the required area of 0.00056 sq. ft. (0.000052 m²) for a BWR/6. Hence, a flow orifice with the scaled throat area of 0.00056 sq. ft. (0.000052 m²) has been installed in the broken loop blowdown line.

VELOCITIES IN DIFFERENT REGIONS

The present TLTA is scaled on a volumetric basis with reference to a BWR/6, except in the case of the bundle region which has a one-to-one similarity to a reactor 8x8 fuel bundle. Consequently, the flow and heat transfer areas of the various regions of TLTA-5 do not bear a one-to-one relationship as shown in Table 1. However, the TLTA flow areas match the scaled reactor values in the primary regions, namely, the core, bypass, and the separator. Hence, the velocity in the bundle would be the same as in the BWR fuel bundles for the same boundary conditions.

As discussed earlier, the core inlet flow during the coastdown period is expected to be less than the predicted reactor values (Figures 1 and 2) due to low initial elevation head in the TLTA downcomer. Subsequent to lower plenum flashing, there is a potential for increased steam generation in the TLTA lower plenum, as mentioned earlier, compared to scaled reactor values (Figures 6 and 7). This would lead to a higher core inlet flow and velocity compared to the reference BWR. This will affect the magnitude of the bundle heat transfer and pressure drop, and the response of the bundle due to CCFL. A similar effect will occur along the guide tube-bypass regions. This higher velocity will also be carried upwards through the upper plenum and separator.

The larger recirculation line areas should not impact the system response since the flow coastdown in these lines is controlled by the pump coastdown and not by the stored momentum at the time of the blowdown initiation.

519 212

T A B L E 1

COMPARISON OF FLOW AND HEAT TRANSFER AREAS
BETWEEN TLTA AND REACTOR SCALED VALUES

	<u>REGION</u>	<u>TLTA</u>	<u>SCALED REACTOR VALUE (= BWR ÷ 624)</u>	
Actual Flow Area	Bundle Inlet	4.64 in ²	4.64 in ² (Hot & Average)	
		4.64 in ²	1.49 in ² (Peripheral)	
	Bundle Exit	11.36 in ²	11.36 in ²	
	Bypass Exit	1.6 in ²	1.73 in ²	
	Separator	20.38 in ²	20.3 in ²	
	Break Area:			
		Suction	0.43 in ²	0.43 in ²
	Drive	0.08 in ²	0.08 in ²	
Volume Average Flow Area	Lower Plenum	0.72 ft ²	0.19 ft ²	
	Bundle	0.105 ft ²	0.105 ft ²	
	Upper Plenum	0.59 ft ²	0.26 ft ²	
	Downcomer	0.90 ft ²	0.108 ft ²	
	Recirculation Line:			
	Suction	0.046	0.0728 ft ²	
	Discharge	0.012	0.0192 ft ²	
Heat Transfer Surface Area	Lower Plenum (including guide tube outer surface area)	42.46 ft ²	9.5 ft ²	
	Bundle	23.49 ft ²	23.49 ft ²	
	Upper Plenum (inside only)	13.64 ft ²	0.6 ft ²	
	Downcomer up to F.W. Sparger	15.9 ft ²	2.7 ft ²	

519 213

SUMMARY

The preceding analysis indicates that the present TLTA would simulate closely the desired phenomena known to be important in a BWR LOCA up to the time of lower plenum refill. The magnitude of the response and the real time response may not be simulated precisely due to scaling compromises. The expected deviations from the system response of the reference BWR due to the above and other scaling compromises are more fully discussed in Reference 1.

519 214

REFERENCES

1. Letzring, W.J., et al. "BWR Blowdown/Emergency Core Cooling Program Preliminary Facility Description Report for the BD/ECC 1A Test Phase", General Electric Company, December 1977 (GEAP-23592).
2. Burnette, G.W., Danielson, D.W, and Nilsson, K.A., "BWR BDHT Preliminary System Design Description of Two-Loop Test Apparatus", General Electric Company, November 1976 (NEDE-21076).
3. Muralidharan, R., et al., "BWR Blowdown Heat Transfer Final Report", General Electric Company, March 1976 (GEAP 21214).

519 215

VAPORIZATION CORRELATION - BASIS AND APPLICABILITY

The purpose of this write up is to provide the details of the facility and the tests which form the data-base for the vaporization correlation. It will also be shown that this data base is representative of the bundle and the system conditions in TLTA (Two Loop Test Apparatus) after the blowdown phase (~40 secs), and thus the correlation is appropriate in view of current TLTA understanding.

1. TEST FACILITY

The data base for the vaporization correlation was obtained from transient tests conducted on a full size, electrically heated mock up of an 8x8 BWR fuel bundle. The test set up is schematically shown in Figure 1. The basic element represented by the test bundle, as compared with the actual reactor geometry, is shown in Figure 2. The dual channel arrangement (inner and outer channels) has the provision for simulating the cooling water flow along the outside of the bundle (bypass region).

A modified prototype 8x8 BWR tie plate was mounted at the top of the bundle. Prototype spacers were located at representative spacings along the bundle. The lower end of the bundle was not prototypical, the rods extended below the channel and terminated at an electrode. The complete heater rod had a stainless steel clad, a nominal length of 167 inches, a 148-inch heated length and a nominal outside diameter of 0.493 inch. The axial power profile represented a chopped cosine distribution with a peak to average power density ratio of 1.4. Fifty of the heater rods were instrumented with up to six thermocouples. The power supply was made of nine individual power units to allow for a local (i.e., rod to rod) peaking pattern. The bundle power transient approximated the decay heat power required by 10CFR50 Appendix K following a postulated accident (ANS + 20%)

An upper plenum chamber, 24½ inches in diameter and 37 inches high, enclosed the top of the bundle (Figure 1). Inside this plenum was a 1 inch spray nozzle for the core spray simulation. Water was introduced into the gap between the two channels using four 1/4 inch lines, one to each of the four channel sides. From the bottom of the bundle, the water emptied into a graduated holding tank for flow measurement.

519 216

2. INSTRUMENTATION

The test facility was instrumented to measure the parameters listed below:

- Spray water temperature
- Spray flow rate
- Bypass flow rate
- Bundle drainage flow rate
- Rods and channel temperature
- Steam flow rate exiting the test section
- Applied power to the rods

3. TEST PROCEDURES AND PARAMETERS

3.1 Test Procedures

Figure 3 schematically shows the test procedures adopted to obtain the data base for the vaporization correlation. These procedures are outlined as follows:

- a) Apply power to the test bundle.
- b) Monitor bundle and channel temperatures.
- c) When prescribed initial conditions are obtained, start spray water flows and simultaneously start bundle power on programmed decay transient.
- d) Terminate test when cladding temperatures have been reduced to prescribed lower values.

3.2 Test Parameters

The data base for the vaporization correlation covers the range of test parameters listed below which is representative of the parameter range used for the evaluation model calculations applied to BWRs.

Bundle Power: 200 - 300 KW

System Pressure: 15 to 25 psia (approx.)

Maximum Cladding Temperature at Spray Initiation: 1040 - 1880°F

Spray Rate: 1.5 - 11.8 GPM

Spray Temperature: 100°F - 208°F

519 217

4. DATA BASE AND APPLICABILITY

The core vaporization correlation used in the evaluation model was empirically developed using data from a full scale bundle, described above, with ECC liquid introduced at the top and no apparent liquid hold up at the bottom. All the vapor generated in the fuel bundle and the surrounding bypass region flowed upward and was measured as a combined value at the top of the core. No additional vapor was injected at the bottom of the core. The tests were conducted by preheating the fuel rods to a determined initial temperature (test parameter), setting the initial decay power level (test parameter), then measuring the core vapor generation as a function of time with power variation to simulate the LOCA decay power transient. Counter-current flow limiting (CCFL) occurred at the upper tie-plate in most of these tests resulting in liquid hold up in the upper plenum.

The vaporization correlation has a large data base, relevant information (Figures 4 and 5) from a representative test run are included here. Additional experimental data were transmitted to NRC in a letter dated January 30, 1979 from E. P. Stroupe of General Electric Company to R.L. Tedesco of Nuclear Regulatory Commission. Figure 4 shows the measured steam flow as a function of time exiting from the test section. Some of the steam generated in the core condenses due to system heat loss and due to subcooled ECC water flow in the upper plenum and in the bypass region. Maximum core steam flow is then determined by adding the steam condensed to the measured maximum steam flow. For conservatism, the maximum core steam flows (Figure 4) were used to establish the vaporization correlation. Further conservatism is introduced in the correlation by assuming that the entire vapor flow measured at the top of the core was generated in the bundle, and that no part of this steam was generated in the bypass region.

Figure 5 shows the bundle power equivalent steam flow (steam that could be generated by all the test power going into steam generation). Also shown in Figure 5 is the bundle steam flow predicted by the vaporization correlation for the initial temperature and peak bundle power for the representative run. Under the test conditions without bundle reflood, the general temperature transient response follows the trends depicted in Figure 3.

519 218

The significance of the results shown in Figure 5 is the comparison of the fraction of decay heat that actually contributes to steam generation. During the initial period of the transient ($t < t_1$), the instantaneous steam generation rate is less than the decay heat due to net increase in the stored energy of the rods. During the later part of the transient ($t > t_1$), the rods are cooling down and the instantaneous steam generation rate is greater than the decay heat due to net decrease in the stored energy of the rods. The physical significance of the point of intersection of the decay heat curve and the predicted maximum vaporization line is that all the decay heat is going into vapor generation at this time ($t = t_1$) and that the net change in the stored energy of the rods is approximately zero. However, because the decay heat rate is decreasing with time, the combined effects of steam generation due to decay heat and stored heat in the rods contribute to a lower net steam generation rate later in the transient ($t > t_1$) as shown in Figure 4. Use of the maximum steam generation rate measured therefore represents an upper bound.

In order to examine the applicability of the vaporization correlation to TLTA (Two Loop Test Apparatus), the schematic diagram showing this test set up is included in Figure 6. Comparison of Figures 1 and 6 indicates that the test section in TLTA is very similar to the one used in obtaining the data base for the vaporization correlation. Detailed results from recent TLTA phenomena analyses are presented in Attachment 1. One of the significant conclusions of these recent analyses on TLTA is that a mixture density sufficient to maintain nucleate boiling persisted in the core region for approximately 40 seconds and, thereafter, the core was entirely depleted of any liquid continuum. This conclusion is supported by the bundle density and pressure drop measurements shown in Figures 7 and 8. Subsequent to the liquid depletion from the core at 40 seconds, the system conditions in the TLTA bundle are quite representative of those present in the "empty bundle" experiments used in the development of the vaporization correlation. For reasons of similarities both in the test sections and the system conditions, it can be concluded that the vaporization correlation also provides a bounding prediction of the steam generation rate in TLTA tests with ECC injection after 40 seconds into the transient.

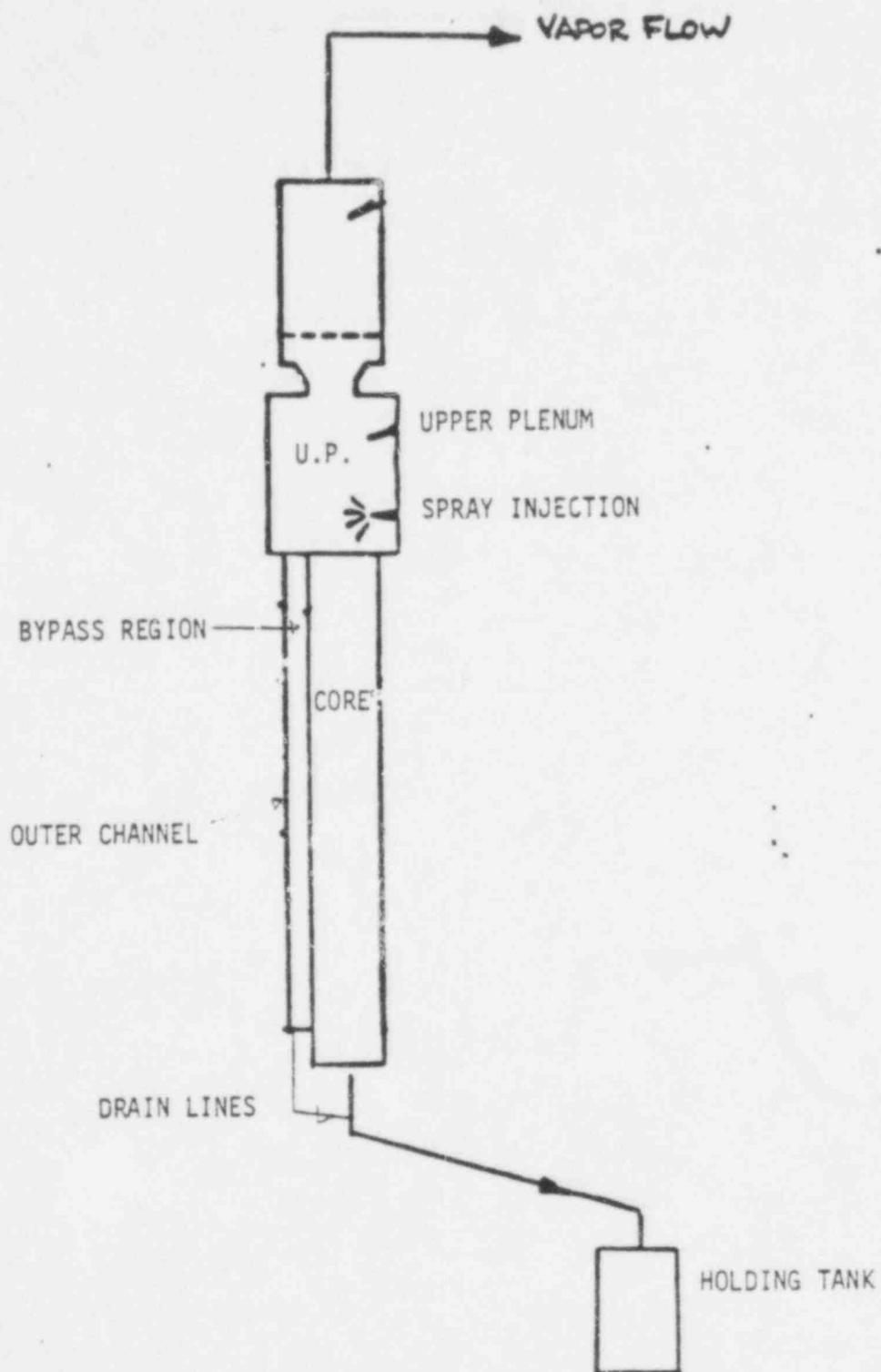
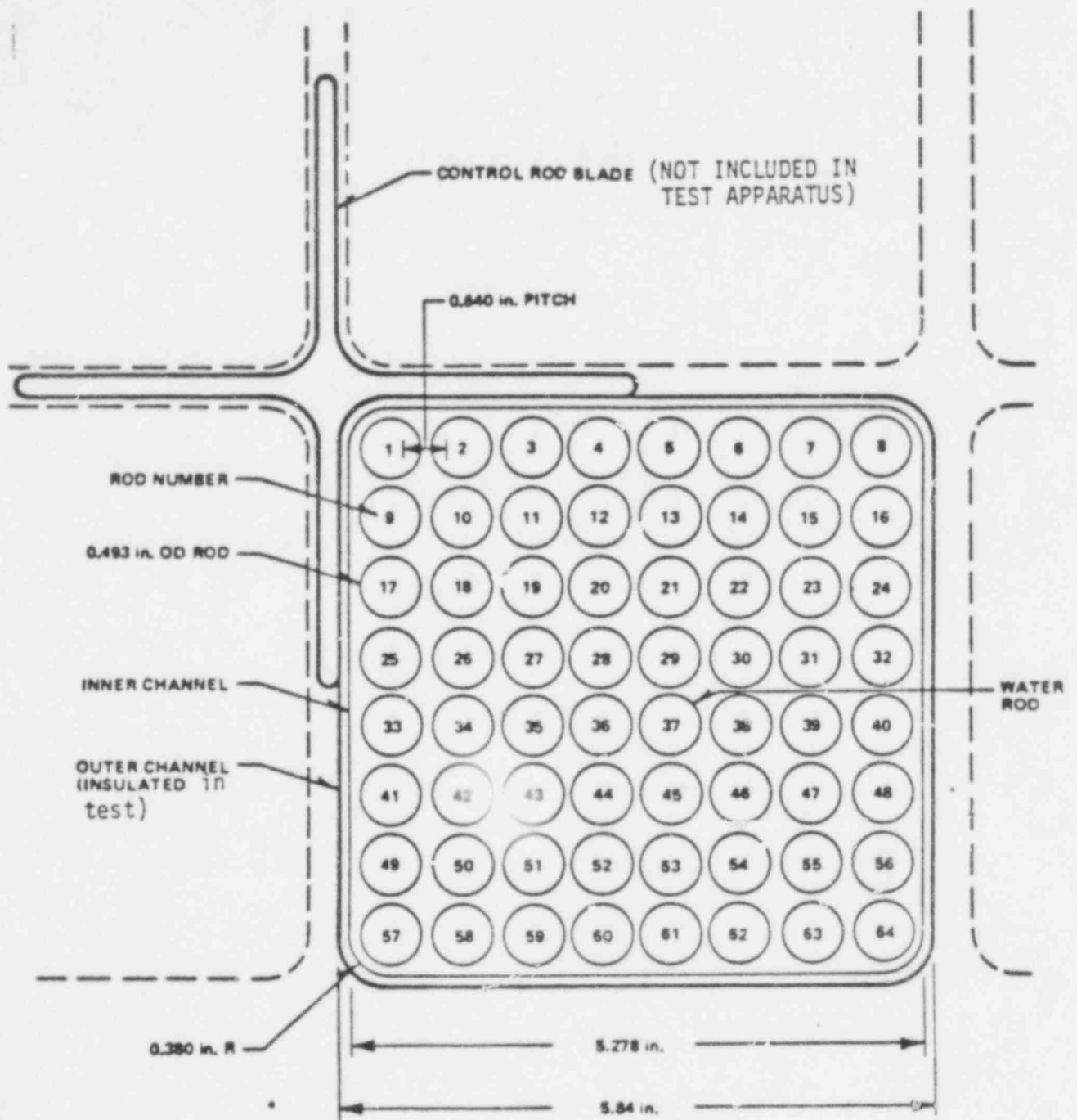


FIGURE 1: SCHEMATIC OF FACILITY USED IN VAPORIZATION TEST. 519 220



519 221

Figure 2: Reactor Channel Geometry and Test Section Simulation

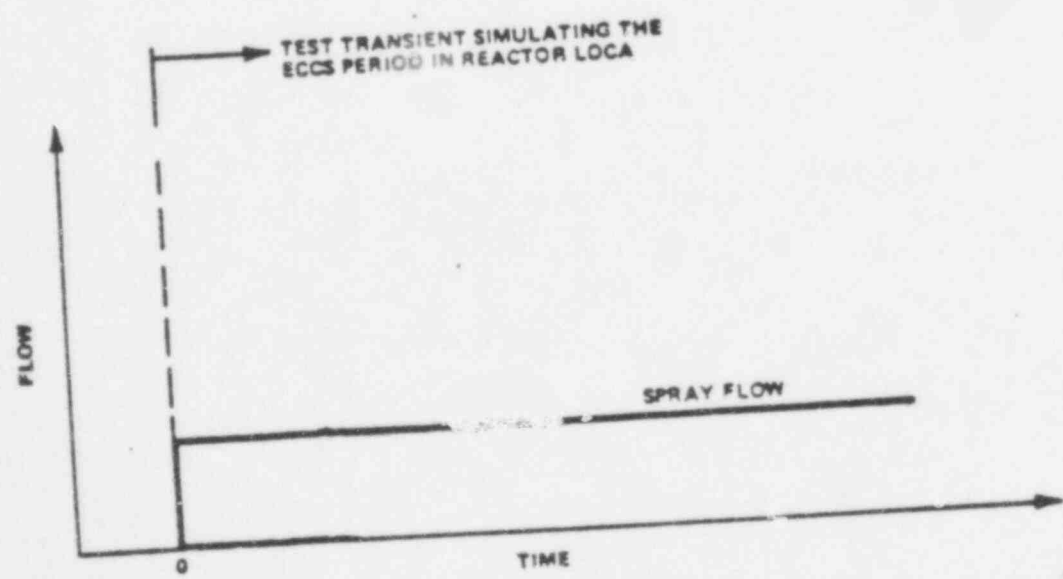
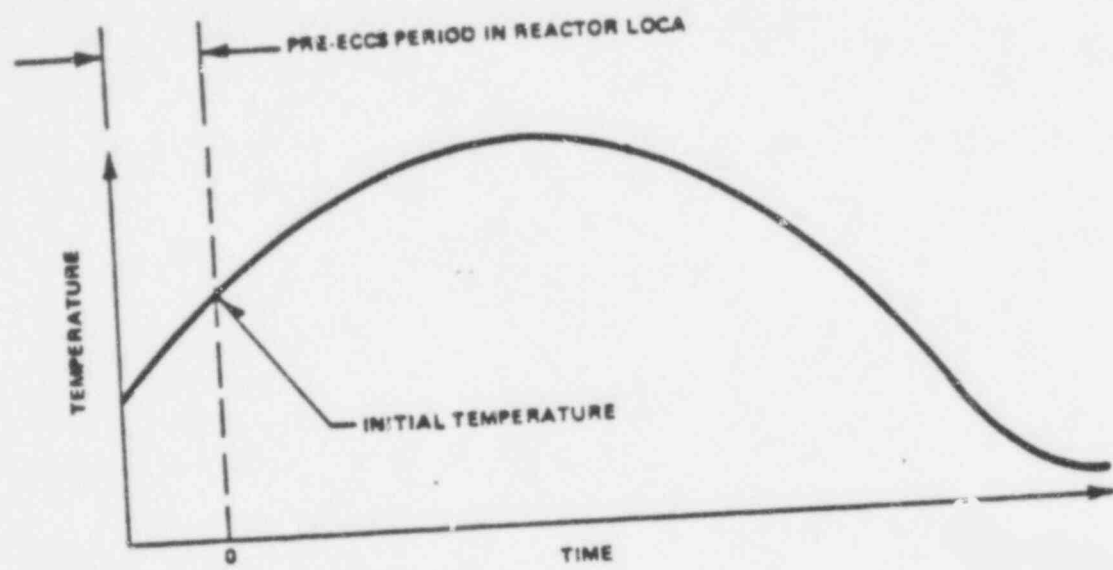
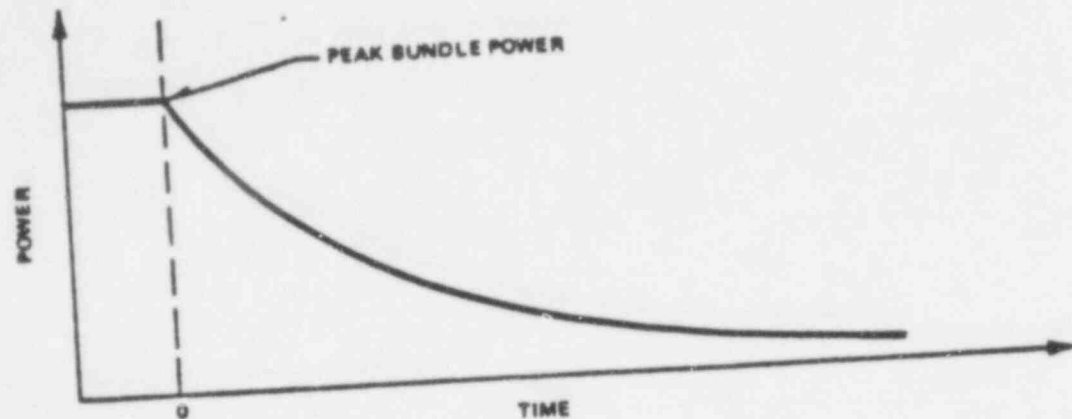
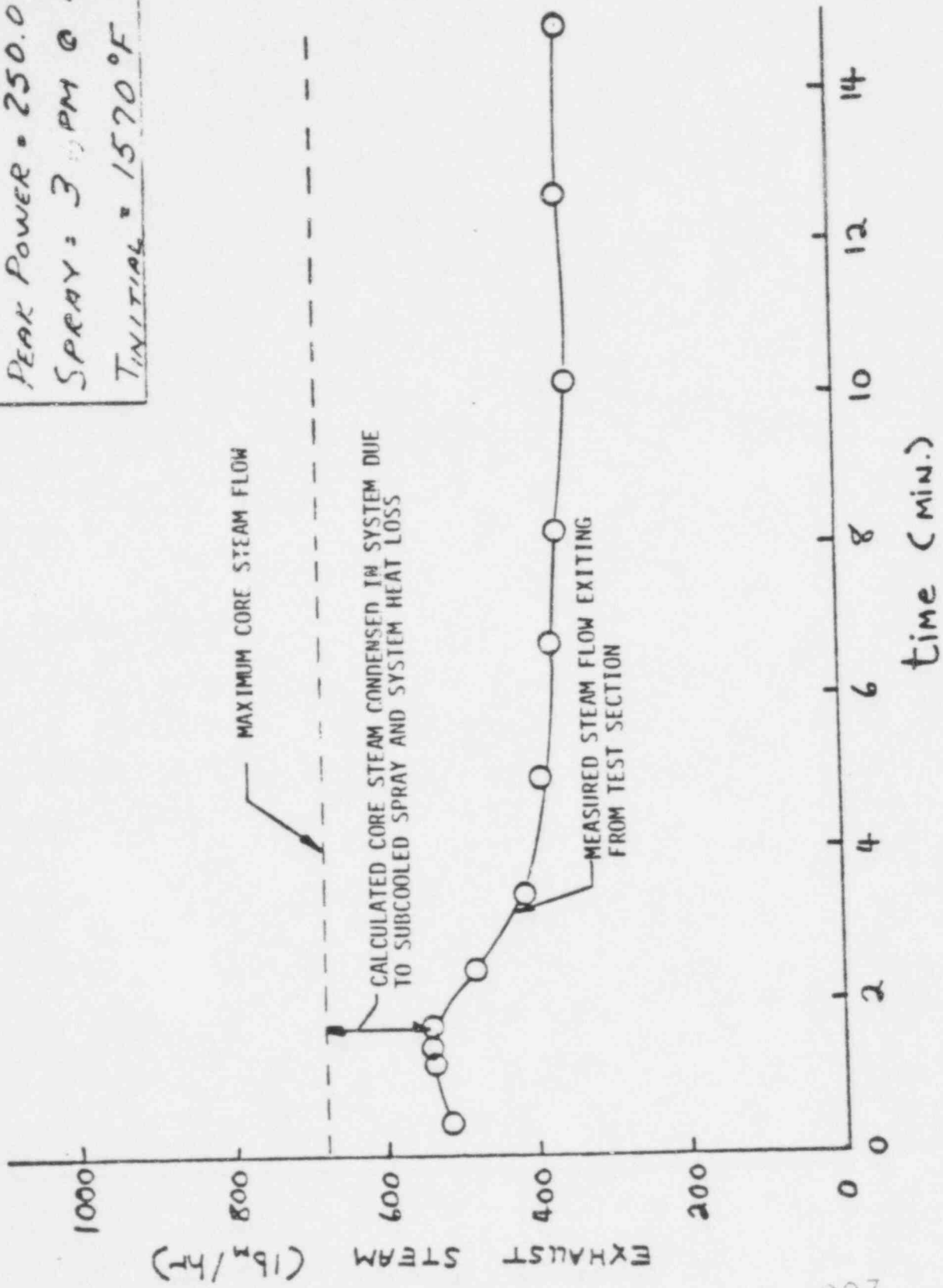


Figure 3: Transient Test Procedure

519 222

RUN 66
 1972-73 SS BUNDLE
 PEAK POWER = 250.0 KW
 SPRAY = 3.0 PM @ 190°F
 T_{INITIAL} = 1570°F



519 223

RUN 66

1972-73 SS BUNDLE

PEAK POWER = 250.0 KW

SPRAY = 3 GPM @ 190°F

T INITIAL = 1570°F

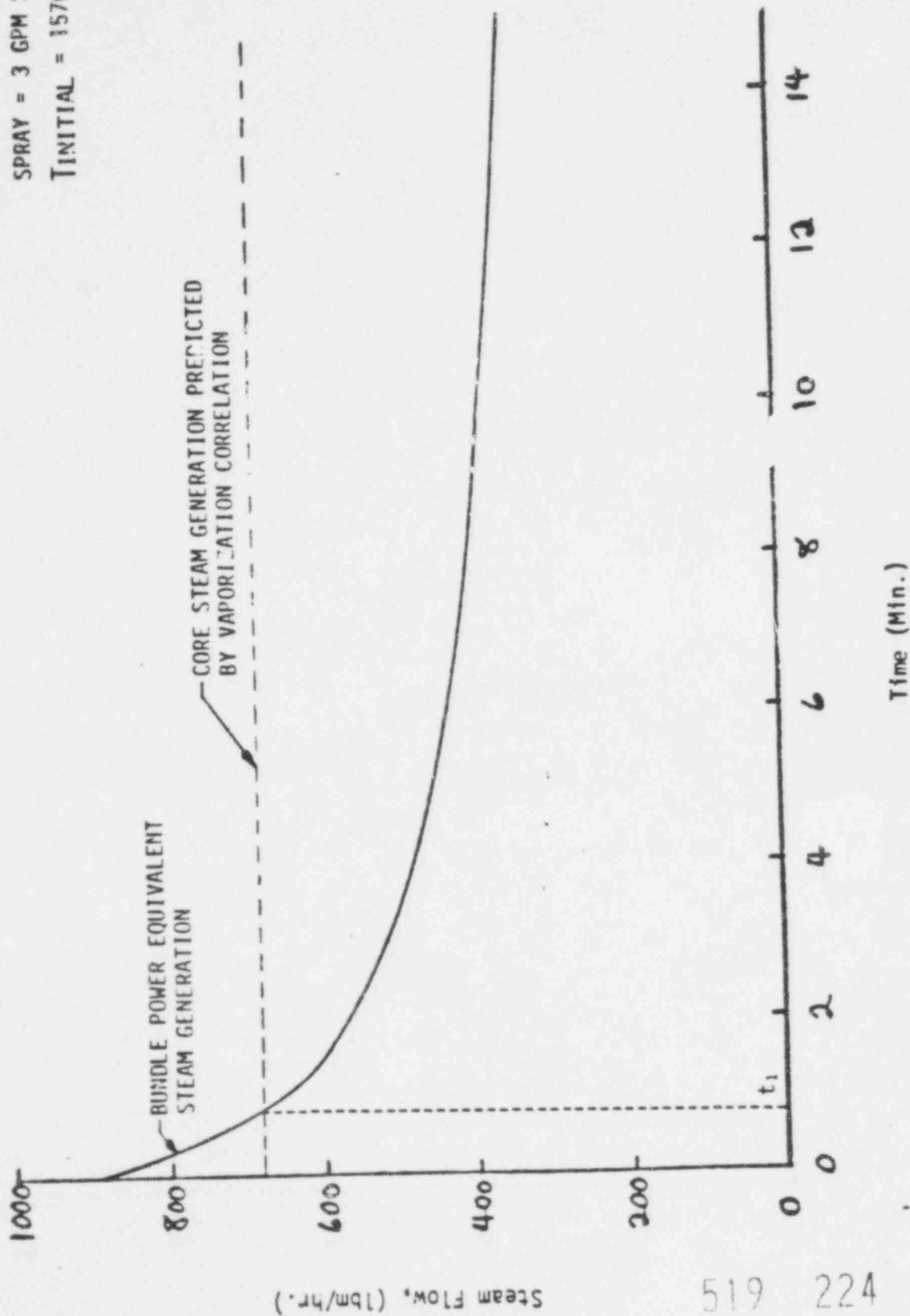


FIGURE 5: COMPARISON OF VAPOR GENERATION ASSUMING ALL TEST POWER GENERATES VAPOR TO THE VAPOR GENERATION CALCULATED USING THE VAPORIZATION CORRELATION FOR TEST RUN 66.

519 224

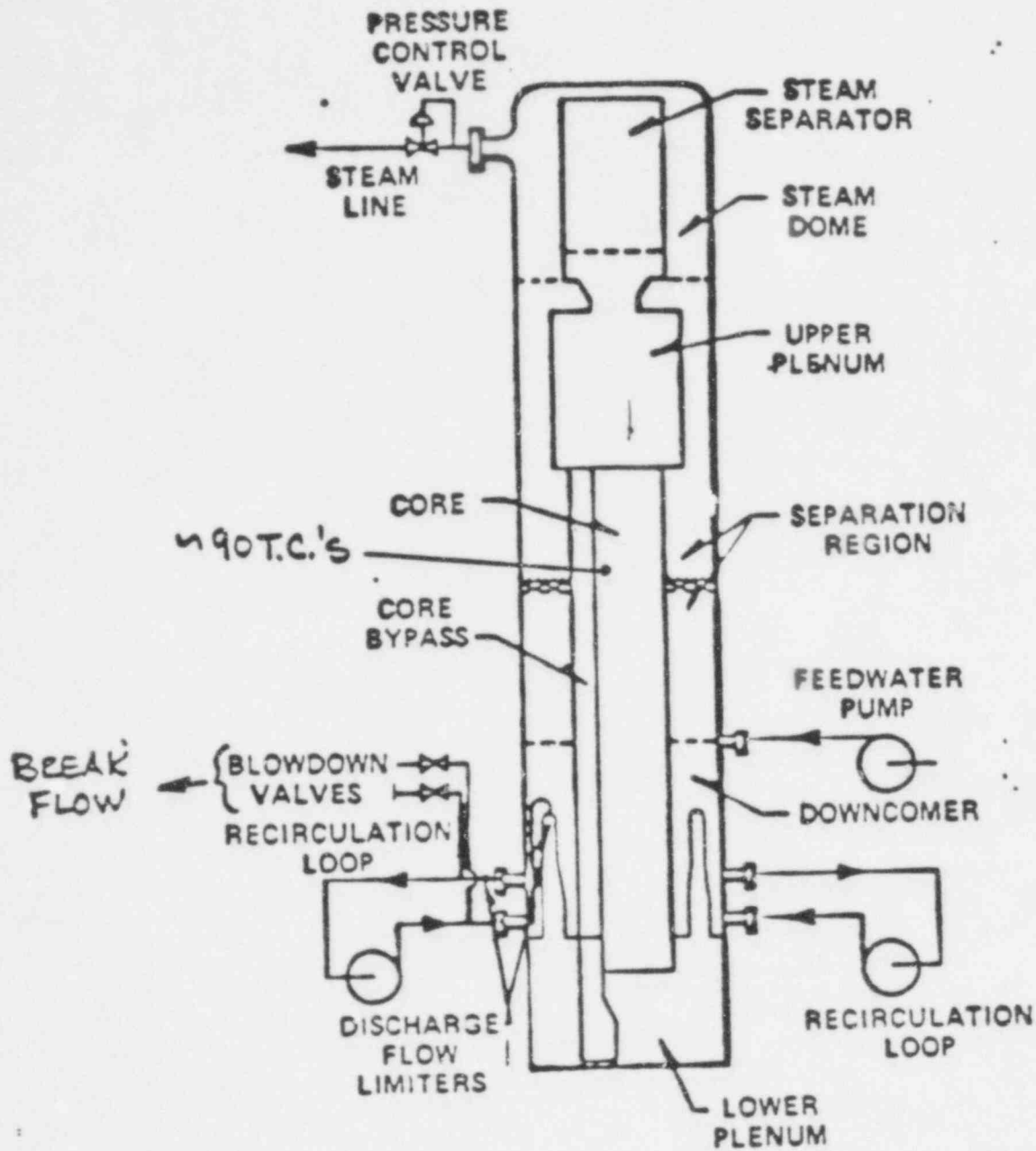


FIGURE 6: TWO-LOOP TEST APPARATUS

519 225

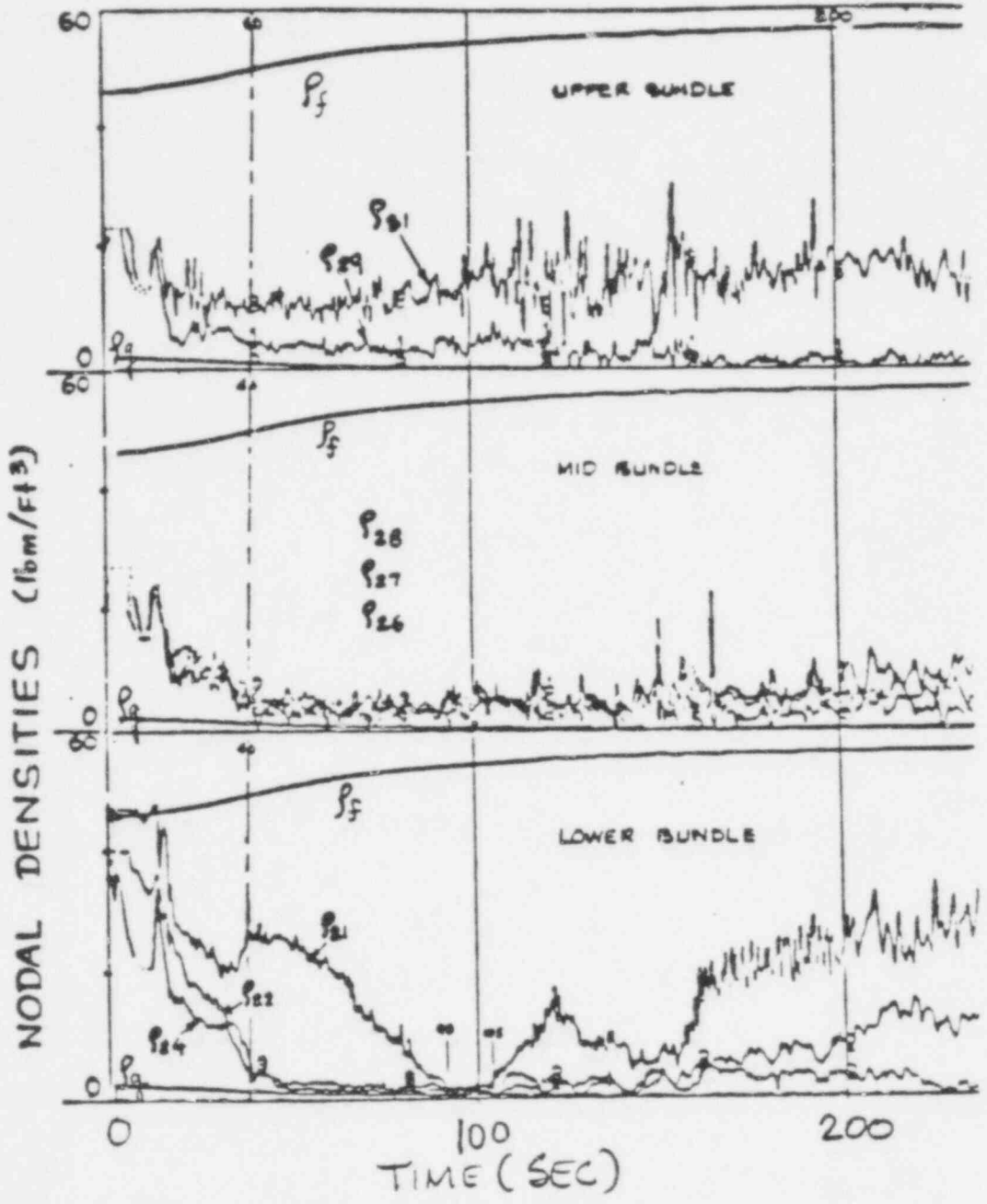
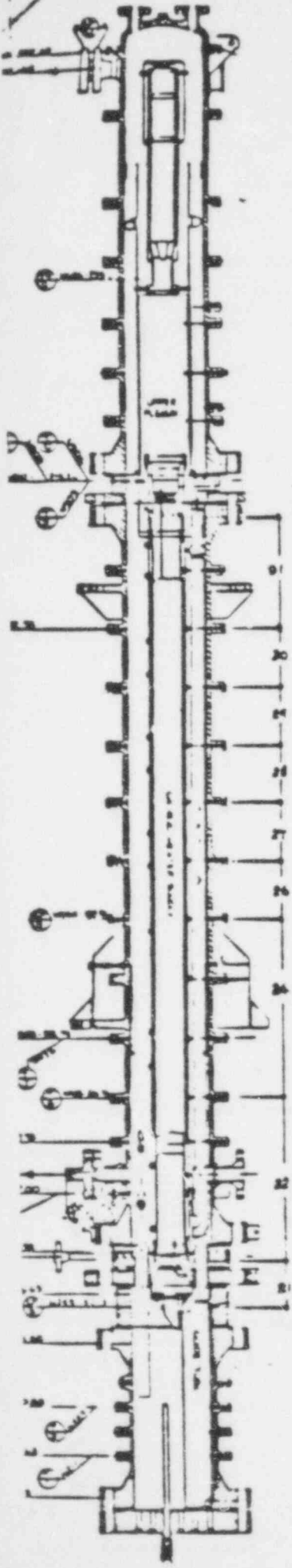


FIGURE 7: DENSITY MEASUREMENTS FROM TLTA FOR AVERAGE POWER AVERAGE ECC TEST.

519 226

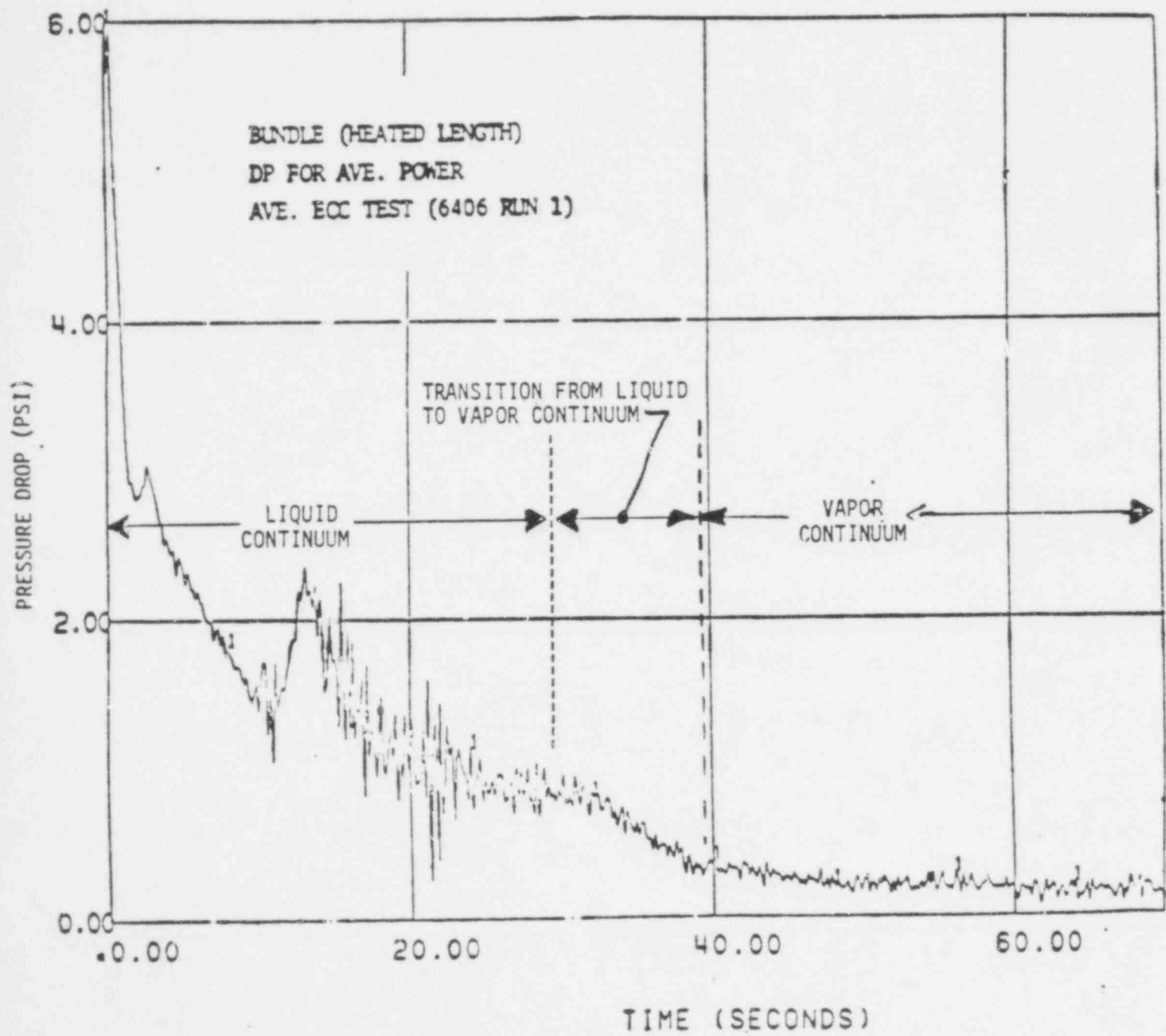


FIGURE 8: MEASUREMENT OF BUNDLE PRESSURE DROP FROM TLTA FOR AVERAGE POWER AVERAGE ECC TEST.

519 227

QUESTION

The conservatism of the heat transfer transition in SAFE should be justified.

RESPONSE

The heat transfer coefficient below the two phase level, used in the SAFE code for current licensing calculations is shown on page I-49 of Reference 1 and is shown in figure 1 as the solid line. As the SAFE code is a system code the core thermal hydraulic calculation is done for the average bundle and not the high powered bundle. Hence the most appropriate heat transfer coefficient to be used is the one most representative of the average bundle. Tests in the TLTA, both with and without ECC, have shown that the most representative heat transfer coefficient for the average bundle, at all elevations below the two phase level, is nucleate boiling (references 2 and 3). Hence, the sensitivity study showing the effect of high heat transfer on calculated peak cladding temperature (PCT) (Reference 4) was performed using the heat transfer observed in the test, which was intended to be most representative i.e. best estimate and not conservative.

QUESTION

GE must either justify that not including CCFL at the bottom (side entry orifice) is conservative or put it into their model.

RESPONSE

The effect of not including liquid holdup in the bundle because of side entry orifice (SEO) CCFL in the EM is conservative for two major reasons:

- a) SEO CCFL during the blowdown phase results in a delay in the mixture level dropping out of the core. If SEO CCFL were included in the evaluation model (EM) a delay in the core uncover and improved heat transfer would be calculated.
- b) SEO CCFL during the ECC phase results in earlier reflooding of the core as the core can be reflooded prior to the lower plenum completely refilling. This earlier reflooding results in much lower PCTs.

There are a number of other minor effects of SEO CCFL on the expected response of the BWR, most of which have been shown (References 5 - 12) to result in earlier reflooding. These are:

- a) Effect of steam redistribution between different bundles (Reference 6). It was shown that if this effect is included it results in a lower PCT.
- b) Effect of liquid in some bundles and only steam in others. Reference 13 discusses this effect in detail and shows that the current evaluation model (EM) calculation is conservative.

- c) Effect of steam generation in the bundle as a result of water holdup. Reference 13 gives a detailed comparison of this possible non-conservatism to the other conservatisms, discussed above. It was shown that the conservatisms of not including SEO CCFL, far outweigh the one possible non-conservatism.

There is no new evidence or test information to show that the NRC's conclusion (Reference 10 and 12) about modelling of SEO CCFL needs to be changed. Hence it can be concluded that the EM need not be changed to include SEO CCFL, as it is conservative without specifically modelling SEO CCFL.

References

- 1) General Electric company analytical model for loss of coolant analysis in accordance with 10CFR50 Appendix K, NEDO 20566 Vol. 1 and 2, Nov. 1975.
- 2) BWR Blowdown Heat Transfer Program - Final Report GEAP 21214, Feb. 1976.
- 3) BWR Blowdown/Emergency Core Cooling Blowdown Heat Transfer (8x8 BDHT) Final Report GEAP-NUREG 23977, Sept. 1978.
- 4) Letter E.P. Stroupe to R.L. Tedesco, "Leibnitz Rule and High Heat Transfer in LOCA Models (Verified Calculations)," May 2, 1979.
- 5) NEDC-20994, September 1975, "Peach Bottom Atomic Power Station Units 2 and 3 Safety Analysis Report for Plant Modifications to Eliminate Significant In-Core Vibrations."
- 6) "Supplemental Information for Plant Modification to Eliminate In-Core Vibration," NEDE-21156, January 1976 (proprietary).
- 7) "Supplemental Information for Plant Modification to Eliminate Significant In-Core Vibrations," Supplement 1, NED-21156-2,
- 8) "Supplemental Information for Plant Modification to Eliminate Significant In-Core Vibrations," Supplement 2, NEDE-21156-2, January 1977.
- 9) Letter, R. Engel to V. Stello, "Answers to NRC Questions on NEDE-21156-2," January 24, 1977.

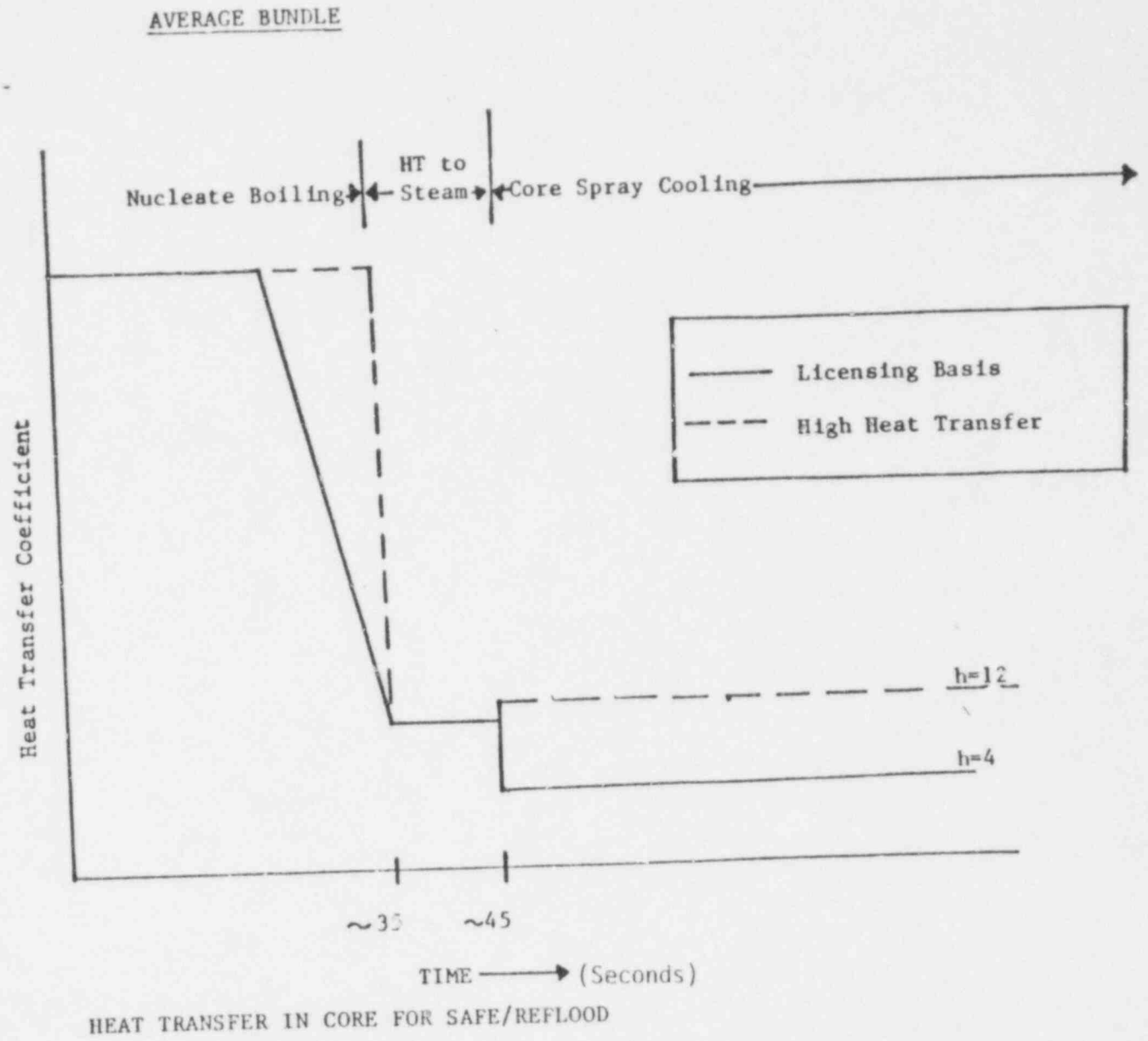
519 229

- 10) NEDE-24094, January, 1978, "LOCA Analysis Methods for BWR 2/3 with Drilled Lower Tie Plates", General Electric Co.
- 11) Letter to Mr. R.L. Baer, USNRC, from R. Engel, GE, "Responses to NRC Questions on NEDE-24094", April 28, 1978.
- 12) Letter, K.R. Goller to G.G. Sherwood, "Safety Evaluation for General Electric ECCS Model Modifications," April 12, 1977.
- 13) Letter E.P. Stroupe to R.L. Tedesco , "TLTA Information Requested by NRC," Jan. Jan. 30, 1979.

519 230

6-4

519 231



QUESTION:

Provide basis for GE conclusion that liquid pools will not collect above grid spacers for the refill/reflood phase of the transient.

RESPONSE:

A "liquid pool" can form above a restriction due to counter current flow limiting (CCFL) when the liquid cannot drain at a sufficient rate due to vapor upflow. Thus, two criteria must be met for such a "liquid pool" to form:

1. The liquid must be draining, i.e., in counter current flow;
2. The vapor velocity must be high enough to restrict the available liquid downflow.

The refill portion of the postulated BWR LOCA is a slow transient which can be treated as a quasi-static calculation. During this phase, spray water falls through the bundle resulting in evaporation of a portion of the water. Thus counter current flow conditions exist in the bundle. The highest vapor upflow and liquid downflow rates occur at the top of the bundle. The upper tie plate also presents the greatest restriction to the flow. All of these conditions result in CCFL only at the upper tie plate. The attached figure shows possible flow situations in a $j_g - j_f$ plane. Flow conditions to the left of the CCFL curve in counter current flow are not possible. This situation is illustrated as line 'AB' in the attached figure. 'A' represents conditions at the bottom of the bundle and 'B' at the top of the bundle and points along 'AB' represent conditions along the bundle. For truly steady-state conditions, AB is a straight line with a slope of $-v_g/v_l$. For a slowly varying transient, the line 'AB' will represent the conditions along the length reasonably well. The figure shows two CCFL curves, based on volumetric fluxes in the open bundle area: curve 1 for the tie plate and curve 2 for the spacer, which is less restrictive. In order that CCFL occur at the spacer, AB must

519 232

intersect 2 before 1. Clearly, under quasi-static conditions this is not possible. Thus, while some axial changes in droplet concentration may be caused by the spacers, 'liquid pools' will not form at the spacers in this situation.

In order that CCFL occur at the spacers before (or together with) the upper tie plate, a significant distortion of the axial flow profile must take place. Curves CD to C'D show such situation. Typically, this could happen during a transient when the inlet liquid flow is sharply reduced from c' to C as during the "flow window" just prior to lower plenum flashing in the early blowdown period. The flow conditions along the bundle prior to the sudden inlet flow reduction would be represented by C'D, whereas, shortly after the flow reduction from C' to C the characteristics would be along C'D. This can lead to CCFL at the spacers and formation of low void fraction regions ("liquid pools") above the spacers and high void fraction regions below the spacers. It should be noted that for Appendix K analysis a "dryout correlation" based on experimental data is used to predict boiling transition during this period. The correlation conservatively assumes that the entire length of the bundle suffers boiling transition rather than small regions near spacers.

LFR: rm/522-523

7/25/79

519 233

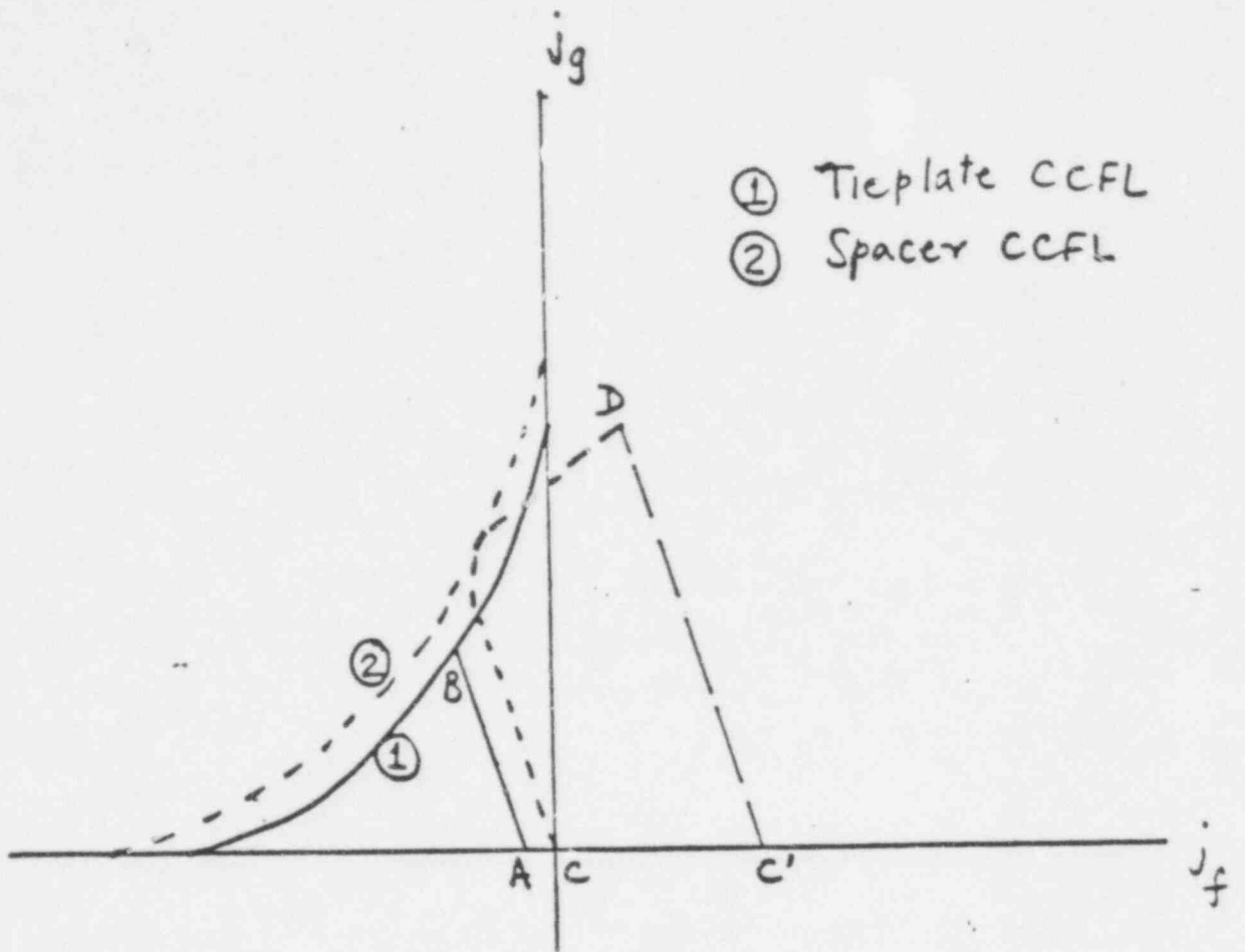


FIGURE: Axial Variation of Flow Rate in $j_g - j_f$ Plane

519 231

COMPARISONS OF THE SAFE

CALCULATION WITH THE TLTA TEST DATA

July, 1979

1. INTRODUCTION

The analytical calculations for the TLTA average power tests with and without ECC were carried out recently with the SAFE code. The evaluation model procedures used in the BWR calculations, which are applicable to the TLTA conditions, were used in the study. SAFE runs were conducted with the initial conditions (bundle power, water level, steam line flow, jet pump flow, etc.) and the boundary conditions (control valve characteristics and ECC flow characteristics) given by the test data. Comparisons of the calculations with the test data are presented below.

2. SAFE CALCULATIONS

Comparisons for the tests without and with ECC are shown in Figures 1 and 2, respectively. Each figure shows the system blowdown (pressure) response and break flow transients given by the calculation and the test.

SAFE calculates a higher break flow and hence more mass depletion in the early transient (<15 seconds) for both tests. This early overcalculation results in less stored mass and energy in the system which correspondingly leads to a faster system blowdown transient (pressure response) and a lower system pressure later in the transient. Over that period where the discharge fluid is predominantly steam, SAFE underestimates the break flow mainly due to the lower calculated system pressure. However, as the calculated pressures become closer to the test results beyond 100 seconds, better agreements of the break flows are seen particularly in the case without ECC.

519 235

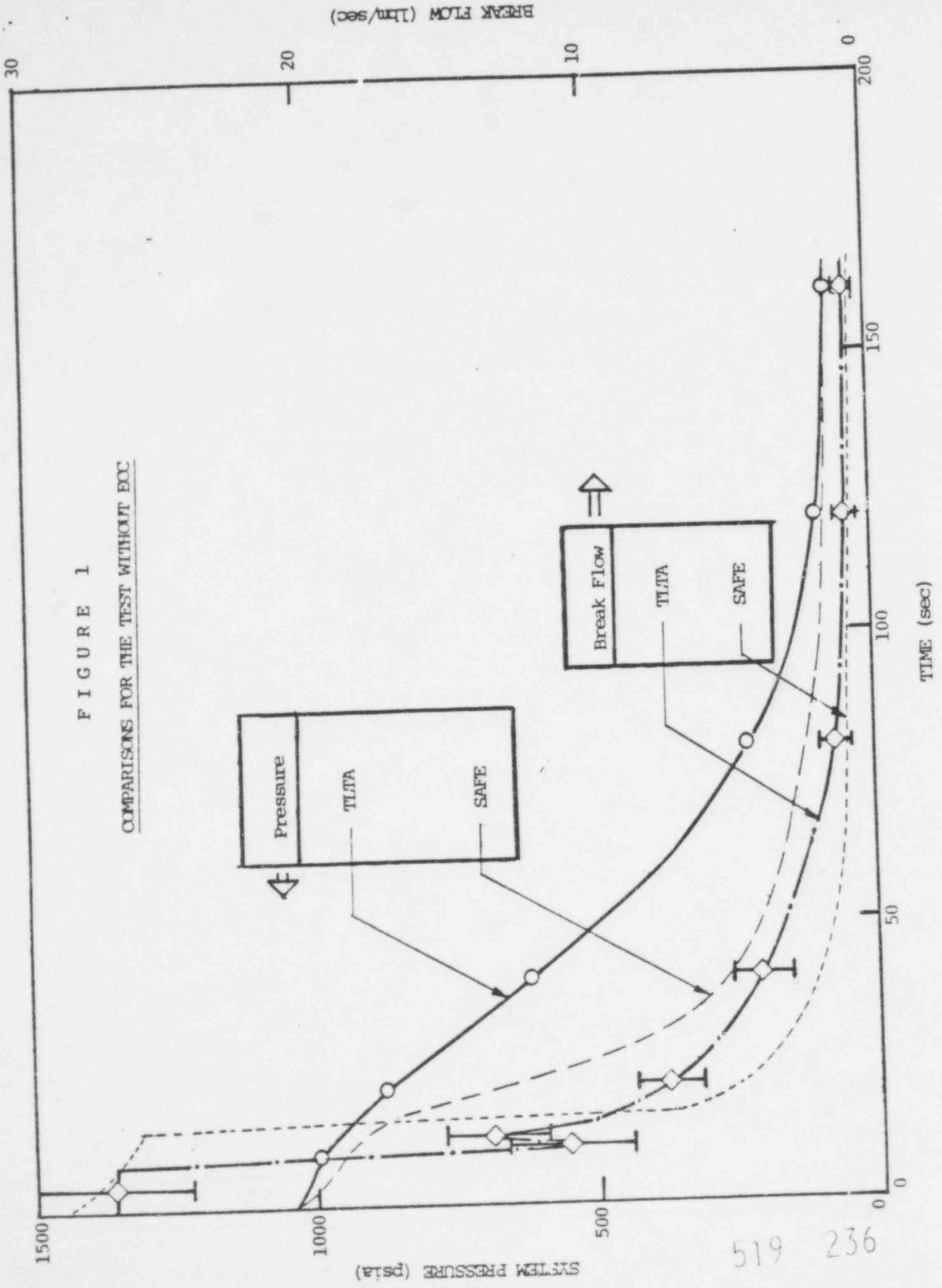


FIGURE 1
COMPARISONS FOR THE TEST WITHOUT ECC

SYSTEM PRESSURE (psia)

BREAK FLOW (lbm/sec)

TIME (sec)

519 236

FIGURE 2

COMPARISONS FOR THE TEST WITH ECC

